Issue 4 2018 | Volume 14

The Journal on Advanced Studies in Theoretical and Experimental Physics, including Related Themes from Mathematics

PROGRESS IN PHYSICS

"All scientists shall have the right to present their scientific research results, in whole or in part, at relevant scientific conferences, and to publish the same in printed scientific journals, electronic archives, and any other media." — Declaration of Academic Freedom, Article 8

ISSN 1555-5534

The Journal on Advanced Studies in Theoretical and Experimental Physics, including Related Themes from Mathematics

PROGRESS IN PHYSICS

A quarterly issue scientific journal, registered with the Library of Congress (DC, USA). This journal is peer reviewed and included in the abstracting and indexing coverage of: Mathematical Reviews and MathSciNet (AMS, USA), DOAJ of Lund University (Sweden), Scientific Commons of the University of St. Gallen (Switzerland), Open-J-Gate (India), Referativnyi Zhurnal VINITI (Russia), etc.

Electronic version of this journal:
http://www.ptep-online.com

Postal Address

Department of Mathematics and Science,
University of New Mexico,
705 Gurley Ave., Gallup, NM 87301, USA

ISSN: 1555-5534 (print)
ISSN: 1555-5615 (online)

Standard Address Number: 297-5092
Printed in the United States of America

October 2018 **Vol. 14, Issue 4**

CONTENTS

Information for Authors

Progress in Physics has been created for rapid publications on advanced studies in theoretical and experimental physics, including related themes from mathematics and astronomy. All submitted papers should be professional, in good English, containing a brief review of a problem and obtained results.

All submissions should be designed in LaTeX format using *Progress in Physics* template. This template can be downloaded from *Progress in Physics* home page http://www.ptep-online.com

Preliminary, authors may submit papers in PDF format. If the paper is accepted, authors can manage LaTeXtyping. Do not send MS Word documents, please: we do not use this software, so unable to read this file format. Incorrectly formatted papers (i.e. not LaTeXwith the template) will not be accepted for publication. Those authors who are unable to prepare their submissions in LaTeXformat can apply to a third-party payable service for LaTeX typing. Our personnel work voluntarily. Authors must assist by conforming to this policy, to make the publication process as easy and fast as possible.

Abstract and the necessary information about author(s) should be included into the papers. To submit a paper, mail the file(s) to the Editor-in-Chief.

All submitted papers should be as brief as possible. Short articles are preferable. Large papers can also be considered. Letters related to the publications in the journal or to the events among the science community can be applied to the section *Letters to Progress in Physics*.

All that has been accepted for the online issue of *Progress in Physics* is printed in the paper version of the journal. To order printed issues, contact the Editors.

Authors retain their rights to use their papers published in *Progress in Physics* as a whole or any part of it in any other publications and in any way they see fit. This copyright agreement shall remain valid even if the authors transfer copyright of their published papers to another party.

Electronic copies of all papers published in *Progress in Physics* are available for free download, copying, and re-distribution, according to the copyright agreement printed on the titlepage of each issue of the journal. This copyright agreement follows the *Budapest Open Initiative* and the *Creative Commons Attribution-Noncommercial-No Derivative Works 2.5 License* declaring that electronic copies of such books and journals should always be accessed for reading, download, and copying for any person, and free of charge.

Consideration and review process does not require any payment from the side of the submitters. Nevertheless the authors of accepted papers are requested to pay the page charges. *Progress in Physics* is a non-profit/academic journal: money collected from the authors cover the cost of printing and distribution of the annual volumes of the journal along the major academic/university libraries of the world. (Look for the current author fee in the online version of *Progress in Physics*.)

Elimination of Anomalies Reported for $b \to s\ell\ell$ and $b \to c\ell\bar{\nu}_\ell$ Semi-Leptonic Decay Ratios R(K,K*) and R(D,D*) when the Lepton Families Represent Discrete Symmetry Binary Subgroups 2T, 2O, 2I of SU(2)

Franklin Potter
Sciencegems.com, 8642 Marvale Drive, Huntington Beach, CA 92646 USA. E-mail: frank11hb@yahoo.com

The large discrepancies between the measured and predicted values of B meson decay ratios R(K) and R(D) could indicate lepton flavor universality violation and new physics beyond the Standard Model. I propose that the only new physics is that each lepton family represents a different discrete symmetry binary subgroup of SU(2) and that lepton flavor mixing exists because the 3 families act collectively to achieve SU(2) symmetry. Successful calculations of the neutrino mixing angles and of the measured ratios R(K,K*) and R(D, D*) by using those mixing angles confirm that the 3 lepton families represent the 3 binary subgroups 2T, 2O, and 2I.

1 Introduction

Perhaps the hottest research topic today in particle physics is whether the door to new physics (NP) has been pried ajar by the Belle, BaBar, and LHCb reports of significant discrepancies from the Standard Model (SM) predicted values in the B meson semi-leptonic decay ratios. In particular, rare $b \to s\ell\ell$ and $b \to c\ell\bar{\nu}_\ell$ decays are now known to exhibit significant deviations from the SM predictions for both their branching ratios and their angular distributions [1]. One possible interpretation of these results would be the violation of lepton flavor universality (LFUV) with regard to the weak interaction.

Over the past two decades these deviations from the SM predicted values have triggered a variety of models of NP, such as Z' models with gauged L_μ - L_τ, models with leptoquarks, models with compositeness, etc. For a complete list of the great variety of proposed NP models, see [2].

I claim that the only NP required is to properly identify the lepton and quark family symmetries. Previously, I have shown [3] that their EW flavor states actually represent 3 specific discrete symmetry subgroups of SU(2). In better words, the true reason for lepton mixing is the collective action of the 3 lepton families with their discrete symmetries to mimic the SU(2) weak isospin eigenstates $\pm\frac{1}{2}$ demanded by the SM gauge interaction bosons representing $SU(2)_W \times U(1)_Y$. The correct statement that the mixing angles represent a mismatch between the EW flavor states and their mass states is the consequence of but not the reason for the mixing. I explain below how this collective action is achieved by the 3 specific discrete symmetry binary subgroups of SU(2), known as 2T, 2O, and 2I, for the electron, muon, and tau families, respectively. The immediate results are the correct mixing angles and the correct ratios of branching ratios for b quark semi-leptonic decays.

Section 2 is a brief review of the recent experimental results for B meson semi-leptonic decays. Section 3 explains how the lepton mixing angles are derived from the generators of the 3 discrete symmetry subgroups of SU(2), or equivalently the group of unit quaternions Q. Section 4 includes a derivation of the electroweak (EW) boson states $W^\pm$, Z^0, and γ as well as the Weinberg angle. Finally, in Section 5, I calculate the ratios for the semi-leptonic b decays $b \to s\ell\ell$ and $b \to c\ell\bar{\nu}_\ell$ using alternative EW boson state assignments. In order to do so, one requires the appropriate discrete symmetry eigenstates for the leptons, quarks, and EW bosons, which I have discussed in the literature [3,4] and at conferences [5,6].

2 The B meson decays

The ratio of branching ratios has been used extensively to summarize both the theoretical and the experimental results because almost all the hadronic uncertainties are eliminated. For example, these four ratios for B meson decays exhibit large discrepancies of more than 2.5σ from their SM predictions [1]:

$$R(K)^{SM} = \frac{\mathcal{B}(B \to K\mu^+\mu^-)}{\mathcal{B}(B \to Ke^+e^-)} = 1.00 \pm O(1\%), \quad (1)$$

$$R(K^*)^{SM} = \frac{\mathcal{B}(B \to K^*\mu^+\mu^-)}{\mathcal{B}(B \to K^*e^+e^-)} = 1.00 \pm O(1\%), \quad (2)$$

$$R(D)^{SM} = \frac{\mathcal{B}(B \to D\tau\nu_\tau)}{\mathcal{B}(B \to D\ell\nu_\ell)} = 0.298 \pm 0.003, \quad (3)$$

$$R(D^*)^{SM} = \frac{\mathcal{B}(B \to D^*\tau\nu_\tau)}{\mathcal{B}(B \to D^*\ell\nu_\ell)} = 0.255 \pm 0.004, \quad (4)$$

valid over a broad range of q^2 values.

LHCb has recently reported [7]

$$R(K)^{exp} = 0.745 \pm 0.090 \pm 0.036 \quad (5)$$

$$R(K^*)^{exp} = 0.685 \pm 0.113 \pm 0.047 \quad (6)$$

in the di-lepton invariant mass range $1\ \text{GeV}^2 < q^2 < 6\ \text{GeV}^2$, exhibiting significant deviations from the SM predictions.

For muonic decays [8]

$$R(D)^{exp} = 0.407 \pm 0.039 \pm 0.024. \quad (7)$$

Table 1: Exact angle contributions by the U_2 generators of 2T, 2O, and 2I. Note that $\phi = (1 + \sqrt{5})/2$, and Angle = arccosine (Factor), which is twice the projection angle to the k-axis.

Family	Group	U_1	U_2	U_3	Factor	Angle	Angle/2
ν_e, e^-	2T	j	$-\frac{i}{2}-\frac{j}{2}+\frac{k}{\sqrt{2}}$	i	-0.26422	105.3204°	52.660°
ν_μ, μ^-	2O	j	$-\frac{i}{2}-\frac{j}{\sqrt{2}}+\frac{k}{2}$	i	+0.80116	36.7581°	18.379°
ν_τ, τ^-	2I	j	$-\frac{i}{2}-\frac{\phi j}{2}+\frac{\phi^{-1}k}{2}$	i	-0.53695	122.4764°	61.238°

$$R(D^*)^{exp} = 0.336 \pm 0.027 \pm 0.030. \quad (8)$$

I propose that the values of the ratios R(K), R(K*), R(D), and R(D*), all can be expressed in terms of the lepton mixing angles, without venturing outside the realm of the SM local interaction symmetry group $SU(3)_C \times SU(2)_W \times U(1)_Y$. For example, I derive in Section 5 how using the lepton family mixing angles predicts

$$R(K) = \frac{Cos\,\theta_{23}}{Cos\,\theta_{13}} = \frac{Cos\,42.859^\circ}{Cos\,8.578^\circ} = 0.74127\ R(K)^{SM}, \quad (9)$$

$$R(D) = \frac{Cos\,\theta_{33}}{Cos\,\theta_{23}} = \frac{Cos\,0.000^\circ}{Cos\,42.859^\circ} = 1.36420\ R(D)^{SM}, \quad (10)$$

which agree with the experimental values 0.745 ±0.090 ± 0.036 and 0.407±0.039±0.024, respectively.

Why does this procedure work? Because the $W^\pm$ and Z^0 bosons have discrete symmetry properties, too, and are eigenstates of the binary product group 2I × 2I'. In the traditional way of thinking, such an alternative way to express $W^\pm$ and Z^0 comes as a big surprise!

3 Brief review of neutrino mixing

In 2013 I derived [3] the exact lepton mixing angles for the neutrino PMNS mixing matrix by first assigning the three lepton families to three special discrete symmetry binary subgroups of the unitary quaternion group Q, which is equivalent to the SU(2) group used for the two electroweak (EW) isospin flavor states $\pm\frac{1}{2}$ in each lepton and quark family. I provide a brief review of that lepton mixing angle derivation here.

The group Q of unitary quaternions has these discrete symmetry subgroups:

$$2T, 2O, 2I, D_{2n}, C_{2n}, C_n \ \ (n\,odd). \quad (11)$$

If I assume that leptons are 3-D entities at the Planck scale, then only 2T, 2O, and 2I, are useful for identifying them. So I assigned these 3 finite binary subgroups to the electron family (ν_e, e^-), to the muon family (ν_μ, μ^-), and to the tau family (ν_τ, τ^-), respectively.

These 3 binary subgroups each have the 3 quaternion generators U_1, U_2, and U_3 as given in Table 1. Notice that for each group only two of the three generators, U_1 = j, and U_3 = i, are the same as for SU(2), which has the three quaternion generators j, k, i. Their other generator, U_2, is different for each binary subgroup and different from each other. By demanding that the three U_2 generators collectively act as the k-generator of SU(2), their linear superposition provides three equations for three unknown factors. Their normalized factors, the corresponding angles calculated by their inverse cosine projections to the k-axis, and the physical rotation angles, are quantities all listed in Table 1.

Defining the lepton mixing angles by $\theta_{ij} = |\ \theta_i - \theta_j\ |$ produces the three neutrino PMNS mixing angles

$$\theta_{12} = 34.281^\circ \quad \text{vs} \quad 33.56^\circ \pm 0.77^\circ\ (exp) \quad (12)$$

$$\theta_{23} = 42.859^\circ \quad \text{vs} \quad 41.6^\circ \pm 1.5^\circ\ (exp) \quad (13)$$

$$\theta_{13} = 8.578^\circ \quad \text{vs} \quad 8.46^\circ \pm 0.15^\circ\ (exp), \quad (14)$$

with their absolute values agreeing with the experimental values. Note that I have no mixing among the charged lepton flavor states, unitarity of the PMNS mixing matrix, a normal mass state hierarchy, and no additional neutrino states beyond those in the three known lepton families.

Therefore, I claim that the three lepton families represent the three chosen discrete symmetry binary subgroups 2T, 2O, 2I, and that they act collectively to mimic the SU(2) symmetry required for the isospin flavor states of the EW component of the SM.

4 Electroweak boson states W^+, Z^0, W^-, γ

The SM local gauge group SU(2) × U(1) has four EW interaction bosons W^+, Z^0, W^-, γ, which can be derived from the four quaternion generators i, j, k, b, with the first three generators for SU(2) or Q and the generator b for U(1) [or, equivalently, for the 2-element inversion group I_2]. These four generators required for the EW boson operations on the lepton flavor states must be able to perform the discrete rotations of the binary subgroups 2T, 2O, and 2I, in order to go from one lepton flavor state $\pm\frac{1}{2}$ to the other in each family. Of course, the Lie groups SU(2), or Q, are capable of doing these discrete rotations because they include all possible operations.

But there exists a smaller group with discrete symmetry that can provide the essential operations. One might expect that the largest group 2I of binary icosahedral operations by itself would be able to perform the required rotations in the normal space $C^2 = R^4$. However, some operations in the binary octahedral group 2O for the muon family would be omitted, so one finds that the product group 2I × 2I' is necessary, where 2I' provides certain "reciprocal" operations, as they are called.

In a 2014 paper [9], by using 2I × 2I', I derived the Weinberg angle, i.e., the weak mixing angle, using $U_2 \times U'_2$ to predict

$$\theta_W = 30^\circ \text{ vs } 28.4^\circ \pm 0.5^\circ \ (exp). \tag{15}$$

The discrepancy between the measured and the theoretical values of the Weinberg angle could be indicating that the 30° value applies at the Planck scale.

One now defines the four EW boson states in terms of the 2I × 2I' weak isospin states by these four relations:

$$|W^+> = |+\tfrac{1}{2}>|+\tfrac{1}{2}> \tag{16}$$

$$|Z^0> = \left(|+\tfrac{1}{2}>|-\tfrac{1}{2}> + |-\tfrac{1}{2}>|+\tfrac{1}{2}>\right)/\sqrt{2} \tag{17}$$

$$|W^-> = |-\tfrac{1}{2}>|-\tfrac{1}{2}> \tag{18}$$

$$|\gamma> = \left(|+\tfrac{1}{2}>|-\tfrac{1}{2}> - |-\tfrac{1}{2}>|+\tfrac{1}{2}>\right)/\sqrt{2}. \tag{19}$$

where the upper state $+\frac{1}{2}$ for 2I is the tau neutrino flavor state ν_τ and the lower state $-\frac{1}{2}$ is the τ^- state. The tau family antiparticle states representing the 2I' discrete symmetry group have the upper and lower states τ^+ and $\bar{\nu}_\tau$.

One would expect that these four EW boson state identifications in terms of 2I × 2I' eigenstates would be important for understanding their decays into leptons and quarks. Indeed, unless one uses these particular identifications, the B meson decays will have large discrepancies with the SM predictions and remain a challenge for the SM traditional approach, paricularly for the semi-leptonic decays

$$b \to s\,\ell^+\ell^- \text{ and } b \to c\ell\bar{\nu}_\ell, \tag{20}$$

precisely the decays for R(K) and R(D).

Therefore, I can re-define the EW boson states in terms of the tau lepton family flavor states for calculation purposes and determine the consequences for the b semi-leptonic decays:

$$|W^+> = |\nu_\tau>|\tau^+> \tag{21}$$

$$|Z^0> = (|\nu_\tau>|\bar{\nu}_\tau> + |\tau^->|\tau^+>)/\sqrt{2} \tag{22}$$

$$|W^-> = |\tau^->|\bar{\nu}_\tau> \tag{23}$$

$$|\gamma> = (|\nu_\tau>|\bar{\nu}_\tau> - |\tau^->|\tau^+>)/\sqrt{2}. \tag{24}$$

That these assignments work well in determining the ratios R(K) and R(D) is discussed in the next section.

5 b → $s\ell\ell$ and b → $c\ell\bar{\nu}_\ell$

The traditional way to handle these decays would be to examine the Wilson coefficients [10] and determine which ones are possibly responsible for the discrepancies of the experimental results from the SM predictions.

However, now that I have proposed explicit expressions for the EW bosons in terms of the tau family flavor states, I can calculate directly the decay ratios reported in the literature. For the decay b → $s\ell\ell$ in which R(K) is expressed in terms of the ratio of the branching ratios of $Z^0 \to \mu^-\mu^+$ and $Z^0 \to e^-e^+$ in Eq. 1, the semi-leptonic B meson decays require the Z^0 decays expressed as

$$|\tau^->|\tau^+> \to |\mu^->|\mu^+> \tag{25}$$

$$|\tau^->|\tau^+> \to |e^->|e^+>, \tag{26}$$

with each decay being proportional to the cosine of the specific lepton mixing angle between families, i.e., one predicts their ratio

$$R(K) = \frac{\cos\theta_{23}}{\cos\theta_{13}} = \frac{0.73303}{0.98888} = 0.74127, \tag{27}$$

which is the measured value of R(K) = 0.745 ±0.090 ±0.36.

The R(K*) ratio has the same Z^0 decays, so the prediction is the same,

$$R(K^*) = \frac{\cos\theta_{23}}{\cos\theta_{13}} = \frac{0.73303}{0.98888} = 0.74127, \tag{28}$$

which is within the measured value of R(K) = 0.685 ±0.113 ±0.47 with its large uncertainties.

In order to use the same procedure for b→ $c\ell\bar{\nu}_\ell$, which involves the W^- decay, the three W^- decays are expressed as

$$|\tau^->|\bar{\nu}_\tau> \to |\tau^->|\bar{\nu}_\tau> \tag{29}$$

$$|\tau^->|\bar{\nu}_\tau> \to |\mu^->|\bar{\nu}_\mu> \tag{30}$$

$$|\tau^->|\bar{\nu}_\tau> \to |e^->|\bar{\nu}_e>, \tag{31}$$

again with each decay being proportional to the cosine of the lepton mixing angle. For example, taking the ratio of the first two, one obtains the factors

$$R(D)^\mu = \frac{\cos\theta_{33}}{\cos\theta_{23}} = \frac{1}{0.73303} = 1.364, \tag{32}$$

and the ratio of the first and third produces

$$R(D)^e = \frac{\cos\theta_{33}}{\cos\theta_{13}} = \frac{1}{0.98888} = 1.011. \tag{33}$$

Either or both of these factors multiplies the SM predicted value in order to achieve the measured values of R(D) and R(D*). The W^- decay to the muon family alone produces

$$R(D)^\mu = 1.364 \text{ x } 0.298 = 0.408, \tag{34}$$

$$R(D^*)^{\mu} = 1.364 \text{ x } 0.255 = 0.348. \quad (35)$$

both predicted values matching the experimental values 0.407 ±0.039 ±0.024 and 0.336 ±0.027 ±0.030, respectively, for purely muonic decays.

And for the other product, the one involving the tau family states decaying to the electron family only, the predicted results are

$$R(D)^{e} = 1.011 \text{ x } 0.298 = 0.301, \quad (36)$$

$$R(D^*)^{e} = 1.011 \text{ x } 0.255 = 0.258. \quad (37)$$

Therefore, if there is a significant electron family contribution to the R(D*) decay channel, that would lower the total predicted R(D*) value for those reports that average both the muon and electron contributions.

6 Summary

There is no evidence in these semi-leptonic decays for lepton flavor violation. The lepton mixing angles are used to successfully calculate the B meson ratios R(K), R(K*), R(D), and R(D*), which involve ratios of the semi-leptonic b quark decays $b \to s\ell\ell$ and $b \to c\ell\bar{\nu}_\ell$. No discrepancies between the predicted values and the experimental values exist when the lepton families are expressed in terms of the 3 discrete symmetry binary subgroups 2T, 2O, and 2I of SU(2) and the EW boson states are expressed in terms of the discrete symmetry product group 2I × 2I'. The predicted values agree with the experimental values for all four ratios when expressed in terms of the appropriate mixing angles.

The key idea is that the lepton mixing angles exist because the 3 binary subgroups identifying the 3 lepton family discrete symmetries are acting collectively to achieve the SU(2) Lie symmetry of the EW part of the SM. One immediate consequence is that the EW boson states W^+, Z^0, W^-, γ can be expressed in terms of the discrete symmetry product group 2I × 2I', a real surprise. With these discrete symmetry groups, I calculate the neutrino mixing angles, the Weinberg angle, and the four B meson ratios, all in agreement with the experimental values.

Acknowledgements

I thank Sciencegems.com for their continued support.

Submitted on June 10, 2018

References

1. Altmannshofer W., Stangl P., Straub D.M. Interpreting Hints for Lepton Flavor Universality Violation. arXiv: 1704.05435v2 [hep-ph]. Includes a complete reference list.
2. Watanabe R. New Physics effect on $B_c \to J/\psi\tau\bar{\nu}$ in relation to the R(D*) anomaly. arXiv: 1709:08644v3 [hep-ph].
3. Potter F. Geometrical Derivation of the Lepton PMNS Matrix Values. *Progress in Physics*, v. 9(3), 2013, 29–30. http://www.ptep-online.com/2013/PP-34-09.PDF.
4. Potter F. CKM and PMNS mixing matrices from discrete subgroups of SU(2). *Progress in Physics*, v. 10(3), 2014, 146–150. http://www.ptep-online.com/2013/PP-34-09.PDF.
5. Potter F. CKM and PMNS mixing matrices from discrete subgroups of SU(2). *J. Phys: Conf. Ser.*, v. 631, 2015, 012024. http://iopscience.iop.org/article/10.1088/1742-6596/631/1/012024/meta.
6. Potter F. Exact Neutrino Mixing Angles from Three Subgroups of SU(2) and the Physics Consequences. Workshop in Neutrinos (WIN) 2017 UC Irvine, June 19-24, 2017 https://indico.fnal.gov/event/9942/session/4/contribution/23/material/slides/0.pdf
7. Albrecht J. Lepton Flavour Universality tests with B decays at LHCb. arXiv: 1805.06243 [hep-ph].
8. Aaij R. et al. [LHCb Collaboration] Measurement of the Ratio of Branching Fractions $\mathcal{B}(\bar{B}^0 \to D^{*+}\tau^-\bar{\tau}_\tau)/\mathcal{B}(\bar{B}^0 \to D^{*+}\mu^-\bar{\nu}_\mu)$. *Phys. Rev. Lett.*, 2015, v. 115(11), 111803. Erratum: [*Phys. Rev. Lett.*, 2015, 115(15), 159901].
9. Potter F. Weinberg Angle Derivation from Discrete Subgroups of SU(2) and All That. *Progress in Physics*, v. 11(1), 2014, 76–77. http://www.ptep-online.com/2015/PP-40-14.PDF.
10. Cornella, C., Feruglio F., Paradisi P. Low-energy Effects of Lepton Flavour Universality Violation. arXiv: 1803:00945v1 [hep-ph].

On the Anomalous Electronic Heat Capacity γ-Coefficient

G. G. Nyambuya

National University of Science and Technology, Faculty of Applied Sciences – Department of Applied Physics, Fundamental Theoretical and Astrophysics Group, P. O. Box 939, Ascot, Bulawayo, Republic of Zimbabwe.
E-mail: physicist.ggn@gmail.com

As is common knowledge, the experimentally measured and theoretically deduced values of the γ-coefficient of the electronic heat capacity of metals exhibit a clear discrepancy. This discrepancy is usually attributed to the neglected effects such as the electron self-interaction and the electron interaction with phonons and the Coulomb potential. Despite the said pointers to the possible cause in the obtaining theoretical and experimental dichotomy, no dedicated effort has been put in order to come up with a theory to explain this. An effort is here made to come-up with an alternative theoretical framework whose endeavour is to proffer a theory that may explain why there is this theoretical and experimental dichotomy by invoking the hypothesis that the temperature of electrons and the lattice may be different. We argue that the different electron and lattice temperatures can – *in-principle* – give an alternative explanation as to the said theoretical and experimental dichotomy in the γ-coefficient of the electronic heat capacity of metals without the need to invoke the effective mass theory as currently obtains.

> "Thermodynamics is a funny subject. The first time you go through it, you don't understand it at all. The second time you go through it, you think you understand it, except for one or two small points. The third time you go through it, you know you don't understand it, but by that time you are so used to it, it doesn't bother you anymore."
>
> Arnold J. W. Sommerfeld (1868–1951)

1 Introduction

The main purpose of the present reading is to provide (propose) an alternative model that seeks to explain the existing discrepancy in the electronic heat capacity γ-coefficients for different metals. That is to say, for temperatures below the Debye (θ_D) and Fermi temperature (θ_F), in terms of the temperature (T) of the metal in question, the total molar heat capacity at constant volume C_V^T of metals is satisfactorily described by the sum of a *linear electronic* ($C_V^e \propto T$) [1, 2] and a *cubic phononic* ($C_V^l \propto T^3$) contribution [3], *i.e.*:

$$C_V^T = \gamma T + AT^3 \,, \tag{1}$$

where $\gamma = \pi^2 n_* \mathscr{R}/2\theta_F$ is the said γ-coefficient in question, with n_* being the number of free electrons per lattice point, $\mathscr{R} = 8.3144600(50)\ \mathrm{Jmol^{-1}K^{-1}}$ is the ideal gas constant and is such that $\mathscr{R} = N_A k_B$, where $N_A = 6.022140857(74) \times 10^{23}$ is the Avogadro number and $k_B = 1.38064852(79) \times 10^{-23}\ \mathrm{JK^{-1}}$ is the Boltzmann's constant, and:

$$A = \frac{9\mathscr{R}}{\theta_D^3} \int_0^{x_D} \frac{x^4 e^x dx}{(e^x - 1)^2} \,, \tag{2}$$

where $x = \hbar\omega/k_B T$ and $x_D = \theta_D/T$, $\hbar$ is Planck's normalized constant and ω is the angular frequency of the oscillating lattice points (*i.e.* atom or molecule). In the low temperature region, *i.e.* $x \lll 1$, A is such that:

$$A \simeq \frac{12\pi^4 \mathscr{R}}{5\theta_D^3} \,. \tag{3}$$

For a given metal in question – the coefficients γ and A are constant coefficients which are determined experimentally.

It was after Albert Einstein's [4] first great insights into the quantum nature of solids that the cubic term $C_V^l \propto T^3$, was successfully explained by Peter Debye [3]. At low temperatures the lattice contribution $C_V^l \propto T^3$ is significantly smaller than the electronic contribution $C_V^e \propto T$, it vanishes faster than the electronic contribution and from this, γ (also known as the *Sommerfeld constant*) can be measured experimentally. As will be seen in the next section, there is a clear marked difference in the theoretical and experimental values of the γ-coefficient and we seek here an answer to as to why this fragment disagreement between theoretical and experiment.

2 Problem

Table 1 lists the theoretical γ_{theo} and experimental γ_{exp} values of twenty one elements and these values are plotted in Figure 1. One finds that they can fit either a linear, quadratic, a general power law or logarithmic curve to these data points. The marked difference in the theoretical and experimental values of the γ-coefficient is clear. From column 3 of Table 1, the percentage deviations are presented and it can be seen from this that the mean square deviation is as high as 35%, while the mean value of the ratio $\gamma_{exp}/\gamma_{theo}$ (column 5 of Table 1) together with its deviation from this mean value is 1.30 ± 0.40.

The said marked difference in the theoretical and experimental values of the γ-coefficient as presented in Figure 1

Table 1: Table of 21 elements for the experimental and theoretical values of the electronic heat capacity coefficients. From left to right, the columns represent the element, its corresponding theoretical and experimental γ-coefficient and the percentage $(1-\gamma_{exp}/\gamma_{theo})\times 100\%$ deviation of the experimental value from the theoretical one, respectively. The values of γ_{exp} and γ_{theo} are adapted from Kittel (2005, 1986) [5, 6] and Tari (2003) [7].

Element	γ_{theo} ($mJmol^{-1}K^{-2}$)	γ_{exp} ($mJmol^{-1}K^{-2}$)	**%Dev.**	$\frac{\gamma_{exp}}{\gamma_{theo}}$
Li	1.63	0.75	+54	2.18
Be	0.17	0.50	+190	0.34
Na	1.38	1.09	+20	1.26
Mg	1.30	0.99	+24	1.31
Al	1.35	0.91	+32	1.48
K	2.08	1.67	+20	1.25
Ca	2.90	1.51	+48	1.92
Cu	0.70	0.51	+27	1.38
Zn	0.64	0.75	−18	0.85
Ga	0.60	1.03	−72	0.58
Rb	2.41	1.91	+21	1.26
Sr	3.60	1.79	+50	2.01
Ag	0.65	0.65	+0.15	1.00
Cd	0.69	0.95	−38	0.73
In	1.69	1.23	+27	1.37
Sn	1.78	1.41	+20	1.26
Cs	3.20	2.24	+30	1.43
Ba	2.70	1.94	+28	1.39
Au	0.73	0.64	+12	1.14
Hg	1.79	0.95	+47	1.88
Pb	2.98	1.51	+49	1.97
Mean Square Deviation	↦		**35**	

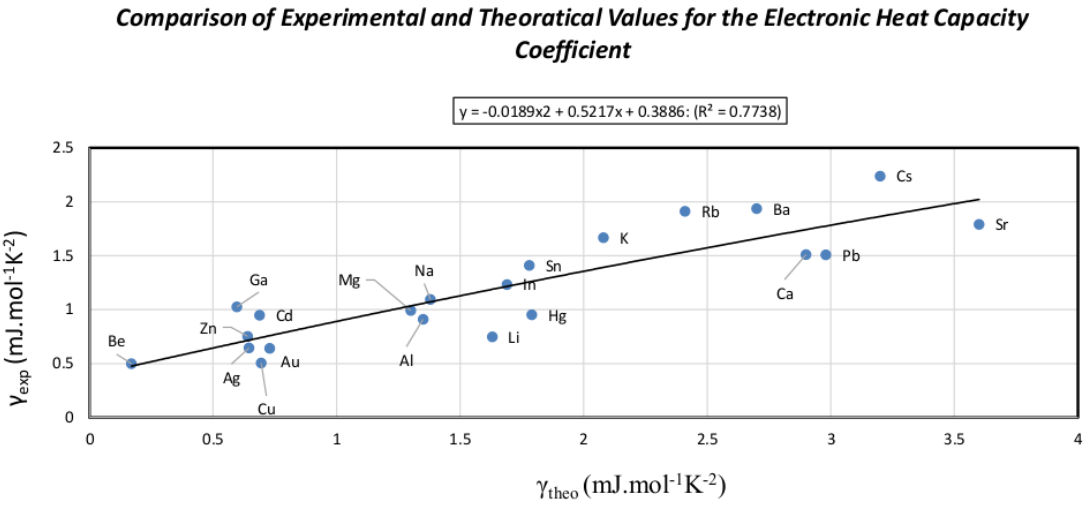

Fig. 1: A comparison graph of the experimental and theoretical values for the electronic heat capacity coefficients for the twenty one elements listed in Table 1. If there was a good agreement between theory and experimental, the values of γ_{exp} and γ_{theo} would lay along the line $\gamma_{exp} = \gamma_{theo}$. This is not the case implying a sure fragment disagreement between theory and experiment.

demonstrates an underlying correlation between these values. Amongst others, a correlation such as this, suggests some correlated physics must be at play – *one way or the other*. Given that electrons do interact with phonons, this correlation must have something to do with the electron-phonon interaction. We are not going to seek a fundamental origin of this correlation but merely suggest that this deviation may (as will be demonstrated) very well be due to a possible inequality in the electron and lattice temperatures.

The general and widely held view (see *e.g.* [5,6,8–10]) as to this discrepancy is that:

1. The interaction of the conduction electrons with the periodic Coulomb potential of the rigid crystal lattice is neglected.
2. The interaction of the conduction electrons with phonons is also neglected. This interaction causes changes in the effective mass of the electron and therefore it affects the electron energy.
3. The interaction of the conduction electrons with themselves is also ignored. For example, a moving electron causes an inertial reaction in the surrounding electron gas.

Since $\gamma \propto m_{\mathrm{e}}$ (see *e.g.* [5, 6]), to bring about agreement between theory and observation, the mass of the electron is corrected by introducing an effective mass m_{e}^{*} for the electron (*e.g.* [5, 6, 8–10]). Whatever difference there exists between theory and experiment, the effective mass is wholly assumed to shoulder this discrepancy (*e.g.* [5, 6, 8, 9]) as follows:

$$\frac{\gamma_{\mathrm{exp}}}{\gamma_{\mathrm{theo}}} = \frac{m_{\mathrm{e}}^{*}}{m_{\mathrm{e}}}\,, \tag{4}$$

where $m_{\mathrm{e}} = 9.10938356(11) \times 10^{-31}$ kg is the usual elementary mass of the electron.

The effective mass theory (see *e.g.* [5, 11] or any good textbook on the subject) is essentially about the equation of motion of a charged particle (electron in this case) inside the energy band of the crystal. In this theory, the electron is treated as a wave-packet in the typical *de Broglie* wave-particle duality model. That is to say, the electron is assumed to be a wave-packet made up of wavefunctions near a particular wavevector $\vec{k}$ and this wave-packet has a group velocity $\vec{v}_{\mathrm{g}} = \partial\omega/\partial\vec{k}$. All the effects of the environment on the electron are contained in the dispersion relation $\omega = \omega(k)$. For an electron whose energy is ϵ, the effective mass theory (see *e.g.* [5,11] or any good textbook on the subject) predicts that:

$$\frac{1}{m_{\mathrm{e}}^{*}} = \frac{1}{\hbar^2}\,\frac{\partial^2\epsilon}{\partial k^2} = \frac{1}{\hbar}\,\frac{\partial^2\omega}{\partial k^2} = \frac{1}{\hbar}\,\frac{\partial v_{\mathrm{g}}}{\partial k}\,, \tag{5}$$

where m_{e}^{*} is the effective mass of the electron as it moves in the energy band of the crystal. For example, in the case of a free electron where $\epsilon = \hbar^2 k^2/2m_{\mathrm{e}}$, we have $m_{\mathrm{e}}^{*} = m_{\mathrm{e}}$, *i.e.* the electron has its usual mass m_{e}. Inside the crystal structure where there is no current flow, the valency electrons are free having only thermal energy, they do not have a net drift velocity, but have random fluctuations whose net velocity is zero – hence, the effective mass theory should not be inapplicable to such electrons since measurements of the electronic γ-factor is conducted on such electrons. It is this that has made us to doubtfully question the effective mass theory in accounting for the γ-factor discrepancy.

The effective mass m_{e}^{*} can be larger or smaller than the electron's actual mass m_{e} and this depends on whether the states within the electron's energy band are denser (more compressed) or less dense (expanded) compared with those of a free gas [5, 6, 11]. The effective mass also reflects the inertia of the charge carriers. The two (effective mass & the inertia of the charge carriers) are related, because narrower, denser, bands reflect a smaller overlap of neighbouring electron clouds and hence greater difficulty for electrons to travel from one atom to the next.

This communication presents an alternative model whose aim is to explain the discrepancy in theoretical and experimental values of the electronic heat capacity coefficient. As pointed above – currently this is explained by invoking the effective mass theory. As shown in Figure 1, there is a clear trend in the experimental and theoretical values of the electronic heat capacity coefficient. We have not seen any theory that tries to explain this trend, not even *within* the effective mass theory. It is our firm belief that the effective mass theory should fail to explain this trend for the reason pointed above about the electrons inside metals during the measurement of γ, namely that they have a net zero group velocity. This communication makes an endeavour to provide an alternative model by invoking the not so unreasonable idea that electrons and atoms (molecules) in solids are at different temperatures.

3 Electron-lattice temperature correction

In our suggested alternative explanation – as to the discrepancy between theory and experiment, we propose to reconsider the issue of the lattice and electron temperatures. That is to say, a solid can be viewed as a homogeneous mixture of the lattice and the valency electrons. Just like any mixture, the different species are not expected to be at the same temperatures. Yes, the mixture will come together to a common temperature T, which is the temperature that we generally assign to the solid in question. The species with "*more heat*" will transfer this heat to the species with "*less heat*". In this case of the electron-lattice mixture, we expect the lattice to have "*more heat*" with the valency electrons having "*less heat*". If ΔQ_l is the heat transfer from the lattice and ΔQ_{e} is the heat received by the free electrons, then we must have:

$$\Delta Q_{\mathrm{e}} + \Delta Q_l = 0\,. \tag{6}$$

So, unlike in the conventional treatment where the lattice and electron temperatures are assumed to be equal, we here as-

sume them to be different. If one accepts this, then what follows is straightforward.

If $M_{\mathrm{e}}, c_v^{\mathrm{e}}, T_{\mathrm{e}}; M_l, c_v^l, T_l$ is the total mass, specific heat capacity and temperature of the electrons gas and the lattice respectively, and T is the common temperature of the mixture, then, from (6), we will have:

$$\underbrace{M_{\mathrm{e}} c_v^{\mathrm{e}} (T - T_{\mathrm{e}})}_{\Delta Q_{\mathrm{e}}} + \underbrace{M_l c_v^l (T - T_l)}_{\Delta Q_l} = 0 \,. \tag{7}$$

Rearranging (7) and making T the subject, we will have:

$$T = \left(\frac{M_{\mathrm{e}} c_v^{\mathrm{e}}}{M_{\mathrm{e}} c_v^{\mathrm{e}} + M_l c_v^l} \right) T_{\mathrm{e}} + \left(\frac{M_l c_v^l}{M_{\mathrm{e}} c_v^{\mathrm{e}} + M_l c_v^l} \right) T_l \,. \tag{8}$$

Further – rearrangement of (8), gives:

$$T = \left(1 + \frac{M_l c_v^l}{M_{\mathrm{e}} c_v^{\mathrm{e}}} \right)^{-1} T_{\mathrm{e}} + \left(1 + \frac{M_{\mathrm{e}} c_v^{\mathrm{e}}}{M_l c_v^l} \right)^{-1} T_l \,. \tag{9}$$

We know that:

$$c_v^{\mathrm{e}} = \frac{C_V^{\mathrm{e}}}{N_A m_{\mathrm{e}}} \quad \text{and} \quad c_v^l = \frac{C_V^l}{N_A \mathcal{A}_l} \,, \tag{10}$$

where $\mathcal{A}_l$ is the atomic mass of the lattice and C_V^{e} and C_V^l are the electronic and lattice molar heat capacity respectively, and that:

$$\frac{M_l}{M_{\mathrm{e}}} = \frac{\mathcal{A}_l}{n_* m_{\mathrm{e}}} \,, \tag{11}$$

and substituting (10) and (11) into (9), we will have:

$$T = \left(1 + \frac{C_V^l}{n_* C_V^{\mathrm{e}}} \right)^{-1} T_{\mathrm{e}} + \left(1 + \frac{n_* C_V^{\mathrm{e}}}{C_V^l} \right)^{-1} T_l \,. \tag{12}$$

Now – because of the different temperatures of the electrons and the lattice, the total internal energy $\mathcal{U}_{\mathrm{e}}$ of the electrons is to be expressed as a function of the electron temperature T_{e} *i.e.* $\mathcal{U}_{\mathrm{e}} = \mathcal{U}_{\mathrm{e}}(T_{\mathrm{e}})$ and likewise, that of the lattice structure is such that $\mathcal{U}_l = \mathcal{U}_l(T_l)$. With the internal energy given in terms of the electron and lattice temperatures respectively, the corresponding electronic and lattice molar heat capacities are:

$$C_V^{\mathrm{e}} = \frac{\partial \mathcal{U}_{\mathrm{e}}(T_{\mathrm{e}})}{\partial T_{\mathrm{e}}} \quad \text{and} \quad C_V^l = \frac{\partial \mathcal{U}_l(T_l)}{\partial T_l} \,. \tag{13}$$

The total internal energy $\mathcal{U}_{\mathrm{T}}$ of the solid is such that:

$$\mathcal{U}_{\mathrm{T}} = \mathcal{U}_{\mathrm{e}}(T_{\mathrm{e}}) + \mathcal{U}_l(T_l) \,. \tag{14}$$

Now, to compute the total molar heat capacity of the solid, one does this by differentiating (14) with respect to the common temperature T as follows:

$$C_V^{\mathrm{T}} = \frac{\partial \mathcal{U}_{\mathrm{T}}}{\partial T} = \frac{\partial \mathcal{U}_{\mathrm{e}}(T_{\mathrm{e}})}{\partial T_{\mathrm{e}}} \frac{dT_{\mathrm{e}}}{dT} + \frac{\partial \mathcal{U}_{\mathrm{e}}(T_l)}{\partial T_l} \frac{dT_l}{dT} \,. \tag{15}$$

Eq. (15) can be re-written as:

$$C_V^{\mathrm{T}} = a_{\mathrm{e}} C_V^{\mathrm{e}} + a_l C_V^l \,, \tag{16}$$

where $a_{\mathrm{e}} = dT_{\mathrm{e}}/dT$ and $a_l = dT_l/dT$. From (12) and (16), it follows that:

$$a_{\mathrm{e}}^{-1} = \frac{1}{1 + C_V^l / n_* C_V^{\mathrm{e}}} + \frac{1}{\eta} \frac{1}{1 + n_* C_V^{\mathrm{e}} / C_V^l} \,, \tag{17}$$

where $\eta = dT_{\mathrm{e}}/dT_l$. Setting:

$$x = n_* \left(\frac{C_V^{\mathrm{e}}}{C_V^l} \right) , \tag{18}$$

it follows that:

$$a_{\mathrm{e}} = \left(\frac{x}{1+x} + \frac{1}{\eta} \frac{1}{1+x} \right)^{-1} = \eta \left(\frac{1+x}{1+\eta x} \right) . \tag{19}$$

It is expected that the lattice contribution will always be significantly larger than that of the electrons and this means or directly translates to: $x \ll 1$. In addition to the said condition $x \ll 1$, if we assume $|\eta x| < 1$, then, to first order approximation, we will have:

$$a_{\mathrm{e}} \simeq \eta \quad \text{and} \quad a_l \simeq 1 \,, \tag{20}$$

hence:

$$C_V^{\mathrm{T}} = \eta C_V^{\mathrm{e}} + C_V^l \,. \tag{21}$$

Clearly, from (21) above, the obvious identification:

$$\gamma_{\mathrm{exp}} = \eta \gamma_{\mathrm{theo}} \,, \tag{22}$$

can be made, the meaning of which is that the theoretical and experimental discrepancy in the values of the γ-coefficient can be ascribed to η.

We shall reiterate: one very important thing to note is that the effective mass of the electron applies only in the case of an electron that is in motion with $v_{\mathrm{g}} \neq 0$ in the crystal structure and this is in the case of an applied potential across the metal. The γ-coefficient is measured not for a metal that has a flow of current in it, but one with no current, thus making is logically inappropriate in this instance to ascribe an effective mass to the electron that is different to its bare mass m_{e}. In such a case, it would make sense to ascribe the different values of γ_{exp} and γ_{theo} to the difference in the electron and lattice temperatures as suggested herein.

4 General discussion

We herein have provided an alternative model whose endeavour is to explain the existing discrepancy between the experimental and theoretical values of the electronic heat capacity γ-coefficient. We must say that – at a reasonable and satisfactory level, the proposed model does explain the discrepancy in the experimental and theoretical γ-values. The prevalent (current mainstream) view is that this discrepancy comes

about as a result of a variable effective mass of the electron – wherein, the difference between the experimental and theoretical γ-values is wholly shouldered by the effective mass of the electron (see *e.g.* [5–10]). This idea of the effective mass may be logically inappropriate because the effective mass theory applies only in the case of an electron that is in motion with $v_g \neq 0$ in the crystal structure whereas the γ-coefficient is measured not for a metal that has a flow of current in it, but one with no current. Current flow implies "*with* $v_g \neq 0$", and no-current flow implies "*with* $v_g = 0$".

In the proposed model, this discrepancy is explained as being due to the different temperatures of the electrons and the lattice. In the mainstream model, the thermodynamic temperature of the electrons and atoms (molecules) of the solid are assumed to be equal. This view may not be correct. It is actually not unreasonable to think that electrons and atoms (molecules) of the solid are at different temperatures as this is common place in *e.g.* the study of molecular clouds in *Astrophysics* and as well as in *Plasma Physics*.

This model does not discard the effective mass model where results of experiments are made to agree with the theoretical value by postulating that the entire discrepancy be shouldered by the resulting effective mass of the electron. What the model does is basically to "*tell*" us that the different electron and lattice temperatures may have a role to play in the said observed discrepancies, or both models may be at play. This is something that can be investigated in a separate study unit altogether. As to what use this model may hold in the immediate future, we can not say, but we hope it will prove useful in the future as our knowledge horizons broaden and push further than where they lie at present.

Acknowledgements

We are grateful for the assistance rendered unto us by the National University of Science and Technology's Research Board toward our research endeavours.

Received on June 7, 2018

References

1. Sommerfeld A. Zur Elektronentheorie der Metalle. *Naturwissenschaften*, 1927, v. 15 (41), 825–832.
2. Bethe H. A. On the Theory of Metals. *Zeitschrift für Physik*, 1931, v. 71, 205–226.
3. Debye P. Zur Theorie der Spezifischen Wärmen. *Annalen der Physik*, 1912, v. 344 (14), 789–839.
4. Einstein A. Die Plancksche Theorie der Strahlung und die Theorie der spezifischen Wärme. *Annalen der Physik*, 1906, v. 327 (1), 180–190.
5. Kittel C. Introduction to Solid State Physics. John Wiley & Sons Inc., New York, Hoboken, USA, 8^{th} edition, 2005, pp. 146, 193–200.
6. Kittel C. Introduction to Solid State Physics. John Wiley & Sons Inc., New York, Chichester, USA, 6^{th} edition, 1986, pp. 140, 193–200.
7. Tari A. The Specific Heat of Matter at Low Temperatures. Imperial College Press, London, 6^{th} edition, 2003, p. 71.
8. Varshney D., Mansuri I., and Khan E. Phonon, Magnon and Electron Contributions to Low Temperature Specific Heat in Metallic State of $La_{0.85}Sr_{0.15}MnO_3$ and $Er_{0.8}Y_{0.2}MnO_3$ Manganites. *Bulletin of Materials Science*, 2013, v. 36 (7), 1255–1260.
9. Varshney D. and Kaurav N. Analysis of Low Temperature Specific Heat in the Ferromagnetic State of the Ca-doped Manganites. *Eur. Phys. J. B*, 2004, v. 37 (3), 301–309.
10. Carbotte J. P. Properties of Boson-Exchange Superconductors. *Rev. Mod. Phys.*, 1990, v. 62, 1027–1157.
11. Stowe K. An Introduction to Thermodynamics and Statistical Mechanics. Cambridge University Press, The Edinburgh Building, Cambridge CB2 8RU, UK, 2^{nd} edition, 2007, p. 486.

The Dirac Electron and Its Propagator as Viewed in the Planck Vacuum Theory

William C. Daywitt
National Institute for Standards and Technology (retired), Boulder, Colorado, USA
E-mail: wcdaywitt@me.com

This paper examines the covariant Dirac equation and its associated quantum-electrodynamic propagator from the perspective of the Planck vacuum (PV) theory. Calculations reveal: that the PV state is a bifurcated state whose two branches provide the electrons and positrons that, under certain conditions, can be scattered from the PV into free space; that the degenerate collection of Planck-particle cores (that pervade the invisible, negative-energy vacuum state) is responsible for the scattering that takes place in the Huygens principle and the propagator theory; and that the two-term coupling force the electron core exerts on the PV state vanishes at the electron Compton radius, preventing the electron core (and its consequent Dirac electron) from being tethered by the coupling force to the vacuum state, assuring that the electron propagates freely in free space. The paper represents a relativistic addendum to an earlier paper [1] concerning the Schrödinger electron.

1 Introduction

Charge conjugation [2] in the PV theory implies that the invisible vacuum state must be a bifurcated state — bifurcation meaning that at each point in free space there exists a vacuum subspace consisting of the charge doublet $(\pm e_*)^2$ that defines the two vacuum branches

$$e_*^2 = (-e_*)(-e_*) \qquad \text{and} \qquad e_*^2 = (+e_*)(+e_*)\,. \tag{1}$$

The first charge in each branch belongs to the electron or positron and the second charge to the corresponding branch of the subspace. For example, if the first charge $(-e_*)$ in the negative branch on the left belongs to the electron, then the first charge $(+e_*)$ in the positive branch at the right belongs to the positron. In other words, in the PV theory charge conjugation simply switches back and forth between the two branches. The equivalence of the two branches can be seen in the Dirac equation

$$ic\hbar\left(\frac{\partial}{c\partial t} + \boldsymbol{\alpha}\cdot\nabla\right)\psi = mc^2\beta\psi \tag{2}$$

or, using $c\hbar = e_*^2$,

$$\left[i(-e_*)(-e_*)\left(\frac{\partial}{c\partial t} + \boldsymbol{\alpha}\cdot\nabla\right) - mc^2\beta\right]\psi = 0 \tag{3}$$

where the negative branch, the electron branch, is used. The Dirac equation (2) applies to both branches; i.e. the equation works for both the electron and positron. A similar statement can also be made for the equations in (5).

The theoretical foundation [3, 4, 5] of the PV theory rests upon the unification of the Einstein, Newton, and Coulomb superforces:

$$\frac{c^4}{G}\left(= \frac{m_*c^2}{r_*}\right) = \frac{m_*^2G}{r_*^2} = \frac{e_*^2}{r_*^2} \tag{4}$$

where the ratio c^4/G is the curvature superforce that appears in the Einstein field equations. G is Newton's gravitational constant, c is the speed of light, m_* and r_* are the Planck mass and length respectively [6, p.1234], and e_* is the massless bare charge. The fine structure constant is given by the ratio $\alpha = e^2/e_*^2$, where $(-e)$ is the observed electronic charge.

The two particle/PV coupling forces

$$F_c(r) = \frac{e_*^2}{r^2} - \frac{mc^2}{r} \quad \text{and} \quad F_*(r) = \frac{e_*^2}{r^2} - \frac{m_*c^2}{r} \tag{5}$$

the electron core $(-e_*, m)$ and the Planck-particle core $(-e_*, m_*)$ exert on the PV state, along with their coupling constants

$$F_c(r_c) = 0 \quad \text{and} \quad F_*(r_*) = 0 \tag{6}$$

and the resulting Compton radii

$$r_c = \frac{e_*^2}{mc^2} \quad \text{and} \quad r_* = \frac{e_*^2}{m_*c^2} \tag{7}$$

lead to the important string of Compton relations

$$r_cmc^2 = r_*m_*c^2 = e_*^2 \quad (= c\hbar) \tag{8}$$

for the electron and Planck-particle cores, where $\hbar$ is the reduced Planck constant. The electron and Planck particle masses are m and m_* respectively. The vanishing of $F_c(r_c)$ in (6) frees the electron from being tethered to the vacuum state, insuring that the electron propagating in free space behaves as a free particle.

The Planck constant is a secondary constant whose structure can take different forms; e.g.

$$\hbar\,[\text{erg sec}] = r_cmc = r_*m_*c = \left(\frac{e_*^2}{r_*}\right)t_* = m_*c^2t_* \tag{9}$$

that are employed throughout the following text, where t_* $(= r_*/c)$ is the Planck time [6, p.1233]. The products to the right of $\hbar$ relate the electron mass m and Compton radius r_c to the vacuum parameters r_*, m_*, t_*, and e_*^2.

Furthermore, the energy and momentum operators expressed as

$$\widehat{E} = i\hbar\frac{\partial}{\partial t} = i(m_*c^2)t_*\frac{\partial}{\partial t} = i(m_*c^2)r_*\frac{\partial}{c\partial t} \tag{10}$$

and

$$c\,\widehat{\mathbf{p}} = -ic\hbar\nabla = -i(m_*c^2)r_*\nabla = -i(mc^2)r_c\nabla \tag{11}$$

will be used freely in what follows.

Section 2 examines the covariant Dirac equation and the covariant Dirac equation with the electromagnetic interaction included. Results show that the two equations can be totally normalized by the vacuum parameters r_* and m_*c^2 from (8).

Section 3 looks at the relativistic Dirac propagator that provides the foundation for the scattering in the Huygens-principle and the propagator formalisms. The propagator equation is normalized by the vacuum parameters r_* and m_*c from (9).

Section 4 traces the scatterings of the Huygens principle and the propagator theory to the pervaded vacuum space, and indicates how electron-positron pair creation is related to PV charge conjugation.

2 Dirac equation

The manifestly covariant form of the Dirac equation [7, p.90] is

$$\left(i\hbar\gamma^\mu\frac{\partial}{\partial x^\mu}\right)\psi - mc\psi = 0 \tag{12}$$

which, using (9), can be expressed as

$$\left(i\gamma^\mu\frac{r_*\partial}{\partial x^\mu}\right)\psi - \frac{mc}{m_*c}\,\psi = 0 \tag{13}$$

with

$$\frac{\partial}{\partial x^\mu} \equiv \left(\frac{\partial}{c\partial t}, \nabla\right) \tag{14}$$

where ψ is the 4x1 Dirac spinor, [$\mu = 0, 1, 2, 3$], and ∇ is the normal 3-dimensional gradient operator. See Appendix A for the definition of the γ^μ matrices. The summation convention over the two μs in the first terms of (12) and (13) is understood.

The Dirac equation with the electromagnetic interaction included is [7, eqn.5.249]

$$\left[i\hbar\gamma^\mu\frac{\partial}{\partial x^\mu} \pm \frac{e\gamma^\mu A_\mu}{c}\right]\psi - mc\psi = 0 \tag{15}$$

which, using (9), can be reduced to

$$\left[i\gamma^\mu\frac{r_*\partial}{\partial x^\mu} \pm \frac{e\gamma^\mu A_\mu}{m_*c^2}\right]\psi - \frac{mc}{m_*c}\psi = 0 \tag{16}$$

where the minimal-substitution ratio [7, p.90]

$$\pm\frac{e\gamma^\mu A_\mu}{c} \tag{17}$$

represents the relativistic electromagnetic interaction of the charge ($\mp e$) with the 4-potential A_μ.

3 Dirac propagator

The relativistic Dirac propagator $S_F(x', x; A)$ is defined to satisfy the Green-function equation [7, eqn.6.91]

$$\left[\gamma_\mu\left(i\hbar\frac{\partial}{\partial x'_\mu} - \frac{eA^\mu(x')}{c}\right) - mc\right]_{\alpha\lambda} S_{F\lambda\beta}(x', x; A)$$

$$= \delta_{\alpha\beta}\delta^4(x' - x) \tag{18}$$

which reduces to

$$\left[\gamma_\mu\left(i\frac{r_*\partial}{\partial x'_\mu} - \frac{\alpha^{1/2}e_*A^\mu(x')}{m_*c^2}\right) - \frac{mc}{m_*c}\right]_{\alpha\lambda} S_{F\lambda\beta}(x', x; A)$$

$$= \delta_{\alpha\beta}\frac{\delta^4(x' - x)}{m_*c} \tag{19}$$

where $e = \alpha^{1/2}e_*$ is used in the reduction and $\delta_{\alpha\beta}$ is the Kronecker delta. The bracket on the left is dimensionless and the δ^4on the right has the units of "1/spacetime-volume". Thus S_F in (19) has the units "$1/mc$·spacetime-volume".

4 Conclusions and comments

The product m_*c^2 in (8) is the upper limit to elementary-particle mass-energy and r_* is the lower limit to the particle Compton radius. With this in mind, and the fact the normalizers in equations (13), (16), and (19) are m_*c and r_*, it is assumed in the PV theory that the Planck-particle cores ($\pm e_*, m_*$) associated with the two branches in (1) that pervade the PV state are the scatterers that provide the scattering for the Huygens-principle and the propagator formalisms. For example, in (13) r_* normalizes the four spacetime gradients $\partial/\partial x^\mu$ and m_*c normalizes the electron product mc.

Finally, the charge ambiguity in (2) due to (1) allows for the creation of an electron-positron pair [7, fig.6.6],

$$\left[i(-e_*)(-e_*)\left(\frac{\partial}{c\partial t} + \boldsymbol{\alpha}\cdot\nabla\right) - mc^2\beta\right]\psi = 0$$

$$\oplus$$

$$\left[i(+e_*)(+e_*)\left(\frac{\partial}{c\partial t} + \boldsymbol{\alpha}\cdot\nabla\right) - mc^2\beta\right]\psi = 0\,, \tag{20}$$

where the first and second equations are related respectively to the electron and positron branches in (1).

Appendix A: The γ and β matrices

The 4x4 γ, β, and α_i matrices used in the Dirac and propagator theories are defined here: where [7, p.75]

$$\gamma^0 \equiv \beta = \begin{pmatrix} I & 0 \\ 0 & -I \end{pmatrix} \tag{A1}$$

and

$$\gamma^i \equiv \beta\alpha_i = \begin{pmatrix} 0 & \sigma_i \\ -\sigma_i & 0 \end{pmatrix} \tag{A2}$$

and where I is the 2×2 unit matrix and

$$\alpha_i = \begin{pmatrix} 0 & \sigma_i \\ \sigma_i & 0 \end{pmatrix} \tag{A3}$$

where the σ_i are the 2×2 Pauli matrices

$$\sigma_1 = \begin{pmatrix} 0 & 1 \\ 1 & 0 \end{pmatrix}, \quad \sigma_2 = \begin{pmatrix} 0 & -i \\ i & 0 \end{pmatrix}, \quad \sigma_3 = \begin{pmatrix} 1 & 0 \\ 0 & -1 \end{pmatrix} \tag{A4}$$

and $\boldsymbol{\alpha} = (\alpha_1, \alpha_2, \alpha_3)$.

Received on June 26, 2018

References

1. Daywitt W.C. The Planck Vacuum Physics Behind the Huygens Principle and the Propagator Theory for the Schrödinger Electron. *Progress in Physics*, 2018, v. 14, issue 3, 111.
2. Daywitt W.C. Antiparticles and Charge Conjugation in the Planck Vacuum Theory. *Progress in Physics*, 2015, v. 11, issue 4, 311.
3. Davies P. Superforce: the Search for a Grand Unified Theory of Nature. Simon and Schuster, New York, 1984.
4. Daywitt W.C. A Model for Davies' Universal Superforce. *Galilean Electrodynamics*, 2006, v. 5, Sept./Oct., 83.
5. Daywitt W.C. The Trouble with the Equations of Modern Fundamental Physics. American Journal of Modern Physics. Special Issue: "Physics without Higgs and without Supersymmetry". 2016, v. 5, no.1–1, 22. See also www.planckvacuumDOTcom.
6. Carroll B.W., Ostlie A.D. An Introduction to Modern Astrophysics. Addison-Wesley, 2007.
7. Gingrich D.M. Practical Quantum Electrodynamics. CRC Press, 2006.

QED Mass Renormalization, Vacuum Polarization and Self-Energies in the Elastodynamics of the Spacetime Continuum (STCED)

Pierre A. Millette

E-mail: PierreAMillette@alumni.uottawa.ca, Ottawa, Canada

In this paper, we consider the explanation of the Quantum Electrodynamics (QED) phenomena of self-energy, vacuum polarization and mass renormalization provided by the Elastodynamics of the Spacetime Continuum (*STCED*). We note that QED only deals with the *wave* aspect of wave-particle objects, and hence QED only deals with the distortion transverse strain energy $W_\perp$, while the dilatation massive longitudinal strain energy term $W_\parallel$ is not considered. Hence there is no possibility of properly deriving the mass, as QED uses an incomplete description of particle energies at the quantum level. Comparison of QED mass renormalization with *STCED* strain energy shows that the interaction of the particle with the medium or the field, δm, is the transverse strain energy present in the spacetime continuum (or vacuum), essentially a field energy. We provide the strain energy equivalence for QED mass renormalization and self-energies for bosons, quarks and leptons.

1 Introduction

In this paper, we consider the explanation of the Quantum Electrodynamics (QED) phenomena of self-energy, vacuum polarization and mass renormalization provided by the Elastodynamics of the Spacetime Continuum (*STCED*) [1–11]. QED is the well-known relativistic quantum field theory of electromagnetic dynamics (electrodynamics) in which charged particle interactions are described by the exchange of (virtual) photons. QED is a perturbative theory of the electromagnetic quantum vacuum [12], and the virtual particles are introduced as an interpretation of the propagators which appear in the perturbation expansion of vacuum expectation values represented by Feynman diagrams.

In *STCED*, energy propagates in the spacetime continuum (*STC*) as wave-like deformations which can be decomposed into *dilatations* and *distortions*. *Dilatations* involve an invariant change in volume of the spacetime continuum which is the source of the associated rest-mass energy density of the deformation. On the other hand, *distortions* correspond to a change of shape (shearing) of the spacetime continuum without a change in volume and are thus massless. Thus the deformations propagate in the continuum by longitudinal (*dilatation*) and transverse (*distortion*) wave displacements.

This provides a natural explanation for wave-particle duality, with the massless transverse mode corresponding to the wave aspects of the deformations and the massive longitudinal mode corresponding to the particle aspects of the deformations. The rest-mass energy density of the longitudinal mode is given by [1, see Eq.(32)]

$$\rho c^2 = 4\bar{\kappa}_0 \varepsilon \tag{1}$$

where ρ is the rest-mass density, c is the speed of light, $\bar{\kappa}_0$ is the bulk modulus of the *STC* (the resistance of the spacetime continuum to *dilatations*), and ε is the volume dilatation

$$\varepsilon = \varepsilon^{\alpha}{}_{\alpha} \tag{2}$$

which is the trace of the *STC* strain tensor obtained by contraction. The volume dilatation ε is defined as the change in volume per original volume $\Delta V/V$ [13, see pp. 149–152] and is an invariant of the strain tensor, as is the rest-mass energy density. Hence

$$mc^2 = 4\bar{\kappa}_0 \Delta V \tag{3}$$

where m is the mass of the deformation and ΔV is the dilatation change in the spacetime continuum's volume corresponding to mass m. This demonstrates that mass is not independent of the spacetime continuum, but rather mass is part of the spacetime continuum fabric itself.

In *STCED*, $\bar{\lambda}_0$ and $\bar{\mu}_0$ are the Lamé elastic constants of the spacetime continuum: $\bar{\mu}_0$ is the shear modulus (the resistance of the spacetime continuum to *distortions*) and $\bar{\lambda}_0$ is expressed in terms of $\bar{\kappa}_0$, the bulk modulus:

$$\bar{\lambda}_0 = \bar{\kappa}_0 - \bar{\mu}_0/2 \tag{4}$$

in a four-dimensional continuum.

2 Energy in the spacetime continuum

In *STCED*, energy is stored in the spacetime continuum as strain energy [5]. As seen in [1, see Section 8.1], the strain energy density of the spacetime continuum is separated into two terms: the first one expresses the dilatation energy density (the mass longitudinal term) while the second one expresses the distortion energy density (the massless transverse term):

$$\mathcal{E} = \mathcal{E}_\parallel + \mathcal{E}_\perp \tag{5}$$

where

$$\mathcal{E}_\parallel = \frac{1}{2}\,\bar{\kappa}_0 \varepsilon^2 \equiv \frac{1}{32\bar{\kappa}_0}\,\rho^2 c^4\,, \tag{6}$$

ρ is the rest-mass density of the deformation, and

$$\mathcal{E}_\perp = \bar{\mu}_0 e^{\alpha\beta} e_{\alpha\beta} = \frac{1}{4\bar{\mu}_0} t^{\alpha\beta} t_{\alpha\beta}\,, \tag{7}$$

with the strain distortion

$$e^{\alpha\beta} = \varepsilon^{\alpha\beta} - e_s g^{\alpha\beta} \tag{8}$$

and the strain dilatation $e_s = \frac{1}{4}\varepsilon^\alpha{}_\alpha$. Similarly for the stress distortion $t^{\alpha\beta}$ and the stress dilatation t_s. Then the dilatation (massive) strain energy density of the deformation is given by the longitudinal strain energy density (6) and the distortion (massless) strain energy density of the deformation is given by the transverse strain energy density (7).

The strain energy W of the deformation is obtained by integrating (5) over the volume V of the deformation to give

$$W = W_\parallel + W_\perp \tag{9}$$

where $W_\parallel$ is the (massive) longitudinal strain energy of the deformation given by

$$W_\parallel = \int_V \mathcal{E}_\parallel \, \mathrm{d}V \tag{10}$$

and $W_\perp$ is the (massless) transverse distortion strain energy of the deformation given by

$$W_\perp = \int_V \mathcal{E}_\perp \, \mathrm{d}V \tag{11}$$

where the volume element $\mathrm{d}V$ in cylindrical polar coordinates is given by $r\mathrm{d}r\,\mathrm{d}\theta\,\mathrm{d}z$ for a stationary deformation.

3 Quantum particles from STC defects

In [8, 10, 11], we show that quantum particles can be represented as defects in the spacetime continuum, specifically dislocations and disclinations. *Dislocations* are translational deformations, while *disclinations* are rotational deformations. In particular, we consider the simplest quantum particle defect given by the edge dislocation [10].

The strain energy density of a stationary edge dislocation is given by

$$W^E = W^E_\parallel + W^E_\perp\,. \tag{12}$$

The longitudinal strain energy of the edge dislocation $W^E_\parallel$ is given by [10, eq. (8)]

$$W^E_\parallel = \frac{\bar{\kappa}_0}{2\pi}\,\bar{\alpha}_0^2\, b^2\,\ell\,\log\frac{\Lambda}{b_c} \tag{13}$$

where

$$\bar{\alpha}_0 = \frac{\bar{\mu}_0}{2\bar{\mu}_0 + \bar{\lambda}_0}\,, \tag{14}$$

ℓ is the length of the dislocation, b_c is the size of the core of the dislocation, of order b_0, the smallest spacetime Burgers dislocation vector [9] and Λ is a cut-off parameter corresponding to the radial extent of the dislocation, limited by the average distance to its nearest neighbours. In (13), the edge dislocation is along the z-axis with Burgers vector b along the x-axis.

The transverse strain energy $W^E_\perp$ is given by [10, eq. (10)]

$$W^E_\perp = \frac{\bar{\mu}_0}{4\pi}\left(\bar{\alpha}_0^2 + 2\bar{\beta}_0^2\right) b^2\,\ell\,\log\frac{\Lambda}{b_c} \tag{15}$$

where

$$\bar{\beta}_0 = \frac{\bar{\mu}_0 + \bar{\lambda}_0}{2\bar{\mu}_0 + \bar{\lambda}_0} \tag{16}$$

and the other parameters are as defined previously.

4 QED mass renormalization

The basic Feynman diagrams can be seen to represent screw dislocations as photons, edge dislocations as bosons, twist and wedge disclinations as fermions [10], and their interactions. The interaction of defects results from the overlap of the defects' strain energy densities. In QED, the exchange of virtual particles in interactions can be seen to be a perturbation expansion representation of the forces resulting from the overlap of the strain energy densities of the dislocations and disclinations.

Similarly, the phenomena of self-energy and vacuum polarization can be understood to result from the strain energy densities of individual defects. QED again represents this situation as a perturbation expansion of an interaction of a photon with the vacuum (photon self-energy also known as vacuum polarization) or of a particle such as an electron with its field (self-energy). In *STCED*, the perturbative expansions are replaced by finite analytical expressions for the strain energy density of individual screw dislocations as photons, edge dislocations as bosons, twist and wedge disclinations as fermions [10].

Quantum Mechanics and QED only deal with the transverse component of spacetime continuum deformations as they are only concerned with the *wave* aspect of wave-particle duality (see [14] for a discussion of this topic). The energy terms used in QED thus correspond to the transverse strain energy $W^E_\perp$. Hence there is no equivalent dilatation massive longitudinal strain energy term ($W^E_\parallel$) used in QED, and no possibility of properly deriving the mass from the theory, as QED uses an incomplete description of particle energies at the quantum level.

The mass term used in the QED equations is external to and not derived from quantum equations. It is thus found to not correspond to the actual mass of the particle and is characterized instead as the bare mass m_0 [15]. To this mass is added the interaction of the particle with the medium or the field, δm, the result of which m_{qm} is "renormalized" (the value of m_0 and the field corrections are infinite) and replaced with the actual experimental mass m according to

$$m_{qm} = m_0 + \delta m \to m\,. \tag{17}$$

Comparing this equation with (12), we find that

$$\begin{aligned} m &= W^E \\ m_0 &= W^E_{\parallel} = \frac{\bar{\kappa}_0}{2\pi}\,\bar{\alpha}_0^2\, b^2\,\ell\,\log\frac{\Lambda}{b_c} \\ \delta m &= W^E_{\perp} = \frac{\bar{\mu}_0}{4\pi}\left(\bar{\alpha}_0^2 + 2\bar{\beta}_0^2\right) b^2\,\ell\,\log\frac{\Lambda}{b_c}\,. \end{aligned} \tag{18}$$

The interaction of the particle with the medium or the field, δm, is the transverse strain energy present in the spacetime continuum (or vacuum), essentially a field energy.

We note that the bare mass (*i.e.* the massive longitudinal strain energy) and the field correction (*i.e.* the transverse strain energy) are both finite in this approach and there is no need for the subtraction of infinities as both terms are well-behaved. If integrated over all of spacetime, they would be divergent, with the divergence being logarithmic in nature. However, contrary to QED, the strain energies are bounded by the density of defects present in the spacetime continuum, which results in an upperbound to the integral of half the average distance between defects. As mentioned by Hirth [16], this has little impact on the accuracy of the results due to the logarithmic dependence. Hence including the longitudinal dilatation mass density term as derived in *STCED* along with the transverse distortion energy density term in the strain energy density provides the expression for the mass m and eliminates the need for mass renormalization as the theory is developed with the correct mass term.

Eq. (18) applies to massive bosons as shown in [10]. For electrons, we have

$$W^{\ell^3} = W^{\ell^3}_{\parallel} + W^{\ell^3}_{\perp}\,, \tag{19}$$

where the defect in this case is the ℓ^3 twist disclination [10] and where (18) is replaced with the following:

$$\begin{aligned} m &= W^{\ell^3} \\ m_0 &= W^{\ell^3}_{\parallel} = \frac{\bar{\kappa}_0}{6\pi}\,\bar{\alpha}_0^2\left(\Omega_x^2 + \Omega_y^2\right)\ell^3\log\frac{\Lambda}{b_c} \\ \delta m &= W^{\ell^3}_{\perp} = \frac{\bar{\mu}_0}{2\pi}\,\frac{\ell^3}{3}\left[\left(\Omega_x^2 + \Omega_y^2\right)\left(\bar{\alpha}_0^2 + \tfrac{1}{2}\,\bar{\beta}_0^2\right) + \right. \\ &\qquad \left. + 2\,\Omega_x\Omega_y\left(\bar{\alpha}_0^2 - 2\bar{\beta}_0^2\right)\right]\log\frac{\Lambda}{b_c} \end{aligned} \tag{20}$$

where Ω^μ is the spacetime Frank vector. The same considerations as seen previously for bosons apply to (20) due to the logarithmic dependence of the expressions.

For quarks, we have

$$W^W = W^W_{\parallel} + W^W_{\perp} \tag{21}$$

where the defect in this case is the wedge disclination [10]. In most cases $\Lambda \gg b_c$, and we have

$$\begin{aligned} m &= W^W \\ m_0 &= W^W_{\parallel} \simeq \frac{\bar{\kappa}_0}{2\pi}\,\Omega_z^2\,\ell\,\Lambda^2\left[\bar{\alpha}_0^2\,\log^2\Lambda + \right. \\ &\qquad \left. + \bar{\alpha}_0\bar{\gamma}_0\log\Lambda + \tfrac{1}{4}(\bar{\alpha}_0^2 + \bar{\gamma}_0^2)\right] \\ \delta m &= W^W_{\perp} \simeq \frac{\bar{\mu}_0}{4\pi}\,\Omega_z^2\,\ell\,\Lambda^2\left[\bar{\alpha}_0^2\,\log^2\Lambda - \right. \\ &\qquad - \left(\bar{\alpha}_0^2 - 3\bar{\alpha}_0\bar{\beta}_0\right)\log\Lambda + \\ &\qquad \left. + \tfrac{1}{2}\left(\bar{\alpha}_0^2 - 3\bar{\alpha}_0\bar{\beta}_0 + \tfrac{3}{2}\,\bar{\beta}_0^2\right)\right] \end{aligned} \tag{22}$$

where

$$\bar{\gamma}_0 = \frac{\bar{\lambda}_0}{2\bar{\mu}_0 + \bar{\lambda}_0}\,. \tag{23}$$

In this case, both the longitudinal strain energy $W^W_{\parallel}$ and the transverse strain energy $W^W_{\perp}$ are proportional to Λ^2 in the limit $\Lambda \gg b_c$. The parameter Λ is equivalent to the extent of the wedge disclination, and we find that as it becomes more extended, its strain energy is increasing parabolically. This behaviour is similar to that of quarks (confinement). In addition, as shown in [10, see eqs. (16) and (20)], as $\Lambda \to b_c$, the strain energy decreases and tends to 0, again in agreement with the behaviour of quarks (asymptotic freedom).

5 Dislocation self-energy and QED self-energies

The dislocation self-energy is related to the dislocation self-force. The dislocation self-force arises from the force on an element in a dislocation caused by other segments of the *same* dislocation line. This process provides an explanation for the QED self-energies without the need to resort to the emission/absorption of virtual particles. It can be understood, and is particular to, dislocation dynamics as dislocations are defects that extend in the spacetime continuum [16, see p. 131]. Self-energy of a straight-dislocation segment of length L is given by [16, see p. 161]:

$$\begin{aligned} W_{self} = \frac{\bar{\mu}_0}{4\pi}\left((\mathbf{b}\cdot\boldsymbol{\xi})^2 + \frac{\bar{\mu}_0 + \bar{\lambda}_0}{2\bar{\mu}_0 + \bar{\lambda}_0}\,|(\mathbf{b}\times\boldsymbol{\xi})|^2\right)\times \\ \times L\left(\ln\frac{L}{b} - 1\right) \end{aligned} \tag{24}$$

where there is no interaction between two elements of the segment when they are within $\pm b$, or equivalently

$$W_{self} = \frac{\bar{\mu}_0}{4\pi}\left((\mathbf{b}\cdot\boldsymbol{\xi})^2 + \frac{\bar{\mu}_0 + \bar{\lambda}_0}{2\bar{\mu}_0 + \bar{\lambda}_0}\,|(\mathbf{b}\times\boldsymbol{\xi})|^2\right) L\,\ln\frac{L}{eb} \tag{25}$$

where $e = 2.71828...$. These equations provide analytic expressions for the non-perturbative calculation of quantum self energies and interaction energies, and eliminate the need for the virtual particle perturbative approach.

In particular, the pure screw (photon) self-energy

$$W^S_{self} = \frac{\bar\mu_0}{4\pi}\,(\mathbf{b}\cdot\boldsymbol{\xi})^2\,L\left(\ln\frac{L}{b}-1\right) \tag{26}$$

and the pure edge (boson) self-energy

$$W^E_{self} = \frac{\bar\mu_0}{4\pi}\,\frac{\bar\mu_0+\bar\lambda_0}{2\bar\mu_0+\bar\lambda_0}\,|(\mathbf{b}\times\boldsymbol{\xi})|^2\,L\left(\ln\frac{L}{b}-1\right) \tag{27}$$

are obtained from (25), while (25) is also the appropriate equation to use for the dual wave-particle "system".

We can relate (27) to (12) and (18) by evaluating W^E from (12) using (13) and (15):

$$W^E = \frac{b^2}{4\pi}\left[2\bar\kappa_0\bar\alpha_0^2+\bar\mu_0\left(\bar\alpha_0^2+2\bar\beta_0^2\right)\right]\ell\,\log\frac{\Lambda}{b_c}\,. \tag{28}$$

Substituting for $\bar\kappa_0$ from (4), for $\bar\alpha_0$ from (14) and for $\bar\beta_0$ from (16), the factor in square brackets in the above equation becomes

$$[\,] = \frac{\bar\mu_0}{(2\bar\mu_0+\bar\lambda_0)^2}\left(4\bar\mu_0^2+6\bar\mu_0\bar\lambda_0+2\bar\lambda_0^2\right) \tag{29}$$

which can be factored as

$$[\,] = \frac{2\bar\mu_0}{(2\bar\mu_0+\bar\lambda_0)^2}\,(2\bar\mu_0+\bar\lambda_0)(\bar\mu_0+\bar\lambda_0)\,. \tag{30}$$

Substituting back into (28), we obtain

$$W^E_{self} = \frac{1}{2}\,W^E = \frac{\bar\mu_0}{4\pi}\,\frac{\bar\mu_0+\bar\lambda_0}{2\bar\mu_0+\bar\lambda_0}\,b^2\,\ell\,\log\frac{\Lambda}{b_c}\,. \tag{31}$$

As noted in [17, see p. 178], the self-energy and the interaction energies are described by the same equations in the non-singular theory, except that the self-energy is half of the interaction energy. We thus see that the above result (28) is essentially the same as (27) from Hirth [16, see p. 161] except that the log factors are slightly different, but similar in intent ($\log\Lambda/b_c$ compared to $\log\ell/eb$).

Dislocation self energies are thus found to be similar in structure to Quantum Electrodynamics self energies. They are also divergent if integrated over all of spacetime, with the divergence being logarithmic in nature. However, contrary to QED, dislocation self energies are bounded by the density of dislocations present in the spacetime continuum, which results in an upperbound to the integral of half the average distance between dislocations.

For a dislocation loop, as each element $d\mathbf{l}$ of the dislocation loop is acted upon by the forces caused by the stress of the other elements of the dislocation loop, the work done against these corresponds to the self-energy of the dislocation loop. The self-energy of a dislocation loop can be calculated from Eq. (4-44) of [16, see p. 110] to give

$$\begin{aligned} W_{self} &= \frac{\bar\mu_0}{8\pi}\oint_{C_1=C}\oint_{C_2=C}\frac{(\mathbf{b}\cdot d\mathbf{l_1})\,(\mathbf{b}\cdot d\mathbf{l_2})}{R}+\\ &+\frac{\bar\mu_0}{4\pi}\,\frac{\bar\mu_0+\bar\lambda_0}{2\bar\mu_0+\bar\lambda_0}\oint_{C_1=C}\oint_{C_2=C}\frac{(\mathbf{b}\times d\mathbf{l_1})\cdot\mathbf{T}\cdot(\mathbf{b}\times d\mathbf{l_2})}{R} \end{aligned} \tag{32}$$

where $\mathbf{T}$ is as defined in Eq. (4-44) of [16, see p. 110].

The photon self-energy also known as vacuum polarization is obtained from the strain energy density of screw dislocations. The longitudinal strain energy of the screw dislocation $W^S_{\parallel}=0$ as given by [10, eq. (6)] *i.e.* the photon is massless. The photon self-energy is given by half the transverse strain energy of the screw dislocation $W^S_{\perp}$ given by [10, eq. (7)]

$$W^S_{self} = \frac{1}{2}\,W^S_{\perp} = \frac{\bar\mu_0}{8\pi}\,b^2\,\ell\,\log\frac{\Lambda}{b_c} \tag{33}$$

which again includes the $\log\Lambda/b_c$ factor. Comparing this expression with (26) and with (32), we find that (26) is likely off by a factor of 2, being proportional to $1/8\pi$ as per Hirth's (32) and (33), not $1/4\pi$ as given in Hirth's (24) and Hirth's (26).

6 Disclination self-energy and QED self-energies

From dislocation self-energies, we can calculate the photon self-energy (also known as the vacuum polarization) and, in the general case, the boson self-energy.

The fermion self-energies are calculated from the corresponding disclination self-energies, with the lepton self-energy calculated from the interaction energy W^{ℓ^3} of the ℓ^3 twist disclination, the neutrino self-energy calculated from the interaction energy W^{ℓ} of the ℓ twist disclination and the quark self-energy calculated from the interaction energy W^W of the wedge disclination, using the result that self-energy is half of the interaction energy as seen previously in Section 5.

6.1 The ℓ^3 twist disclination self-energy and lepton self-energies

The lepton (electron) self-energy is calculated from the interaction energy W^{ℓ^3} of the ℓ^3 twist disclination by evaluating W^{ℓ^3} from (19) using $W^{\ell^3}_{\parallel}$ and $W^{\ell^3}_{\perp}$ from (20):

$$\begin{aligned} W^{\ell^3} &= \frac{\bar\kappa_0}{6\pi}\,\bar\alpha_0^2\left(\Omega_x^2+\Omega_y^2\right)\ell^3\log\frac{\Lambda}{b_c}+\\ &+\frac{\bar\mu_0}{2\pi}\,\frac{\ell^3}{3}\Big[\left(\Omega_x^2+\Omega_y^2\right)\left(\bar\alpha_0^2+\tfrac{1}{2}\,\bar\beta_0^2\right)+\\ &+2\,\Omega_x\Omega_y\left(\bar\alpha_0^2-2\bar\beta_0^2\right)\Big]\log\frac{\Lambda}{b_c}\,. \end{aligned} \tag{34}$$

Substituting for $\bar\kappa_0$ from (4), for $\bar\alpha_0$ from (14) and for $\bar\beta_0$ from (16), (34) becomes

$$\begin{aligned} W^{\ell^3} &= \frac{\ell^3}{6\pi}\,\frac{\bar\mu_0}{(2\bar\mu_0+\bar\lambda_0)^2}\times\\ &\times\Big[\left(\Omega_x^2+\Omega_y^2\right)\left(2\bar\mu_0^2+2\bar\mu_0\bar\lambda_0+\tfrac{1}{2}\,\bar\lambda_0^2\right)-\\ &-2\,\Omega_x\Omega_y\left(\bar\mu_0^2+4\bar\mu_0\bar\lambda_0+2\bar\lambda_0^2\right)\Big]\log\frac{\Lambda}{b_c} \end{aligned} \tag{35}$$

which can be factored as

$$W^{\ell^3} = \frac{\ell^3}{12\pi}\,\frac{\bar{\mu}_0}{(2\bar{\mu}_0+\bar{\lambda}_0)^2}\left\{\left(\Omega_x^2+\Omega_y^2\right)\left(2\bar{\mu}_0+\bar{\lambda}_0\right)^2 - \right. \\ \left. - 4\Omega_x\Omega_y\left[\left(\bar{\mu}_0+\bar{\lambda}_0\right)\left(\bar{\mu}_0+2\bar{\lambda}_0\right)+\bar{\mu}_0\bar{\lambda}_0\right]\right\}\log\frac{\Lambda}{b_c}. \tag{36}$$

The lepton self-energy is then given by

$$W^{\ell^3}_{self} = \frac{1}{2}\,W^{\ell^3} = \frac{\bar{\mu}_0}{24\pi}\left\{\left(\Omega_x^2+\Omega_y^2\right) - \right. \\ \left. - 4\,\Omega_x\Omega_y\,\frac{\left(\bar{\mu}_0+\bar{\lambda}_0\right)\left(\bar{\mu}_0+2\bar{\lambda}_0\right)+\bar{\mu}_0\bar{\lambda}_0}{(2\bar{\mu}_0+\bar{\lambda}_0)^2}\right\}\ell^3\,\log\frac{\Lambda}{b_c}\,, \tag{37}$$

where we have used the result that self-energy is half of the interaction energy as seen previously in Section 5.

6.2 The ℓ twist disclination self-energy and the neutrino self-energy

The neutrino self-energy is calculated from the strain energy W^ℓ of the ℓ twist disclination. The longitudinal strain energy of the ℓ twist disclination $W^\ell_\parallel = 0$ as given by [10, eq. 33)] *i.e.* the neutrino is massless. In most cases $\Lambda \gg b_c$, and the strain energy W^ℓ of the ℓ twist disclination is given by the transverse strain energy $W^\ell = W^\ell_\perp$ given by [10, eq. (35)]:

$$W^\ell = \frac{\bar{\mu}_0}{2\pi}\,\ell\,\Lambda^2\left[\left(\Omega_x^2+\Omega_y^2\right)\left(\bar{\alpha}_0^2\,\log^2\Lambda+\bar{\alpha}_0\bar{\gamma}_0\,\log\Lambda - \right. \right. \\ \left. \left. - \tfrac{1}{2}\,\bar{\alpha}_0\bar{\gamma}_0\right) - 2\,\Omega_x\Omega_y\left(\bar{\alpha}_0\bar{\beta}_0\log\Lambda+\tfrac{1}{2}\,\bar{\beta}_0\bar{\gamma}_0\right)\right]. \tag{38}$$

Substituting for $\bar{\alpha}_0$ from (14), for $\bar{\beta}_0$ from (16) and for $\bar{\gamma}_0$ from (23), (38) becomes

$$W^\ell = \frac{\bar{\mu}_0}{2\pi}\,\frac{\ell\,\Lambda^2}{(2\bar{\mu}_0+\bar{\lambda}_0)^2}\left\{\left(\Omega_x^2+\Omega_y^2\right)\left[\bar{\mu}_0^2\,\log^2\Lambda+ \right. \right. \\ \left. + \bar{\mu}_0\bar{\lambda}_0\left(\log\Lambda-\tfrac{1}{2}\right)\right] - \\ \left. - 2\,\Omega_x\Omega_y\left[\bar{\mu}_0\left(\bar{\mu}_0+\bar{\lambda}_0\right)\log\Lambda+\tfrac{1}{2}\,\bar{\lambda}_0\left(\bar{\mu}_0+\bar{\lambda}_0\right)\right]\right\}. \tag{39}$$

The neutrino self-energy is then given by

$$W^\ell_{self} = \frac{1}{2}\,W^\ell = \frac{\bar{\mu}_0}{4\pi}\,\frac{\ell\,\Lambda^2}{(2\bar{\mu}_0+\bar{\lambda}_0)^2}\times \\ \times\left\{\left(\Omega_x^2+\Omega_y^2\right)\left[\bar{\mu}_0^2\,\log^2\Lambda+\bar{\mu}_0\bar{\lambda}_0\left(\log\Lambda-\tfrac{1}{2}\right)\right] - \right. \\ \left. - 2\,\Omega_x\Omega_y\left(\bar{\mu}_0+\bar{\lambda}_0\right)\left(\bar{\mu}_0\log\Lambda+\tfrac{1}{2}\,\bar{\lambda}_0\right)\right\} \tag{40}$$

where we have used the result that self-energy is half of the interaction energy as seen previously in Section 5.

6.3 The wedge disclination self-energy and quark self-energies

The quark self-energy is calculated from the interaction energy W^W of the wedge disclination by evaluating W^W from (21) using $W^W_\parallel$ and $W^W_\perp$ from (22). In most cases $\Lambda \gg b_c$, and we have

$$W^W \simeq \frac{\bar{\kappa}_0}{2\pi}\,\Omega_z^2\,\ell\,\Lambda^2\left[\bar{\alpha}_0^2\,\log^2\Lambda+ \right. \\ + \bar{\alpha}_0\bar{\gamma}_0\log\Lambda+\tfrac{1}{4}(\bar{\alpha}_0^2+\bar{\gamma}_0^2)\big]+ \\ + \frac{\bar{\mu}_0}{4\pi}\,\Omega_z^2\,\ell\,\Lambda^2\left[\bar{\alpha}_0^2\,\log^2\Lambda- \right. \\ - \left(\bar{\alpha}_0^2-3\bar{\alpha}_0\bar{\beta}_0\right)\log\Lambda+ \\ \left. + \tfrac{1}{2}\left(\bar{\alpha}_0^2-3\bar{\alpha}_0\bar{\beta}_0+\tfrac{3}{2}\,\bar{\beta}_0^2\right)\right]. \tag{41}$$

Substituting for $\bar{\kappa}_0$ from (4), for $\bar{\alpha}_0$ from (14) for $\bar{\beta}_0$ from (16) and for $\bar{\gamma}_0$ from (23), (41) becomes

$$W^W \simeq \frac{\Omega_z^2}{2\pi}\,\frac{\ell\,\Lambda^2}{(2\bar{\mu}_0+\bar{\lambda}_0)^2}\left[\bar{\mu}_0^2\left(\bar{\mu}_0+\bar{\lambda}_0\right)\log^2\Lambda+ \right. \\ + \bar{\mu}_0\left(\bar{\mu}_0^2+2\bar{\mu}_0\bar{\lambda}_0+\bar{\lambda}_0^2\right)\log\Lambda+ \\ \left. + \tfrac{1}{4}\,\bar{\lambda}_0\left(\bar{\mu}_0^2+2\bar{\mu}_0\bar{\lambda}_0+\bar{\lambda}_0^2\right)\right] \tag{42}$$

which can be factored as

$$W^W \simeq \frac{\Omega_z^2}{2\pi}\,\frac{\ell\,\Lambda^2}{(2\bar{\mu}_0+\bar{\lambda}_0)^2}\left[\bar{\mu}_0^2\left(\bar{\mu}_0+\bar{\lambda}_0\right)\log^2\Lambda+ \right. \\ \left. + \left(\bar{\mu}_0+\bar{\lambda}_0\right)^2\left(\bar{\mu}_0\log\Lambda+\tfrac{1}{4}\,\bar{\lambda}_0\right)\right]. \tag{43}$$

The quark self-energy is then given by

$$W^W_{self} = \frac{1}{2}\,W^W \simeq \frac{\Omega_z^2}{4\pi}\,\frac{(\bar{\mu}_0+\bar{\lambda}_0)^2}{(2\bar{\mu}_0+\bar{\lambda}_0)^2}\,\ell\,\Lambda^2\times \\ \times\left[\frac{\bar{\mu}_0^2}{\bar{\mu}_0+\bar{\lambda}_0}\,\log^2\Lambda+\bar{\mu}_0\log\Lambda+\tfrac{1}{4}\,\bar{\lambda}_0\right] \tag{44}$$

where we have used the result that self-energy is half of the interaction energy as seen previously in Section 5.

7 Discussion and conclusion

In this paper, we have considered how the Elastodynamics of the Spacetime Continuum (*STCED*) explains the Quantum Electrodynamics (QED) phenomena of self-energy, vacuum polarization and mass renormalization. We have noted that QED only deals with the *wave* aspect of wave-particle objects, and hence QED only deals with the distortion transverse strain energy $W^E_\perp$, while the dilatation massive longitudinal strain energy term $W^E_\parallel$ is not considered. Hence there

is no possibility of properly deriving the mass, as QED uses an incomplete description of particle energies at the quantum level.

Comparison of mass renormalization with *STCED* strain energy shows that the interaction of the particle with the medium or the field, δm, is the transverse strain energy present in the spacetime continuum (or vacuum), essentially a field energy. We provide the strain energy equivalence for QED mass renormalization for bosons, leptons and quarks.

Both the bare mass (*i.e.* the massive longitudinal strain energy) and the field correction (*i.e.* the transverse strain energy) are finite in this approach and there is no need for the subtraction of infinities as both terms are well-behaved. Contrary to QED, the strain energies are bounded by the density of defects present in the spacetime continuum, which results in an upperbound to the integral of half the average distance between defects. Hence including the longitudinal dilatation mass density term as derived in *STCED* along with the transverse distortion energy density term in the strain energy density provides the expression for the mass m and eliminates the need for mass renormalization as the theory is developed with the correct mass term. We have also derived the self-energy expressions for bosons including photons, leptons including neutrinos, and quarks.

It is important to note that

1. The expressions derived are for stationary (time independent) defects.
2. The case of time-dependent screw and edge dislocations moving with velocity v is covered in §16.1.2 and §16.2.2 of [11] respectively. The calculations involve integrals of the form

$$\int_y \frac{1}{\alpha y} \arctan\left(\frac{x-vt}{\alpha y}\right) \mathrm{d}y = -\frac{i}{2}\left[\mathrm{Li}_2\left(-i\,\frac{x-vt}{\alpha y}\right) - \mathrm{Li}_2\left(i\,\frac{x-vt}{\alpha y}\right)\right] \tag{45}$$

where

$$\alpha = \sqrt{1-\frac{v^2}{c^2}} \tag{46}$$

and where $\mathrm{Li}_n(x)$ is the polylogarithm function which arises in Feynman diagram integrals. For $n = 2$ and $n = 3$, we have the dilogarithm and the trilogarithm special cases respectively. This is a further indication that the interaction of strain energies are the physical source of quantum interaction phenomena described by Feynman diagrams as discussed in section 4.

The results obtained are found to provide a physical explanation of QED phenomena in terms of the interaction resulting from the overlap of defect strain energies in the spacetime continuum in *STCED*.

Received on July 18, 2018

References

1. Millette P. A. Elastodynamics of the Spacetime Continuum. *The Abraham Zelmanov Journal*, 2012, vol. 5, 221–277.
2. Millette P. A. On the Decomposition of the Spacetime Metric Tensor and of Tensor Fields in Strained Spacetime. *Progress in Physics*, 2012, vol. 8 (4), 5–8.
3. Millette P. A. The Elastodynamics of the Spacetime Continuum as a Framework for Strained Spacetime. *Progress in Physics*, 2013, vol. 9 (1), 55–59.
4. Millette P. A. Derivation of Electromagnetism from the Elastodynamics of the Spacetime Continuum. *Progress in Physics*, 2013, vol. 9 (2), 12–15.
5. Millette P. A. Strain Energy Density in the Elastodynamics of the Spacetime Continuum and the Electromagnetic Field. *Progress in Physics*, 2013, vol. 9 (2), 82–86.
6. Millette P. A. Dilatation–Distortion Decomposition of the Ricci Tensor. *Progress in Physics*, 2013, vol. 9 (4), 32–33.
7. Millette P. A. Wave-Particle Duality in the Elastodynamics of the Spacetime Continuum (STCED). *Progress in Physics*, 2014, vol. 10 (4), 255–258.
8. Millette P. A. Dislocations in the Spacetime Continuum: Framework for Quantum Physics. *Progress in Physics*, 2015, vol. 11 (4), 287–307.
9. Millette P. A. The Burgers Spacetime Dislocation Constant b_0 and the Derivation of Planck's Constant. *Progress in Physics*, 2015, vol. 11 (4), 313–316.
10. Millette P. A. Bosons and Fermions as Dislocations and Disclinations in the Spacetime Continuum. *Progress in Physics*, 2018, vol. 14 (1), 10–18.
11. Millette P. A. Elastodynamics of the Spacetime Continuum: A Spacetime Physics Theory of Gravitation, Electromagnetism and Quantum Physics. American Research Press, Rehoboth, NM, 2017.
12. Milonni P. W. The Quantum Vacuum: An Introduction to Quantum Electrodynamics. Academic Press, San Diego, 1994.
13. Segel L. A. Mathematics Applied to Continuum Mechanics. Dover Publications, New York, 1987.
14. Millette P. A. On the Classical Scaling of Quantum Entanglement. *Progress in Physics*, 2018, vol. 14 (3), 121–130.
15. Schweber S. S. An Introduction to Relativistic Quantum Field Theory. Dover Publications, Mineola, NY, (1962), 2005, pp. 510–511.
16. Hirth R. M. and Lothe J. Theory of Dislocations, 2nd ed. Krieger Publishing Co., Florida, 1982.
17. Bulatov V. V. and Cai W. Computer Simulation of Dislocations. Oxford University Press, Oxford, 2006.

The Nature of the Electron and Proton as Viewed in the Planck Vacuum Theory

William C. Daywitt

National Institute for Standards and Technology (retired), Boulder, Colorado. E-mail: wcdaywitt@me.com

There is a long-standing question whether or not the proton obeys the Dirac equation. The following calculations answer that question in the affirmative. The paper argues that, even though the proton has an internal structure, unlike the electron, it is still a Dirac particle in the sense that it obeys the same Dirac equation

$$\pm\left[ie_*^2\gamma^\mu\frac{\partial}{\partial x^\mu}-mc^2\right]\psi=0$$

as the electron, where the upper and lower signs refer to the electron and proton respectively with their masses m_e and m_p. Calculations readily show why the proton mass is orders-of-magnitude greater than the electron mass, and suggest that the constant 1836 can be thought of as the 'proton structure constant'.

1 Introduction

The electron is assumed to be a structureless particle [1, p.82] that obeys the Dirac equation; so it is somewhat surprising that the structured proton also obeys that same equation. The reason for this apparent conundrum is tied to the nature of the Planck vacuum (PV) state itself [2].

The manifestly covariant form of the Dirac equation [1, p.90] is

$$\left[i\hbar\gamma^\mu\frac{\partial}{\partial x^\mu}-mc\right]\psi=0 \tag{1}$$

which, using $c\hbar=e_*^2$, can be expressed as

$$\left[ie_*^2\gamma^\mu\frac{\partial}{\partial x^\mu}-mc^2\right]\psi=0 \tag{2}$$

with

$$\frac{\partial}{\partial x^\mu}\equiv\left(\frac{\partial}{c\partial t}\,,\ \nabla\right) \tag{3}$$

where ψ is the 4x1 Dirac spinor, $[\mu=0,1,2,3]$, and ∇ is the normal 3-dimensional gradient operator. See Appendix A for the definition of the γ^μ matrices. The summation convention over the two μs in the first terms of (1) and (2) is understood.

The two particle/PV coupling forces [3]

$$F_e(r)=\frac{e_*^2}{r^2}-\frac{m_ec^2}{r}\quad\text{and}\quad F_p(r)=\frac{e_*^2}{r^2}-\frac{m_pc^2}{r} \tag{4}$$

the electron and proton cores $(-e_*,m_e)$ and $(+e_*,m_p)$ exert on the PV state, along with their coupling constants

$$F_e(r_e)=0\quad\text{and}\quad F_p(r_p)=0 \tag{5}$$

and the resulting Compton radii

$$r_e=\frac{e_*^2}{m_ec^2}\quad\text{and}\quad r_p=\frac{e_*^2}{m_pc^2} \tag{6}$$

lead to the important string of Compton relations

$$r_em_ec^2=r_pm_pc^2=e_*^2=r_*m_*c^2\quad(=c\hbar) \tag{7}$$

where $\hbar$ is the reduced Planck constant. The electron and proton masses are m_e and m_p respectively. The vanishing of $F_e(r_e)$ and $F_p(r_p)$ in (5) frees the electron and proton from being tethered by their coupling forces to the vacuum state, insuring that both particles propagate in free space as free particles. The Planck particle mass and Compton radius are m_* and r_*.

2 Electron and positron

The Dirac electron equation from (2) with the positive sign from the abstract leads to [3]

$$\left[i(-e_*)(-e_*)\gamma^\mu\frac{\partial}{\partial x^\mu}-m_ec^2\right]\psi=0 \tag{8}$$

where the first charge $(-e_*)$ comes from the electron core, and the second charge $(-e_*)$ from any one of the Planck-particle cores in the negative branch of the PV state (Appendix B).

Charge conjugation of (8) then leads to the positron equation

$$\left[i(+e_*)(+e_*)\gamma^\mu\frac{\partial}{\partial x^\mu}-m_ec^2\right]\psi=0\,. \tag{9}$$

where the first charge $(+e_*)$ comes from the positron core $(+e_*,m_e)$, and the second charge $(+e_*)$ from any one of the Planck-particle cores in the positive branch of the PV state.

3 Proton and antiproton

The proton equation from the preceding abstract

$$-\left[ie_*^2\gamma^\mu\frac{\partial}{\partial x^\mu}-m_pc^2\right]\psi=0 \tag{10}$$

can be expressed as

$$\left[i(+e_*)(-e_*)\gamma^\mu\frac{\partial}{\partial x^\mu}+m_pc^2\right]\psi=0 \tag{11}$$

where the first charge $(+e_*)$ comes from the proton core, and the second charge $(-e_*)$ from any one of the Planck-particle cores in the negative branch of the PV state.

Charge conjugation of (11) then leads to the antiproton equation

$$\left[i(-e_*)(+e_*)\gamma^\mu \frac{\partial}{\partial x^\mu} + m_p c^2\right]\psi = 0 \qquad (12)$$

where the first charge $(-e_*)$ comes from the antiproton core $(-e_*, m_p)$, and the second charge $(+e_*)$ from any one of the Planck-particle cores in the positive branch of the PV state.

4 Proton structure

The reason for the proton structure is easily seen from the nature of the charge products in equations (8) and (9), as opposed to those in equations (11) and (12). In (8) and (9) both products yield a positive e_*^2, signifying that the electron and positron charges repel their corresponding degenerate collection of PV charges (Appendix B); isolating the characteristics of the electron/positron from the PV state.

In (11) and (12), however, things are reversed. Both products yield a negative e_*^2, signifying that the proton and antiproton charges are attracting their corresponding degenerate collection of PV charges; converting a small portion of the PV energy into the proton and antiproton states, elevating the proton/antiproton masses orders-of-magnitude over those of the electron/positron masses.

5 Conclusions and comments

From (7) the mass energies of the electron and proton are [2]

$$m_e c^2 = \frac{e_*^2}{r_e} \qquad \text{and} \qquad m_p c^2 = \frac{e_*^2}{r_p} \qquad (13)$$

which lead to

$$m_p = \frac{r_e}{r_p} \cdot m_e \qquad (14)$$

where the ratio $r_e/r_p \approx 1836$. Thus, since m_e is assumed to be structureless, (14) suggests that the constant 1836 can be thought of as the 'proton structure constant'.

Finally, in the PV theory the so-called structure appears in the proton rest frame as a small spherical 'collar' surrounding the proton core [5].

Appendix A: The γ and β matrices

The 4x4 γ, β, and α_i matrices used in the Dirac theory are defined here: where [1, p.91]

$$\gamma^0 \equiv \beta = \begin{pmatrix} I & 0 \\ 0 & -I \end{pmatrix} \qquad (A1)$$

and $(i = 1, 2, 3)$

$$\gamma^i \equiv \beta\alpha_i = \begin{pmatrix} 0 & \sigma_i \\ -\sigma_i & 0 \end{pmatrix} \qquad (A2)$$

and where I is the 2x2 unit matrix and

$$\alpha_i = \begin{pmatrix} 0 & \sigma_i \\ \sigma_i & 0 \end{pmatrix} \qquad (A3)$$

where the σ_i are the 2x2 Pauli spin matrices

$$\sigma_1 = \begin{pmatrix} 0 & 1 \\ 1 & 0 \end{pmatrix}, \sigma_2 = \begin{pmatrix} 0 & -i \\ i & 0 \end{pmatrix}, \sigma_3 = \begin{pmatrix} 1 & 0 \\ 0 & -1 \end{pmatrix} \qquad (A4)$$

and $\boldsymbol{\alpha} = (\alpha_1, \alpha_2, \alpha_3)$.

Appendix B: Charge conjugation

Charge conjugation [4] in the PV theory implies that the invisible vacuum state must be a bifurcated state—bifurcation meaning that at each point in free space there exists a vacuum subspace consisting of the charge doublet $(\pm e_*)^2$ that leads to two vacuum branches

$$e_*^2 = (-e_*)(-e_*) \qquad \text{and} \qquad e_*^2 = (+e_*)(+e_*) \qquad (B1)$$

where, by definition, the second charge in each product defines the branch. The first charge in each branch belongs to the electron or positron. For example, if the first charge $(-e_*)$ in the negative branch on the left belongs to the electron, then the first charge $(+e_*)$ in the positive branch at the right belongs to the positron. In the PV theory charge conjugation simply switches back and forth between the two PV branches, which amounts to changing the signs in the four products $(\pm e_*)(\pm e_*)$. For example, if C is the charge conjugation operator, then

$$C(\pm e_*)(\pm e_*) = (\mp e_*)(\mp e_*)\,. \qquad (B2)$$

In the proton case (the negative sign in the abstract)

$$-e_*^2 = (+e_*)(-e_*) \quad \text{and} \quad -e_*^2 = (-e_*)(+e_*) \qquad (B3)$$

where the first charge on the left belongs to the proton and the first charge on the right belongs to the antiproton. Again, the second charge in each product defines the branch.

Submitted on July 19, 2018

References

1. Gingrich D.M. Practical Quantum Electrodynamics. CRC, The Taylor & Francis Group, Boca Raton, London, New York, 2006.
2. Daywitt W.C. The Trouble with the Equations of Modern Fundamental Physics. American Journal of Modern Physics. Special Issue: "Physics without Higgs and without Supersymmetry". 2016, v. 5, no.1-1, 22. See also www.planckvacuumDOTcom.
3. Daywitt W.C. The Dirac Electron and Its Propagator as Viewed in the Planck Vacuum Theory. *Progress in Physics*, 2018, Issue 4, v. 14, 194.
4. Daywitt W.C. Antiparticles and Charge Conjugation in the Planck Vacuum Theory. *Progress in Physics*, 2015, Issue 11, v. 4, 311.
5. Daywitt W.C. A Planck Vacuum Pilot Model for Inelastic Electron-Proton Scattering. *Progress in Physics*, 2015, Issue 4, v. 11, 308.

Theory of Anomalous Magnetic Moment and Lamb Shift of Extended Electron in Stochastic Electrodynamics

Muralidhar Kundeti[1], Prasad M. B. Rajendra[2]

[1] B-74, Kendriya Vihar, Gachibowli, Hyderabad-500032, India. E-mail: kundetimuralidhar@gmail.com
[2] Physics Department, National Defence Academy, Khadakwasla, Pune-411023, India. E-mail: rajendraprasadmb75@gmail.com

The very presence of zero-point field allows us to consider the structure of the electron with center of charge in circular motion around center of mass. Considering extended electron structure in stochastic electrodynamics, mass and charge corrections are derived without any logarithmic divergence terms. Using these corrections, the anomalous magnetic moment of the electron has been expressed in a series as a function of fine-structure constant. The evaluated magnetic moment is found to be accurate up to ninth decimal place with a difference of 90.22×10^{-12} from the experimental value. In the case of an orbital electron, due to its motion, the surrounding zero-point field is modified and the zero-point energy associated with these modifications leads to a shift in the energy level. By imposing a cut-off frequency equal to the de Broglie frequency, the zero-point energy associated with the orbital electron is attributed to the Lamb shift. The estimated Lamb shift in hydrogen atom is found to be in agreement with the experimental value. These theoretical derivations give a new classical approach to both the anomalous magnetic moment of the electron and the Lamb shift.

1 Introduction

An electron is visualized as a point particle in both quantum mechanics and quantum field theories in general. Efforts to find the size of the electron have led to a very small size $\sim 10^{-20}$ m in high energy scattering experiments [1] and in the penning trap experiment, the finite size effect was considered to be of the order of experimental uncertainty in the measurement of the anomalous magnetic moment of the electron. Thus any sub-structure of the electron is ruled out in quantum field theories and the particles are treated as point particles without any size. The point particle limit of the electron, in most of the theoretical approaches is fine and excellent except for the singularity syndrome and any cut-off procedure leads to a finite structure of the electron.

The concept of an extended structure of the electron originates from the zitterbewegung motion (rapid oscillations of Dirac electron) and such random oscillations are invariably attributed to the presence of zero-point field throughout the universe. The extended electron theories were developed over several decades [2–10] and the perception of point particle having charge and mass or rigid sphere with charge distribution was denied and the structure of the electron had been considered with the charge in an average circular motion about the center of mass. While dealing with extended electron models, a natural question arises that why such extended structure is not detected in scattering experiments. The reason being the charge rotation is at the speed of light and therefore, it cannot be detected at all. However, the footprints of such extended electron can be seen from the recent detection of the de Broglie wave of the electron in the scattering of a beam of electrons in thin silicon crystal [11] and from the high resolution scanning tunneling microscopy images [12].

Recently, the role of spin and the internal electron structure in complex vector formalism was studied by the author [13–15] and it had been shown that the mass of the particle may be interpreted to the zero-point field energy associated with the local complex rotation or oscillation confined in a region of space of the order of the Compton wavelength. Further, the logical classical foundations of quantum mechanics were explored from the consideration of extended electron structure [16, 17]. It is of particular interest whether the calculations of the electron magnetic moment and Lamb shift are possible with the extended electron theories.

In the charge shell model of the electron, Puthoff [18] has shown that the zero-point energy of the particle is equal to the Coulomb energy in the limit when the shell radius tends to zero. The zero-point energy within the shell was found to be proportional to the fine-structure constant. Therefore, it may be expected that the zero-point energy associated with an electron in the point particle limit may be attributed to the charge correction rather than any mass correction which was considered earlier in the stochastic electrodynamics theories.

In stochastic electrodynamics (classical electrodynamics along with zero-point field), a charged point particle is considered as an oscillator and its equation of motion is given by the Brafford-Marshall equation which is simply the Abraham-Lorentz equation with zero-point field. In the stochastic electrodynamics approach, the energy of the electron oscillator was estimated by Boyer [19] and without imposing any cut-off frequency the zero-point energy of the oscillator was found to be $\hbar\omega_0/2$ per mode, where ω_0 and $\hbar$ are the oscillator frequency and reduced Planck constant respectively. Though many quantum phenomena were explained in the stochastic electrodynamics approach, the theory was found to be incom-

plete [20]. However, it has been found that the introduction of spin into the problem leaves the theory to overcome such failures. The detailed discussion of stochastic electrodynamics with spin was given by Cavelleri *et al* [21] and in this theory, the electron has an extended structure. In view of the extended electron structure, one can impose a cut-off frequency ω_0 and in that case, in the absence of radiation damping and binding terms, the energy associated with the electron has been derived in Section 2.

In the point particle limit, the energy associated with the electron is found to be

$$\Delta E_0 = \frac{2\alpha}{3\pi}\hbar\omega_0\,, \tag{1}$$

where $\alpha = (1/4\pi\epsilon_0)(e^2/\hbar c)$ is the fine-structure constant and $-e$ is the electron charge. This energy may be attributed to the charge correction and the ratio $\Delta E_0/\hbar\omega_0$ corresponds to a correction to fine-structure constant due to interaction of random zero-point field fluctuations. In general, the effective or observed fine-structure constant can be expressed by the relation $\alpha_{obs} \to \alpha_{th} + \Delta\alpha$. Now, the ratio $\Delta\alpha/\alpha$ can be expressed in the following form:

$$\frac{\Delta\alpha}{\alpha} = \frac{\Delta E_c}{\hbar\omega_0} = \frac{2\alpha}{3\pi}\,. \tag{2}$$

In quantum electrodynamics such charge correction was calculated considering the vacuum polarization and it may be noted that the above estimate gives a similar result except for the diverging logarithmic term. The incorporation of this charge correction leads to a replacement of fine-structure constant in the theoretical calculations by $\alpha\,(1 - 2\alpha/3\pi)$.

The total energy of the electron immersed in the zero-point field can be expressed by substituting $\left(\mathbf{p} - e\mathbf{A}_{zp}/c\right)$ for momentum in the relation $E^2 = p^2c^2 + m^2c^4$ [15]:

$$E^2 = p^2c^2 - 2ec\mathbf{p}.\mathbf{A}_{zp} + e^2A_{zp}^2 + m^2c^4, \tag{3}$$

where $\mathbf{A}_{zp}$ is the electromagnetic vector potential of zero-point field. The energy in the last two terms in the above equation can be written in the form $E_0 = mc^2 + e^2A_{zp}^2/2mc^2$. Thus under the influence of zero-point field, there appears a correction to mass and such correction to mass must be of the order of fine-structure constant. The derivation of such mass correction of extended electron in stochastic electrodynamics is given in Section 2. We find that the mass correction Δm depends on the reduced particle velocity $\beta = \mathbf{v}/c$ and the ratio $\Delta m/m$ is expressed by the relation

$$\frac{\Delta m}{m} = \frac{\alpha}{2\pi}\left(1 + \beta^2\right). \tag{4}$$

From the knowledge of mass and charge corrections, the anomalous magnetic moment a_e of the electron is estimated in Section 3.

Under the influence of central Coulomb potential, an orbital electron moves with a velocity proportional to the fine structure constant. When the electron moves in the zero-point field, it induces certain modifications in the surrounding zero-point field. Since these zero-point field modifications may be considered at least of the order of the de Broglie wavelength, the energy associated with the shift in the electron energy levels can be obtained by imposing a cut-off frequency equal to the de Broglie frequency ω_B and the derived zero-point energy is attributed to the Lamb shift. The derivation of Lamb shift and its calculation are given in Section 4. The energy shift in the electron circular orbit is found to be

$$\Delta E_L = \frac{4\alpha^5}{3\pi}m_rc^2, \tag{5}$$

where $m_r = mM/(m + M)$ is the reduced mass and M is the nuclear mass. The calculation of the Lamb shift has been performed using charge correction in the Coulomb field and the mass correction for the electron. Finally, the conclusions are presented in Section 5. The derived formulas elucidate a complete classical approach to both the anomalous magnetic moment of the electron and the Lamb shift.

2 Zero-point energy associated with an extended electron

When an electron moves in the zero-point field, we mean that the center of mass moves with velocity $\mathbf{v}$. The particle motion then contains both internal rotational motion and the translational motion. Denoting the center of mass motion by a position vector $\mathbf{x}$ and the radius of internal rotation by a vector ξ, a complex vector connected with both internal and translational motions of an extended electron can be expressed by a complex vector $X = \mathbf{x} + \mathbf{i}\xi$, where $\mathbf{i}$ is a pseudoscalar representing an oriented volume in geometric algebra. A complete account of complex vector algebra was elaborately discussed in the reference [14].

In stochastic electrodynamics, the expression for the electric field vector of electromagnetic zero-point field can be written in the following form

$$E_{zp}(\mathbf{x},t) = Re\left\{\sum_{\lambda=1}^{2}\int d^3k\,\epsilon(\mathbf{k},\lambda)\,\frac{H(\omega)}{2}\times \times\left[ae^{i(\mathbf{k}.\mathbf{x}-\omega t)} + a^*e^{-i(\mathbf{k}.\mathbf{x}-\omega t)}\right]\right\}, \tag{6}$$

where $\epsilon(\mathbf{k},\lambda)$ is the polarization vector which is a function of wave vector $\mathbf{k}$, polarization index $\lambda = 1, 2$ and $Re\{\}$ represents the real part. We define $a = e^{i\theta(\mathbf{k},\lambda)}$ and $a^* = e^{-i\theta(\mathbf{k},\lambda)}$ and the phase angle is introduced to generate random fluctuations of the zero-point field. The normalization constant in (6) is set equal to unity. The spectral function $H(\omega)$ represents the magnitude of zero-point energy and in stochastic electrodynamics its value is found to be $\left(\hbar\omega/8\pi^3\epsilon_0\right)^{1/2}$. In the

complex vector formalism, we replace $\mathbf{x}$ by X in the electric field $E_{zp}(\mathbf{x}, t)$ and expanding in terms of Taylor series yields

$$E_{zp}(X,t) = E_{zp}(\mathbf{x},t) + \mathbf{i}\xi \left.\frac{\partial E_{zp}(\mathbf{x},t)}{\partial x}\right|_{x\to 0} - \frac{\xi^2}{2}\left.\frac{\partial^2 E_{zp}(\mathbf{x},t)}{\partial x^2}\right|_{x\to 0} + O(\xi^3) + \dots \tag{7}$$

Neglecting higher order terms and denoting

$$E_{zp}(\xi,t) = \xi \left.\frac{\partial E_{zp}(\mathbf{x},t)}{\partial x}\right|_{x\to 0}, \tag{8}$$

one can express the electric field vector in a complex form

$$E_{zp}(X,t) = E_{zp}(\mathbf{x},t) + \mathbf{i}E_{zp}(\xi,t)\,. \tag{9}$$

The random zero-point fluctuations influence both the center of mass and the center of charge and therefore the force acting on the extended particle can be decomposed into force acting on center of charge and force acting on center of mass. The equation of motion of center of mass is then expressed in the form

$$m\ddot{\mathbf{x}} - \Gamma_a m\dddot{\mathbf{v}} + m\omega_0^2\mathbf{x} = eE_z p(\mathbf{x},t), \tag{10}$$

where $\mathbf{v} = \dot{\mathbf{x}}$, $\Gamma_a = 2e^2/3mc^3$ and an over dot represents differentiation with respect to time. The second and third terms on the left are radiation damping and binding terms. It should be noted that for the zero-point field acting on center of mass, both particle charge and mass appear at the center of mass point. On the other hand, for the field acting on the center of charge, the effective mass seen by the zero-point field is the potential equal to $e^2/2\xi \sim m_z c^2$, where m_z is the effective mass at the center of charge and the magnitude of ξ is of the order of the Compton wavelength. In this case both radiation damping and binding forces are absent and the equation of motion of center of charge can be written in the form

$$m_z\ddot{\xi} = eE_{zp}(\xi,t)\,. \tag{11}$$

The average zero-point energy of the electron in its rest frame was previously estimated and it had been shown to be equivalent to the zitterbewegung energy [15]. Further, it was shown that the particle mass arises from the internal complex rotations and a relation between particle spin and mass had been derived previously in the following form [13]:

$$mc^2 = \Omega_s \cdot S \tag{12}$$

In the above equation, S is the spin bivector, Ω_s is the angular frequency bivector and it shows that the mass of an electron is equal to the zero-point energy associated with the local complex rotation in the spin plane.

In the case of center of mass motion of the particle with velocity $\mathbf{v}$, as a result of super position of internal complex rotations on translational motion, the particle is associated with a modulated wave containing internal high frequency ω_0 and envelop frequency ω_B which is the de Broglie frequency of the particle. Differentiating the position complex vector $X = \mathbf{x} + \mathbf{i}\xi$ with respect to time gives the velocity complex vector $U = \mathbf{v} + \mathbf{iu}$ and the complex conjugate of U is obtained by taking reversion operation on it, $\bar{U} = \mathbf{v} - \mathbf{iu}$ and the product $U\bar{U} = v^2 + u^2$ [13]. Dividing this equation throughout by ξ^2 and denoting $\omega_B = |v|/\xi$, $\omega_0 = |u|/\xi$ and $\omega_c = |U|/\xi$, we obtain the effective cut-off frequency ω_c of the modulated wave in the particle frame of reference in the form $\omega_c^2 = \omega_0^2 + \omega_B^2 = \omega_0^2(1+\beta^2)$. In the equation of motion of center of mass (9), the strength of radiation damping and binding terms are much smaller than the force term on the right. Therefore, neglecting radiation damping and binding terms in (10) and integrating the expression with respect to time gives

$$\dot{\mathbf{x}} = \frac{e}{m}\int_0^\tau E_{zp}(\mathbf{x},t)\,dt, \tag{13}$$

where the upper limit of integration is chosen to be the characteristic time $\tau = 2\pi/\omega_c$. Substituting the electric field vector $E_{zp}(\mathbf{x}, t)$ given in (6) into (13) and performing the integration gives

$$\dot{\mathbf{x}} = \frac{e}{m}\sum_{\lambda=1}^{2}\int d^3k\epsilon(\mathbf{k},\lambda)\frac{H(\omega)}{2} \times \left\{ae^{i\mathbf{k}.\mathbf{x}}\left(\frac{e^{-i\omega\tau}-1}{-i\omega}\right) + a^* e^{-i\mathbf{k}.\mathbf{x}}\left(\frac{e^{i\omega\tau}-1}{i\omega}\right)\right\}. \tag{14}$$

Now, using $|\dot{\mathbf{x}}|^2 = \dot{\mathbf{x}}\dot{\mathbf{x}}^*$, we find

$$|\dot{\mathbf{x}}|^2 = \frac{e^2}{m^2}\sum_{\lambda,\lambda'=1}^{2}\iint d^3k d^3k'\epsilon(\mathbf{k},\lambda)\epsilon(\mathbf{k}',\lambda')\frac{H^2(\omega)}{2\omega^2} \times (1-\cos\omega\tau)\left\{aa^{*\prime}e^{-i(\mathbf{k}-\mathbf{k}').\mathbf{x}} + a^*a'e^{i(\mathbf{k}-\mathbf{k}').\mathbf{x}}\right\}, \tag{15}$$

where the terms containing aa' and $a^*a^{*\prime}$ are dropped because of their stochastic averages are zero. Taking the stochastic average of (15) on both sides and using the following relations

$$\left\langle aa^{*\prime}e^{-(\mathbf{k}-\mathbf{k}').\mathbf{x}}\right\rangle = \left\langle a^*a'e^{+(\mathbf{k}-\mathbf{k}').\mathbf{x}}\right\rangle = \delta^3(k-k')\,\delta(\lambda-\lambda')\,,$$

$$\left\langle \sum_{\lambda,\lambda'=1}^{2}\epsilon(\mathbf{k},\lambda)\epsilon(\mathbf{k},\lambda')\delta(\lambda-\lambda')\right\rangle = \left\langle\sum_{\lambda=1}^{2}|\epsilon(\mathbf{k},\lambda)|^2\right\rangle = 1 - \frac{k_x^2}{k^2} = \frac{2}{3}\,,$$

$$\int d^3k = \int d\Omega\,k^2dk = 4\pi\int k^2dk = \frac{4\pi}{c^3}\int\omega^2d\omega\,,$$

the average value $\langle|\dot{\mathbf{x}}|^2\rangle$ is found to be

$$\langle|\dot{\mathbf{x}}|^2\rangle = \frac{4\alpha}{3\pi}\frac{\hbar^2}{m^2c^2}\int_0^{\omega_c}\omega(1-\cos\omega\tau)d\omega\,, \tag{16}$$

where the upper limit of integration is the chosen cut-off frequency ω_c. Because of this cut-off frequency, the zero-point field spectral components of wavelength of the order of $2\pi c/\omega_c$ are only effective and thus there exists an upper bound to the energy available from the electromagnetic zero-point field. For an extended particle of radius R, a convergence form factor can be obtained by finding the upper bound to the energy available from the electromagnetic zero-point field. A detailed calculation of such convergence form factor was calculated by Reuda [22]. This convergence form factor is given by

$$\eta(\omega) = \eta(\delta) = \frac{9}{\delta^4}\left(\frac{\sin\delta}{\delta}\right)^2\left(\frac{\sin\delta}{\delta} - \cos\delta\right)^2, \qquad (17)$$

where $\delta = \omega R/c$ and the values of $\eta(\delta)$ lie in the range 0 to 1. For $\omega \sim \omega_0$ and $R \sim 2\hbar/3mc$, we have $\delta \sim 2/3$ and the convergence form factor $\eta(2/3) \sim 3/4$. In view of the extended structure of the particle, the convergence form factor is introduced in the energy calculation. In general, the total energy of an oscillator is a sum of both kinetic and potential energies and it is equal to twice the kinetic energy. Now, the zero-point energy associated with the particle is expressed in the form

$$\Delta E_c = m\langle|\dot{\mathbf{x}}|^2\rangle = \frac{2\alpha}{3\pi}\frac{\hbar^2\omega_c^2}{mc^2}\eta(\omega_c) \times\left[1 + \frac{2}{\omega_c^2\tau^2}(1 - \cos\omega_c\tau - \omega_c\tau\sin\omega_c\tau)\right]. \qquad (18)$$

Substituting $\omega_c\tau = 2\pi$, $\omega_c^2 = \omega_0^2(1+\beta^2)$, using the Einstein de Broglie relation $\hbar\omega_0 = mc^2$ and approximating $\eta(\omega_c) \sim 3/4$ in (18) gives finally

$$\Delta E_c = \frac{\alpha}{2\pi}mc^2(1+\beta^2). \qquad (19)$$

This energy change gives the correction to the mass, $\Delta m = \Delta E_c/c^2$ and we get the relation (4). The result in (19) differs from our previous calculation in reference [15] by the term $(1+\beta^2)$, where we have assumed $\omega_c = \omega_0$. It may be noted that the energy associated with the particle derived in (19) depends on the particle velocity. However, in the point particle limit, $R \to 0$, $\omega_c \to \omega_0$ and $\eta(\omega_0 R/c) \to 1$. Thus in the point particle limit the energy in (18) reduces to the expression (1). It may be noted that both mass correction and charge correction are derived from the common origin zero-point field.

3 Estimation of the anomalous magnetic moment

Dirac theory of the electron predicts the magnetic moment of the electron $g = 2$. However, a small deviation of magnetic moment $a_e = (g-2)/2$ is known as the anomalous magnetic moment and it was discovered by Kusch and Foley [23]. The quantization of electromagnetic field led to quantum electrodynamics and the first theoretical calculation of a_e in the purview of quantum electrodynamics was due to Schwinger [24] and it was estimated to be $a_e = \alpha/2\pi$. The quantum electrodynamics theoretical calculations of a_e almost over fifty years by several authors showed an excellent agreement between theory and experiment and an extensive review of a_e was given by Kinoshita [25]. High precession penning trap measurements of a_e were done by several authors and a recent measurement of a_e was given by Henneke *et al.* [26], $a_e(exp) = 1.15965218073(28)\times10^{-3}$. In this section we shall explore an entirely different classical approach for the calculation of a_e.

Any change in the mass of the particle due to particle motion in the fluctuating zero-point field brings a change in the spin angular frequency in (12).

$$(m + \Delta m)c^2 = \Omega\cdot S\,. \qquad (20)$$

Combining (12) and (20) gives the ratio

$$\frac{\Delta m}{m} = \left|\frac{\Omega - \Omega_s}{\Omega_s}\right|. \qquad (21)$$

The ratio of change in spin frequency to the spin frequency represents the anomalous magnetic moment. In an alternative way, this can be arrived by considering the energy term $(ge\mathbf{B}/2mc)\cdot S$ and identifying m as the theoretical mass and replacing $m_{th} = m_{obs} - \Delta m$. To a first approximation we get $g/2\,(1 + \Delta m/m)$ in place of $g/2$. Now, from (4) the anomalous magnetic moment of the electron can be expressed in the form

$$a_e = \frac{\Delta m}{m} = \frac{\alpha}{2\pi} + \frac{\alpha}{2\pi}\beta^2\,. \qquad (22)$$

The first term on right of the above equation gives the well known Schwinger's result and to obtain this result we have chosen $\eta(\omega_c) \sim 3/4$ in (18). The velocity of an orbital electron in an atom is proportional to α. For a linear motion of the electron we approximate $\beta^2 = \alpha^2/3$ and to account for two modes of polarization of zero-point field, it is multiplied by 2. The reduced velocity is now written in the form $\beta^2 = 2\alpha^2/3$. Substituting this result in (22) and using charge correction relation $\alpha \to \alpha\,(1 - 2\alpha/3\pi)$ gives finally the anomalous magnetic moment of the electron as a function of fine-structure constant:

$$a_e = \frac{1}{2}\left(\frac{\alpha}{\pi}\right) - \frac{1}{3}\left(\frac{\alpha}{\pi}\right)^2 + \frac{\pi^2}{3}\left(\frac{\alpha}{\pi}\right)^3 - \frac{2\pi^2}{3}\left(\frac{\alpha}{\pi}\right)^4 + + \frac{4\pi^2}{9}\left(\frac{\alpha}{\pi}\right)^5 - \frac{8\pi^2}{81}\left(\frac{\alpha}{\pi}\right)^6. \qquad (23)$$

The calculation of a_e is performed using the CODATA recommended fine-structure constant $\alpha = 7.2973525376(50)\times10^{-3}$ [27] and from (23) the value is estimated to be $a_e(th) = 1.15965227095\times10^{-3}$. Though this classical estimate is not at par with the quantum electrodynamics calculations, the difference $a_e(th) - a_e(exp) = 90.22\times10^{-12}$ shows the result is at least accurate up to ninth decimal place. With proper approximation to the reduced velocity, equation (22) may be used for finding the anomalous magnetic moment of any other lepton.

4 Lamb shift

Relativistic theory of a bound electron predicts that the energy levels $2S_{1/2}$ and $2P_{1/2}$ are degenerate. However, the energy level shift $2S_{1/2} - 2P_{1/2}$ was experimentally found to be 1058.27 + 1.0 MHz in 1947 by Lamb and Rutherford [28]. For the Lamb shift calculation, we consider the average deviation in the path of orbital electron is equal to twice the radius of rotation (diameter) of the extended electron. Thus the orbital radius spreads out over a distance 2ξ and the corresponding change in the Coulomb potential is expressed in the form $V(\mathbf{r} + 2\mathbf{i}\xi)$. Expanding this function in terms of Taylor series gives

$$V(\mathbf{r} + 2\mathbf{i}\xi) - V(\mathbf{r}) = 2\mathbf{i}\xi \frac{\partial V(\mathbf{r})}{\partial \mathbf{r}} - 2\xi^2 \left(\frac{\partial^2 V(\mathbf{r})}{\partial r^2} \right) + \dots \quad (24)$$

In the Welton's approach of Lamb shift calculation [29], considering the symmetric potential, an additional multiplying factor $1/3$ was introduced in the second term on right of (24). Since the deviation is considered as a bivector which represents rotation in local space, any such factor is not required in the present calculation. The radius of rotation is a vector in the spin plane and therefore, it can be expressed in the form $\xi = |\xi| \exp(-\mathbf{i}\sigma_s \omega_0 t)$, where $\mathbf{i}\sigma_s$ is a unit bivector in the spin plane [14]. Then, the stochastic average $\langle \xi \rangle = 0$ and the average of square of radius of rotation $\langle \xi^2 \rangle = \langle |\xi|^2 \rangle / 2$. Using the relation $\dot{\xi} = -\mathbf{i}\sigma_s \omega_0 \xi$, we find $\langle |\xi^2| \rangle = \langle |\dot{\xi}|^2 \rangle / \omega_0^2$. Now, taking the stochastic average on both sides of (24), we obtain the stochastic average of change in the potential energy:

$$\Delta E_L = \langle V(\mathbf{r} + 2\mathbf{i}\xi) - V(\mathbf{r}) \rangle = \frac{\langle |\dot{\xi}^2| \rangle}{\omega_0^2} \left| \frac{\partial^2 V(\mathbf{r})}{\partial r^2} \right| \quad (25)$$

where the higher order terms are neglected. The energy in (25) corresponds to the Lamb shift in the energy levels due to the interaction of the electron with the zero-point field. We consider that the zero-point field around the atom is modified due to the extended electron in the orbit and as a consequence the electron orbit spreads out around the Coulomb source. Since the modifications in the zero-point field takes place at the atomic size, we choose the cut-off frequency equal to the de Broglie frequency ω_B. Such low frequency cut-off was not considered previously and this may be one of the reasons for not finding the exact estimate of the Lamb shift in stochastic electrodynamics. Considering the equation of motion of center of charge $\ddot{\xi} = eE_{zp}(\xi, t)/m$ and using the same method of derivation given in Section 3, and imposing the upper cut-off frequency ω_B, we obtain the zero-point energy associated with the orbital electron shift in the form

$$m\langle |\dot{\xi}|^2 \rangle = \frac{2\alpha}{3\pi} \frac{\hbar^2 \omega_B^2}{mc^2} \eta(\omega_B) \times \left[1 + \left\{ \frac{2}{\omega_B^2 \tau^2} (1 - \cos \omega_B \tau + \omega_B \tau \sin \omega_B \tau) \right\} \right] . \quad (26)$$

Since $\omega_B \tau \ll 1$,we neglect the terms in curly brackets and the converging form factor $\eta(\omega_B) = 1$. Now, (26) can be expressed in the form

$$\langle |\dot{\xi}|^2 \rangle = \frac{2\alpha}{3\pi} \frac{\hbar^2 \omega_B^2}{m^2 c^2} . \quad (27)$$

Substituting this result in (25) and using the relation $\hbar\omega_0 = mc^2$ gives

$$\Delta E_L = \frac{2\alpha}{3\pi} \frac{\omega_B^2 c^2}{\omega_0^4} \left| \frac{\partial^2 V(\mathbf{r})}{\partial r^2} \right| . \quad (28)$$

For an orbital electron in a circular orbit, the magnitude of Coulomb potential is equal to twice the kinetic energy of the electron:

$$V(r) = \frac{Ze^2}{r} = m_r v^2 = m_r \omega_B^2 r^2 . \quad (29)$$

Differentiating (29) twice with respect to r yields

$$\left| \frac{\partial^2 V(\mathbf{r})}{\partial r^2} \right| = m_r \omega_B^2 . \quad (30)$$

Substituting the above result in (28) gives

$$\Delta E_L = \frac{4\alpha}{3\pi} \beta^4 m_r c^2 . \quad (31)$$

Considering $\beta^2 = \alpha^2$, we finally arrive at the required energy shift given in (5). The charge correction of a free electron is given in (2) and in the case of an atomic electron it may be expected that it is three times that of the free electron. Then the correction for the fine-structure constant is $2\alpha/\pi$. Further, one may consider the mass correction of the reduced mass, same as $\alpha/2\pi$. Using these corrections in (5) and substituting the CODATA values of the electron mass, proton mass and other fundamental constants [27], the calculated Lamb shift in hydrogen spectra is found to be 1058.3696 MHz. Thus the present calculation is considerably in agreement with the standard value of Lamb shift 1057.8439 MHz [27] and the difference 0.5257 MHz may be attributed to the finite size of the proton.

In the quantum electrodynamics treatment, normally the expectation value of $|\nabla^2 V(r)|$ is found to be $\langle |\nabla^2 V(r)| \rangle \propto \alpha^4$ [30], the upper bound of integration is chosen to be ω_0 and the integration yields a logarithmic term. Comparing (5) with the Welton's result given by [31]

$$\Delta E_n = \frac{4\alpha^5}{3\pi} \frac{Z^4}{n^3} \ln \left(\frac{2}{16.55\alpha^2} \right) m_r c^2 , \quad (32)$$

we get the correct order of fine-structure constant. The logarithmic term $\ln\left(2/16.55\alpha^2\right) \sim 8$ and one can approximate $\beta^4 = 8(Z\alpha)^4/n^3$. Then, if one wishes to include the principal quantum number, (5) may be rewritten in the form

$$\Delta E_L = \frac{4\alpha}{3\pi} \frac{8(Z\alpha)^4}{n^3} m_r c^2 . \quad (33)$$

It may be noted that a complete relativistic quantum electrodynamics evaluation is free from high energy cut-off. However, the above calculation of Lamb shift is entirely different from the quantum electrodynamics treatment, where we consider radiative corrections, and the present calculation is purely based on classical considerations along with the extended structure of the electron.

5 Conclusions

Consideration of extended structure of the electron in zero-point field yields a classical, straightforward and simple approach to find mass and charge corrections. We find the mass correction depends on the particle velocity. The orbital electron reduced velocity is assumed to be proportional to the fine-structure constant. The anomalous magnetic moment of the electron has been expressed as a function of fine-structure constant and the estimated $a_e(th)$ value is found to be correct up to ninth decimal place. Using a low frequency cut-off equal to the de Broglie frequency, the Lamb shift of an extended electron in stochastic electrodynamics is derived and the estimated result deviates from the experimental value by 0.5257 MHz. The theory presented elucidates a classical approach to both anomalous magnetic moment of the electron and Lamb shift and paves the way for further research.

Received on August 13, 2018

References

1. Gabrielse G., Hanneke D., Kinoshita T., Nio M., Odom B. New Determination of the Fine Structure Constant from the Electron *g* Value and QED. *Phys. Rev Lett.*, 2006, v. 97, 030802.
2. Mathisson M. Neuemekhanikmaterietter system. *Acta. Phys. Pol.*, 1937, v. 6, 163–200.
3. Weyssenhoff J., Raabbe A. Relativistic dynamics of spin fluids and spin particles. *Acta. Phys. Pol.*, 1947, v. 9, 7.
4. Barut O. A., and Zanghi A. J. Classical model of the Dirac electron. *Phys. Rev. Lett.*, 1984, v. 52, 2009–2012.
5. Barut O. A., Bracken A. J. Zitterbewegung and the internal geometry of electron. *Phys. Rev. D*, 1981, v. 23, 2454.
6. Corben H. C. Classical and Quantum Theories of Spinning Particles. Holden and Day, New York, 1968.
7. Horvathy P. A. Mathisson's spinning electron: Non commutative mechanics and exotic Galilean symmetry 66 years ago. *Acta. Phys. Pol. B*, 2003, v. 34, 2611–2622.
8. Recami E., Salesi G. Kinematics and hydrodynamics of spinning particles. *Phys. Rev. A*, 1998, v. 57, 98–105.
9. Pavšič M, Recami E., Rodrigues W. A., Maccarrone G. D., Raciti F., Salesi G. Spin and electron structure. *Phys. Lett. B*, 1993, v. 318, 481.
10. Maruani J. The Dirac electron as a massless charge spinning at light speed: Implications on some basic physical concepts. *Prog. Theor. Chem. and Phys. B*, 2013, v. 27, 53–74.
11. Gouanère M., Spighel M., Cue N., Gaillard M. J., Genre R., Kirsch R., Poizat J. C., Remillieux J., Catillon P., Roussel L. Experimental observation compatible with the particle internal clock. *Annales de la Fondation Louis de Broglie*, 2005, v. 30, 109.
12. Hofer W. A. An extended model of electrons: experimental evidence from high-resolution scanning tunneling microscopy. *J. Phys. Conference Series*, 2012, v. 361, 012023.
13. Muralidhar K. Complex vector formalism of harmonic oscillator in geometric algebra: Particle mass, spin and dynamics in complex vector space. *Found. Phys.*, 2014, v. 44, 266–295.
14. Muralidhar K. Algebra of complex vectors and applications in electromagnetic theory and quantum mechanics. *Mathematics*, 2015, v. 3, 781–842.
15. Muralidhar K. Mass of a charged particle with complex structure in zerpoint field. *Progress in Physics*, 2016, v. 12, 224–230.
16. Muralidhar K. Theory of stochastic Schrödinger equation in complex vector space. *Found. Phys.*, 2017, v. 47, 532.
17. Muralidhar K. Classical approach to the quantum condition and biaxial spin connection to Schrödinger equation. *Quantum Stud.: Math. Found.*, 2016, v. 3, 31–39.
18. Puthoff H. E. Casimir Vacuum Energy and the Semiclassical Electron. *Int. J. Theor. Phys.*, 2007, v. 46, 3005–3008.
19. Boyer T. H. Random electrodynamics: The theory of classical electrodynamics with classical electromagnetic zeropoint radiation. *Phys. Rev. D*, 1975, v. 11, 790–808.
20. Boyer T. H. A brief survey of stochastic electrodynamics. In: Barut O. A., ed. Foundations of Radiation Theory and Quantum Electrodynamics. Springer Science + Bissinessmedia, New York, 1980, pp. 49–63.
21. Cavalleri G., Barbero F., Bertazzi G., Casaroni E., Tonni E., Bosi L., Spavieri G., Gillies G. T. A quantitative assessment of stochastic electrodynamics with spin (SEDS): Physical principles and novel applications. *Front. Phys. China*, 2010, v. 5, 107–122.
22. Rueda A. Behavior of classical particles immersed in electromagnetic zero-point field. *Phys. Rev. A*, v. 23, 2020.
23. Kusch P., Foley H. M. The Magnetic Moment of the Electron. *Phys. Rev.*, 1948, v. 74, 250.
24. Schwinger J. Collected Papers on Quantum Electrodynamics. Dover Publications Inc, New York, 1958.
25. Kinoshita T. Theory of the Anomalous Magnetic Moment of Electron – Numerical Approach. World Scientific, Singapore, 1990.
26. Henneke D., Fogwell S., Gabrielse G. New measurement of electron magnetic moment and the fine structure constant. *Phys. Rev. Lett.*, 2008, v. 100, 120801.
27. Mohr P. J., Taylor B. N., Newell D. B. CODATA recommended values of the fundamental physical constants: 2006. *Rev. Mod. Phys.*, 2008, v. 80, 633.
28. Lamb W. E. Jr., and Rutherford R. C. Fine structure of hydrogen atom by a microwave method. *Phys. Rev.*, 1947, v. 72, 241–243.
29. Welton T. A. Some observable effects of quantum mechanical fluctuations of electromagnetic field. *Phys. Rev.*, 1948, v. 74, 1157.
30. Milonni P. W. The Quantum Vacuum: An Introduction to Quantum Electrodynamics. Academic Press, San Diego, 1994, p. 410.
31. Schwabl F. Advanced Quantum Mechanics, Springer, New Delhi, 2005, p. 189.

On the Speed of Light and the Continuity of Physical Vacuum

Anatoly V. Belyakov

E-mail: belyakov.lih@gmail.com

It is shown that the speed of light can be calculated on the basis of the velocity equation of the waves propagating along a liquid surface. This gives a reason to believe that the vacuum medium, being discrete, simultaneously possesses the property of continuity like the surface of an ideal fluid.

The speed of light is one of a few fundamental values, which are not deducible from theory. However, it turns out that the propagation of light is similar to wave motion on a liquid surface, and *has a maximum, which is equal to the speed of light*. This maximum is determined on the basis of the well-known equation

$$v^2 = \frac{g\lambda}{2\pi} + \frac{2\pi\sigma}{\rho\lambda}\,, \tag{1}$$

where g is the acceleration, λ is the wavelength, σ is the surface tension (force-to-perimeter ratio, [N/m]), while ρ is the specific density. The first term means the influence of gravity on the wave speed, the second — the influence of surface tension.

Of course, various physical phenomena described by the same equations are not reducible to each other. Nevertheless, there must be something common between them. In this case, the common feature should be the *continuity of the medium* (physical vacuum). Thus, the physical vacuum, being discrete and being a source of virtual particles, at the same time also possesses the property inherent in the inviscid continuous medium surface through which electromagnetic oscillations propagate in the form of surface transverse waves!

In order to apply formula (1) and determine the parameters entering into it, it is necessary to isolate some unit element of the medium (a radiating cell), which they would apply to. In [1], when determining the critical vacuum density, it was shown that such an element can be a hydrogen atom as the most common element in the Universe.

From the point of view of John Wheeler's geometrodynamic concept, charged microparticles are singular points on a the three-dimensional surface of our world, connected by a "wormhole", i.e. a vortex tube or power current line (of the input-output kind) located in an additional dimension. As a result, a closed contour is formed along which the physical vacuum or some other medium circulates. The presence of contours (vortex tubes) is also postulated, for example, in [2], where the vacuum structure is considered as a network of one-dimensional flow tubes (knotted/linked flux tubes) and it is claimed that it is such a network that provides the spatial three-dimensionality of the Universe. Such a tube or a vacuum unit can be regarded as a field unit, in contrast to an atom — a matter unit [3].

Geometrodynamics in the mechanistic interpretation does not introduce any additional entities. On the contrary, it reduces them. So, from the dimensions set, Coulomb is eliminated: it is replaced by the ultimate momentum of the electron $m_e c$ [4]. In this case, the vortex tube is characterized by the electric constant and magnetic constant ε_0 and μ_0, where the electric constant becomes linear density of the vortex tube, and the reciprocal of the magnetic constant is the centrifugal force produced by rotation of a vortex tube element with the light velocity c along the electron radius r_e. It is also the force acting between elementary charges at a distance r_e:

$$\varepsilon_0 = m_e/r_e\,, \tag{2}$$

$$\mu_0 = \frac{1}{c^2\varepsilon_0} = \frac{r_e}{m_e c^2}\,. \tag{3}$$

It is assumed that the medium circulating along a contour with a radius R in the same time rotates spirally inside it, so that the contour (toroid) contains z structurally ordered units (in this case — the waves or photons). The speed of circulation and rotation is:

$$v = \frac{c\, c_0^{1/3}}{a^2 n^2}\,, \tag{4}$$

where c_0 is the dimensionless speed of light c/[m/sec], a is the inverse fine structure constant, and n is the main quantum number. In this interpretation for the single element (hydrogen atom) accepted, there is only g — the centrifugal acceleration appearing when the medium moves along the contour, i.e. square of the velocity-to-the radius of the spiral rotation ratio:

$$g = \frac{v^2}{R/z} = \frac{z c^2 c_0^{2/3}}{a^4 n^4 R}\,, \tag{5}$$

where

$$R = n^2 R_B = n^2 a^2 r_e\,, \tag{6}$$

where R_B is the Bohr radius.

The surface tension of a unit cell [N/m], using the force $1/\mu_0$ (there is no other force there), is represented as:

$$\sigma = \frac{1/\mu_0}{R} = \frac{m_e c^2}{r_e R}\,, \tag{7}$$

and the hydrogen atom density for an arbitrary n is:

$$\rho_H = \frac{m_p m_e}{R^3}\,, \tag{8}$$

where m_p is the proton relative mass in units of m_e. The wavelength is defined for the case of ionization:

$$\lambda = \frac{n^2}{R_\infty}\,, \tag{9}$$

where R_∞ is the Rydberg constant. As a result, assuming the speed of light to be unknown, replacing c by v and bearing in mind the above formulas, (1) can be represented as:

$$v^2 = \frac{z\,v^2 v_0^{2/3}}{2\pi a^4 n^4 R_B R_\infty} + \frac{2\pi a^2 n^2 R_B R_\infty v^2}{m_p}\,. \tag{10}$$

Making the transformations and bearing in mind that $R_B R_\infty = 1/(4\pi a)$, we obtain from (10):

$$v_0^{2/3} = \left(1 - \frac{an^2}{2m_p}\right)\frac{a^3 n^4}{2z}\,, \tag{11}$$

when differentiating (11) with respect to n, the value of n for the maximum velocity is found:

$$n_m = \sqrt{\frac{4m_p}{3a}} = 4.23. \tag{12}$$

It is noteworthy that the radiation wavelength during ionization, i.e. at the transition $n_m \leftarrow \infty$, corresponds to the temperature of blackbody radiation 1840°K, which is close to the temperatures of the red and brown dwarfs — the most common bodies in the Universe.

Further, replacing n^2 in formula (11) with the value n_m^2, from (11) the maximum of the velocity is determined by:

$$v_m = \left(\frac{a^3 n^4}{6\,z}\right)^{3/2} \times [\text{m/sec}] = 2.81 \times 10^8 \left(\frac{n^4}{z}\right)^{3/2} \times [\text{m/sec}]. \tag{13}$$

In [4], we give additional relations connecting the parameters v_0, z, n, and also the sine of the projection angle (the cosine of the Weinberg angle), which follow from that n^4/z does not depend on n and this value is slightly more than one. As a result, we obtained the value of v, which is very close to the speed of light and is determined only by the fine structure constant and velocity dimensionality as well as the Weinberg angle cosine. The last calculations as not having fundamental importance are not given here.

The obtained solution can be considered as a special case of the wave velocity maximum. However, unlike a liquid where the surface wave velocity has a minimum and these capillary and gravitational waves velocity depends on the surface tension and the basin depth, there is a natural mechanism for electromagnetic waves ensuring the independence of their speed from the wavelength. This follows even from the above formulas, which have a model-simplified character.

Indeed for this, it is necessary that there in formula (11) the ratio n^2/m_p remains constant. Since the wavelength is proportional to n^2, then, with increasing the interval between waves, the mass of the medium in a given interval must grow proportionally, which means that the medium remains homogeneous in the direction of wave propagation. This is true, because equation (1) is based on the law of a simple one-dimensional oscillation of a pendulum. Perhaps, someday, a more accurate equation for the general case made in electrodynamics terms will be deduced.

It should be noted that the fundamental difference between long-wave radiations and particle-like X-rays (gamma radiations) is associated with their different nature: the first is due to the medium surface tension, while the second is due to the medium acceleration in the radiating cell of the contour.

Thus, the physical vacuum as a medium is discrete at a certain level, and its unit is a vortex tube (the field unit). At the same time, it is capable of being infinitely densely filled with such units forming a continuous surface (the possibility of this was proved in the 19th century by J. Peano [5]). This surface, in turn, as it becomes more complex, can form three-dimensional material objects. When driving in such a continuous medium body does not feel any resistance up to the speed of light, i.e., until a surface wave forms, and, for the observer, the vacuum medium remains undetectable. Recall that even when moving in a real liquid body, an observer does not feel a resistance up to the speed when a surface wave is formed (for water, the speed is 0.3 ... 0.5 m/sec).

Conclusion

The fact that the vacuum manifests properties of a continuous surface while electromagnetic waves propagate in the form of surface waves gives grounds to combine the light speed constancy with its wave nature and with the physical vacuum as a transmitting medium (and, at the same time, we can remain within the framework of Newtonian space and time). For this it is sufficient to accept the postulate that *an observer is always at rest with respect to the vacuum medium, and a source always moves with respect to it and, accordingly, with respect to the observer*. Thus, the passive element (an observer) does not detect the vacuum medium, but at the same time he receives an evidence of its existence as a continuous medium, namely — a change in the radiation wavelength (the Doppler effect) due to the motion of the active element (source).

Received on August 28, 2018

References

1. Belyakov A.V. On the independent determination of the ultimate density of physical vacuum. *Progress in Physics*, 2011, v.7, issue 2, 27–29.
2. Berera A., Buniy R. V., Kephart T. W., Päs H., and Rosa J. G. Knotty inflation and the dimensionality of spacetime. arXiv: 1508.01458.
3. Belyakov A.V. On Materiality and Dimensionality of the Space. *Progress in Physics*, 2014, v.10, issue 4, 203–206.
4. Belyakov A.V. Charge of the electron, and the constants of radiation according to J. A. Wheeler's geometrodynamic model. *Progress in Physics*, 2010, v.6, issue 4, 90–94.
5. Peano G. Sur une courbe, qui remplit toute une aire plane. *Mathematische Annalen*, 1890, v.36, issue 1, 157–160.

Unfalsifiable Conjectures in Mathematics

Craig Alan Feinstein
2712 Willow Glen Drive, Baltimore, Maryland 21209, USA
E-mail: cafeinst@msn.com

It is generally accepted among scientists that an unfalsifiable theory, a theory which can never conceivably be proven false, can never have any use in science. In this paper, we shall address the question, "Can an unfalsifiable conjecture ever have any use in mathematics?"

1 Introduction

It is generally accepted among scientists that an unfalsifiable theory, a theory which can never conceivably be proven false, can never have any use in science. As the philosopher Karl Popper said, "the criterion of the scientific status of a theory is its falsifiability, or refutability, or testability" [4]. In this paper, we shall address the question, "Can an unfalsifiable conjecture ever have any use in mathematics?" First, we shall present a famous mathematical conjecture and prove that it is unfalsifiable. Next, we shall discuss the implications of proving that a mathematical conjecture is unfalsifiable. And finally, we shall present some open problems.

2 An unfalsifiable conjecture

Landau's fourth problem is to prove that there are an infinite number of prime numbers of the form n^2+1, where $n \in \mathbb{N}$ [6]. We shall call this conjecture the $n^2 + 1$-Conjecture. And we shall prove that the n^2+1-Conjecture is unfalsifiable, i.e., that its negation is unprovable in any reasonable axiom system:

Theorem: The $(n^2 + 1)$-Conjecture is unfalsifiable.

Proof: Suppose there exists a proof that there are only a finite number of primes of the form $n^2 + 1$. Then there would exist an $N \in \mathbb{N}$ such that for any $n \in \mathbb{N}$ in which $n > N$, $n^2 + 1$ would be composite; thus, one could deduce that $n^2 + 1$ is composite from only the assumption that $n - N \in \mathbb{N}$. But this is impossible, since the polynomial $n^2 + 1$ is irreducible over the integers. Hence, it is impossible to prove that there are only a finite number of primes of the form $n^2 + 1$. So the $n^2 + 1$-conjecture is unfalsifiable. □

3 Implications

Let us assume that the ZFC axioms are consistent [10]. Then what are the implications of proving that a mathematical conjecture is unfalsifiable? The answer is that even though an unfalsifiable conjecture might not be true, there is still no harm in assuming that it is true, since there is no chance that one could derive any provably false statements from it; if one could derive any provably false statements from an unfalsifiable conjecture, this would imply that the conjecture is falsifiable, which is a contradiction.

For example, there is a probabilistic heuristic argument that the $n^2 + 1$-Conjecture is true [3]. This implies that all statements which can be derived from the $n^2 + 1$-Conjecture are almost certainly true. Since our theorem above says that the $n^2 + 1$-Conjecture is unfalsifiable, there is no chance that any of these statements could be proven false.

As a different type of example, in 2006 the author showed that the Riemann Hypothesis is unprovable in any reasonable axiom system [1]. This implies that the negation of the Riemann Hypothesis is unfalsifiable, so one might conjecture that the Riemann Hypothesis is false. However, there is a probabilistic heuristic argument that the Riemann Hypothesis is true [2]; therefore, if one were to assume that the Riemann Hypothesis is false, one could derive statements which are almost certainly false from this assumption. However, these statements could never be proven false, since the negation of the Riemann Hypothesis is unfalsifiable.

4 Open problems

Can the following famous conjectures also be proven to be unfalsifiable?

1. There are an infinite number of pairs of primes which differ by two. These are called twin primes [9].
2. There are an infinite number of primes of the form $2^p - 1$, where p is also prime. These are called Mersenne primes [7].
3. There are an infinite number of primes p, where $2p + 1$ is also prime. These are called Sophie Germain primes [8].
4. There are an infinite number of primes of the form $2^{2^n} + 1$. These are called Fermat primes [5].

5 Conclusion

An unfalsifiable theory can never have any use in science; however, an unfalsifiable conjecture can be very useful in mathematics: When an unfalsifiable conjecture is difficult to prove, one can assume that the conjecture is true and not have to worry about deriving any provably false statements from it, assuming that the ZFC axioms are consistent.

Acknowledgements

The author would like to thank Florentin Smarandache for his very helpful comments.

Received on September 6, 2018

References

1. Feinstein C.A. Complexity science for simpletons. *Progress in Physics*, 2006, issue 3, 35–42.
2. Good I.J. and Churchhouse R.F. The Riemann hypothesis and pseudo-random features of the Möbius Sequence". *Math. Comp.*, 1968, v.22, 857–861.
3. Hardy G.H. and Littlewood J.E. Some problems of "Partitio Numerorum". III. On the expression of a number as a sum of primes. *Acta Math.*, 1923, v.44, 1–70.
4. Popper K. Conjectures and Refutations: The Growth of Scientific Knowledge. London, Routledge, 1963.
5. Fermat Prime. From *MathWorld — A Wolfram Web Resource*. http://mathworld.wolfram.com/FermatPrime.html
6. Landau's Problems. From *MathWorld — A Wolfram Web Resource*. http://mathworld.wolfram.com/LandausProblems.html
7. Mersenne Prime. From *MathWorld — A Wolfram Web Resource*. http://mathworld.wolfram.com/MersennePrime.html
8. Sophie Germain Prime. From *MathWorld — A Wolfram Web Resource*. http://mathworld.wolfram.com/SophieGermainPrime.html
9. Twin Prime Conjecture. From *MathWorld — A Wolfram Web Resource*. http://mathworld.wolfram.com/TwinPrimeConjecture.html
10. Zermelo-Fraenkel Axioms. From *MathWorld — A Wolfram Web Resource*. http://mathworld.wolfram.com/Zermelo-FraenkelAxioms.html

The Helicon: A New Preon Model

Oliver Consa
Department of Physics and Nuclear Engineering, Universitat Politècnica de Catalunya
Campus Nord, C. Jordi Girona, 1-3, 08034 Barcelona, Spain
E-mail: oliver.consa@gmail.com

A new preon model is presented as an extension of the semiclassical Helical Solenoid Electron Model that was previously proposed by the author. This helicon model assumes as postulates both the Atomic Principle and the equality between matter and electric charge. These postulates lead us to a radical reinterpretation of the concepts of antimatter and dark matter and form a new framework for future preon theories.

1 Introduction

According to the Atomic Principle, "matter is composed of indivisible, indestructible and immutable elementary particles." This principle has guided the greatest successes in the history of science [2]. However, the currently-accepted Standard Model of Particle Physics (SM) does not comply with this principle since most of this model's elementary particles are unstable, and all of them can be created or destroyed by matter-antimatter interactions. In concurrence with Kalman [3], we consider the current state of particle physics to be anomalous. We propose that the Atomic Principle is an unrenounceable postulate. Any fundamental theory of elementary particles should strictly respect this principle. If necessary, we should reinterpret the experimental results and discard any theory that does not strictly comply with the Atomic Principle.

The large number of elementary particles described by the SM and the regularities of their properties suggest that there is a lower level of matter organization. In 1974, Pati and Salam [11] proposed that both leptons and quarks were composite particles formed by fundamental particles called preons. To date, no preon model has attracted the general interest of the particle physics community. However, preon models have continued to evolve with new proposals, including those by Terazawa (1977) [12], Harari (the Rishon Model, 1979) [13], Mandelbaum (the Haplon Model, 1981) [14], Dehmelt (the Cosmon Model, 1989) [15], Kalman and d'Souza (the Primon Model, 1992) [17], Dunge and Fredriksson (1997) [16], Bilson-Thompson (the Helon Model, 2005) [18], Yershov (the Y-particle Model, 2006) [19] and Lucas (the Intertwining Charged Fibers Model, 2006) [20].

The objective of this paper is to propose a new preon model as an extension of the Helical Solenoid Model of the electron [1] that is applicable to any subatomic particle and that strictly complies with the Atomic Principle. The Helicoidal Solenoid Model is a semiclassical model that proposes that the electron is a point-like electric charge that moves at the speed of light following a helical solenoid trajectory with an angular momentum equal to the reduced Planck constant. This model assumes that the Zitterbewegung is the mechanism that causes the helical movement of the electron (spin) and its corresponding magnetic moment.

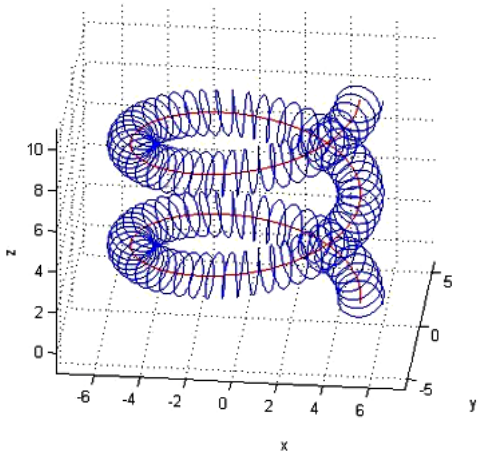

Fig. 1: Trajectory of the electron in the Helical Solenoid Model.

2 Nuclear Forces

The main challenge for preon theories is to explain the force that holds the preons together. Quantum Chromodynamics (QCD) defines a strong nuclear force based on the existence of gluons, but this theory is incompatible with the preon hypothesis. To date, it has not been possible to identify an extension of the QCD theoretical basis that would allow for the incorporation of a substructure common to both leptons and quarks. In addition, all attempts to expand the QCD theory involve an exponential increase in mathematical complexity, the opposite of what is intended with preon theories. Therefore, a preon theory that is compatible with the Atomic Principle will be, predictably, incompatible with QCD.

We are not bothered by this incompatibility because we start from a semiclassical Helical Solenoid Model that is incompatible in fundamental aspects with many of the modern dominant theories (Quantum Mechanics (QM), Quantum Electrodynamics (QED) and Quantum Chromodynamics (QCD)). This is not an insurmountable problem since it is well known that mutually incompatible theories can explain

the same experimental results and, in certain cases, may even be useful. For example, the Bohr-Sommerfeld model was surpassed by QM but, nevertheless, produces the same results for the fine structure of the hydrogen atom.

In 1986, Barut [4] proposed that nuclear forces are manifestations of electromagnetic forces at very short distances. While electric fields decrease with the square of the distance, magnetic fields decrease with the cube of the distance. Magnetic forces are dominant over very small distances, but their influence decreases rapidly with respect to electrical forces as distances expand

$$F_{mag} \propto \frac{1}{R^3} , \tag{1}$$

$$F_{elec} \propto \frac{1}{R^2} . \tag{2}$$

This hypothesis is shared by Pati [5], the creator of the first preon theory, and by other lesser-known researchers such as Schaeffer [6], Dallacasa [7], Cook [8], Kaliambos [9], Kanarev [10] and Lucas [20].

Historically, it has been assumed that magnetic forces at the subatomic level are negligible, but in our Helical Solenoid Model, the magnetic field density at the center of the nucleon is enormous, about 100 trillion tesla. This magnetic field density is thousands of times greater than that of a neutron star. A magnetic field of these proportions must necessarily produce significant effects

$$R = \lambda\!\!\!^{-}_N = \frac{\hbar}{m_N c} = 2.103 \times 10^{-16} \text{ m}, \tag{3}$$

$$f = \frac{v_r}{2\pi R} = \frac{c}{2\pi \lambda\!\!\!^{-}_N} = 2.268 \times 10^{23} \text{ Hz}, \tag{4}$$

$$B = \frac{\mu_0 I}{2R} = \frac{\mu_0 e f}{2\lambda\!\!\!^{-}_N} = 1.088 \times 10^{14} \text{ T}. \tag{5}$$

In our preon model, we do not contemplate the existence of particles that mediate nuclear forces, such as gluons. Instead, we assume that elementary particles interact with each other through their respective electromagnetic fields. While it is outside the present work to explain the physical nature of photons, we conclude that photons (i) are not particles of matter, (ii) are not composed of preons and (iii) do not have to comply with the Atomic Principle. Therefore, photons can be created (by emission) and destroyed (by absorption) without any limitations. Many theories have tried to explain the photon as the union of an electron and a positron, however, all the experiments conducted to date are consistent with the idea that a photon transports electromagnetic energy but does not carry any type of electrical or magnetic charge.

3 Topology

The SM assumes that fermions are point particles and that it is impossible for a point particle to be formed by other point subparticles. For this reason, the more advanced preon models, such as those proposed by Bilson-Thompson [18], Yershov [19] and Lucas [20], describe preons and fermions as structures with a determined topology. In most cases, the proposed topology is toroidal or helical. This topology is suggested by the helical and chiral properties of the subatomic particles. The helical topology allows the composite particles to establish different structures that can be analyzed using knot theory (e.g., Rañada [21]) or braid theory (e.g., Bilson-Thompson [18]). The different combinations would give rise to the various symmetries of the subatomic particles, such as the conservation of the color charge.

The experimental data obtained in particle colliders suggest that fermions are point particles, so we need a model that can combine both point and helical topologies. Our Helical Solenoid Model [1] proposes a dynamic point-particle model, in which a point particle always moves at the speed of light in a closed path. This allows the advantages of the point particle to be combined with helical topology (which corresponds to the particle's trajectory).

In the Helical Solenoid Model, several point particles can form a single helical structure. For example, several particles could share the same closed trajectory in an equidistant fashion or they could share the trajectory in the same plane but with different radii. Finally, Lucas's Intertwining Charged Fibers Model [20] illustrates graphically how several helical paths could interlink with each other, giving rise to different subatomic particles.

4 Matter

In classical physics, matter is any substance that has mass and volume (i.e., that occupies space). This definition is valid for all matter composed of atoms, but when we analyze the subatomic particles that make up the atoms, this definition loses its meaning. In the SM, mass is considered only one form of energy, and the subatomic particles are considered quantum entities that do not have a definite volume or size. In this framework, matter no longer has a precise definition nor is it considered a fundamental concept.

But, to apply the Atomic Principle, matter must have a precise definition and be considered a fundamental concept. To define the concept of matter, we need to identify a fundamental property that strictly complies with three requirements: it must be absolute (the amount of matter cannot depend on the observer or the reference system), conserved (the amount of matter must be retained in any iteration) and quantified (the amount of matter must be composed of whole units).

Mass is an indicator of the kinetic energy and electromagnetic potential associated with the internal structure of each subatomic particle. But, as a property of matter, mass does not meet any of the three requirements. Only one property of matter satisfies the test, the electric charge. Therefore, we propose a new postulate: Electric charge is the fundamental

property of matter.

All matter is composed of unitary electric charges. Phrased in a different manner, matter is everything that is composed of electric charges. Consequently, our second postulate is that matter and electric charge represent exactly the same thing. This postulate has important implications. It implies that all neutral particles must necessarily be composite particles of an equal number of negative and positive electric charge particles. Combining this postulate with the Atomic Principle, we conclude that all subatomic particles must be composed of a whole number of fundamental electric charges.

We also assume the validity of the minimalist hypothesis that postulates that all matter is composed of only two fundamental particles, the positive fundamental electric charge and the negative fundamental electric charge. In our model, we call these elementary particles helicons (H^+ and H^-), to differentiate them from those discussed in other preon models and to emphasize the relationship of this elementary particle with the Helical Solenoid Model. The three preon models that we consider the most advanced (Bilson-Thompson, Yershov and Lucas) concur with this minimalist hypothesis of only two fundamental particles.

All the preon models we have analyzed treat the mass of subatomic particles as an additive property. The greater the number of components in each subatomic particle and the more complex its internal structure, the greater the particle's mass. These models all group elementary particles into several sublevels of organization, forming increasingly complex structures. These models also assume that hadrons have a much more complex structure than leptons. The exact composition of each subatomic particle depends on the proposed preon model. We do not propose any particular organization scheme for subatomic particles; their composition should explain the value of the masses of each subatomic particle and explain all known modes of decay.

5 Antimatter

The concept of antimatter originated in 1898 when Schuster [22] speculated that there were particles with negative gravitational mass. Since antimatter would have negative gravity, antimatter would have a propensity to join together and separate from the matter of positive masses. Over time, antimatter would separate from matter, forming atoms, molecules or even stars and entire galaxies of antimatter. The difficulty occurs in the analysis of negative inertial mass. Negative inertial mass is a strange concept in physics; it causes serious problems and contradictions with the principles of conservation of energy and movement. For example, according to these theories, the more a particle of negative inertial mass accelerates, the more energy is created. In 1905, Einstein demonstrated that mass is only an expression of a particle's energy, implying that negative mass would be equivalent to negative energy.

In 1928, Dirac presented his electron equation, a relativistic half-integer spin version of the Schrodinger Equation, that correctly predicted the value of the electron's magnetic moment and the fine structure of the hydrogen atom. The Dirac Equation elegantly solved the main problems plaguing QM at that time. However, the Dirac Equation created new problems, since it predicted quantum electron states with negative energy. To resolve these issues, Dirac proposed the extravagant "sea of Dirac," where empty space would be formed by an infinite sea of negative energy particles that would occupy all the negative energy quantum states. In 1930, Dirac [23] proposed that there could be "gaps" in this "sea" of negative energy states. These "gaps" would be observed as a particle of positive energy with a positive charge, otherwise known as protons.

Oppenheimer [24] criticized Dirac's proton hypothesis. The positively charged particle predicted by Dirac could not be the proton since it would have the same mass as the electron; they would then annihilate each other upon contact, making the hydrogen atom unstable. Coincidentally, in 1932, while analyzing traces of cosmic rays in a cloud chamber, Anderson identified a particle with a positive electric charge and a mass identical to the mass of the electron that he called a positron. The positron corresponded with the particle predicted by Dirac, confirming the validity of his equation. In 1933, he was awarded the Nobel Prize for the discovery of antimatter.

However, there are many inconsistencies in antimatter theory that have been overlooked. According to Schuster, by definition, antimatter would have a negative mass, which does not happen with the positron. In addition, Dirac's antimatter is a consequence of his "sea of Dirac" theory, an implausible hypothesis that has been ruled out by modern physics. In reality, the current concept of antimatter is the result of a temporal coincidence between Dirac's hypothesis and Anderson's experiments, combined with a factual misinterpretation.

If we set aside the Dirac hypothesis and analyze the positron identified in Anderson's experiments, we find an unstable particle that is identical to the electron but with a positive charge. When a positron comes into contact with an electron, a large amount of energy is emitted, and neither the electron nor the positron presence is longer detected. The currently accepted explanation for this phenomenon is that there is a mutual annihilation of the positron with the electron, but this explanation is not supported by theory or experience. The annihilation theory is only applicable to particles with negative mass, but both the electron and the positron have positive masses. However, if we rely on experience, when a positive electric particle joins a negative electric particle, the result is a neutral electric particle (and radiation emission). There is a similar occurrence when an anion is attached to a cation, forming a neutral molecule, or when an electron is attached to a proton, forming a hydrogen atom.

Instead of mutual annihilation, a more logical explanation

of the matter-antimatter interaction is the creation of neutral matter. This alternative explanation complies with the principles of conservation of electric charge and conservation of matter. According to our postulates, the electric charge is neither created nor destroyed, so the result of the electron-positron interaction must be the creation of one or several neutral particles that are currently unknown. Symmetrically, the creation of an electron-positron pair from energy would also not be possible. Instead, one or more of these unknown neutral particles would need to intervene, in addition to the necessary energy. Therefore, we should not call these processes of creation or annihilation of matter but of decomposition and aggregation of matter.

According to our interpretation, antimatter is characterized by having a topology that is symmetric to the topology of matter. Due to this symmetry, when particles of matter and antimatter come into contact, they have a strong tendency to decompose and reorder, producing simpler neutral particles. However, there is an asymmetry in the universe by which negative helicons tend to organize into simple subatomic structures (electrons), while positive helicons tend to organize into complex subatomic structures (protons and neutrons). This asymmetry in helicon grouping tendencies means that some structures are more common (electrons, protons and neutrons), while other structures form less frequently and decompose rapidly (antimatter). This asymmetry can be explained by assuming that the positive helicon is not exactly symmetric to the negative helicon, but that there is a slight asymmetry in some property of the helicon that causes this predisposition for different grouping tendencies.

The three preon models that we consider the most advanced (Bilson-Thompson, Yershov and Lucas) agree that antimatter is formed by positive and negative preons, in the same fashion as matter, and they reject the possibility of antipreons. Our interpretation of the matter-antimatter interaction is also consistent with Lucas's Intertwining Charged Fibers Model.

6 Dark Matter

Continuing with our minimalist hypothesis, a positive helicon bound to a negative helicon would result in a neutral particle ($H^o = H^+ + H^-$). This neutral particle would be the simplest possible composite particle; therefore, it should be the most abundant stable particle in the universe. The rest of the particles should be produced with a much lower probability. What we currently consider to be empty space would actually be space that is full of neutral particles. The hypothesis of an empty space full of neutral particles is not unusual for physics. Most of the matter in the universe is currently considered to be dark matter that does not correspond to known matter. The electromagnetic properties of this quantum vacuum could also be caused by a sea of neutral particles. We propose the term etheron for the neutral particle that is formed by the binding of a positive helicon to a negative helicon, to emphasize that the etherons form a sea that covers the entire universe, like the old concept of ether. In this case, the sea of etherons is not a fluid of a substance that is different from matter but a sea of neutral particles of ordinary matter.

An indirect consequence of the Sea of Etherons Hypothesis is the recovery of the Principle of Causality or Laplace's Principle of Causal Determinism, according to which every effect has a cause. According to this theory, apparently random processes, such as the disintegration of atomic nuclei or the decay of subatomic particles, are not in reality random processes but are instead determined by collisions with particles from the sea of etherons. Etherons have mass, so their spatial distribution should not be homogeneous. This allows us to establish the first experimentally testable hypothesis of this model: the average lifetime of atoms and subatomic particles must be different in different parts of the universe.

And there is experimental evidence: unexpected and unexplained fluctuations in the decay rates of ^{32}Si and ^{226}Ra have been reported and evidence of correlations between nuclear decay rates and Earth-Sun distance has been found (Jenkins-Fishbach effect [25]).

7 Conclusions

We are convinced of the validity of the Helical Solenoid Model's applicability to the electron, and we believe that this model can be extended to all subatomic particles. We must dispense with the mathematical and conceptual complexities of the SM and the theories that support it (QM, QED and QCD).

As a basis for our preon model, we postulate that the Atomic Principle should be strictly followed and that the fundamental property of matter is the electric charge. From there, we assume the minimalist hypothesis of only two fundamental particles, the negative helicon (H^-) and the positive helicon (H^+). These two point-like particles always move at the speed of light following a helical movement. When several helicons are combined, they form a subatomic particle. There is an asymmetry between the negative helicon and the positive helicon that leads to a propensity of the negative helicons to organize into simple structures (electrons), while the positive helicons tend to organize into complex structures (protons and neutrons). This asymmetry causes opposing structures to be generated with much less probability, as these structures are easily disorganized upon contact with a symmetric structure (matter-antimatter iteration). The union of a negative helicon and a positive helicon forms an etheron, the simplest and most abundant stable particle in the universe. What we know as empty space is actually replete with these neutral particles, forming a sea of etherons. Collisions of particles of matter with particles from the sea of etherons are the cause of many phenomena that are considered random, including:

- Spontaneous disintegration of atomic nuclei;

- Spontaneous disintegration of subatomic particles;
- Antimatter interactions;
- Gravitational dark matter; and
- Quantum effects of vacuum, as the Casimir effect.

Since etherons have mass, their distribution in the universe is not perfectly homogeneous. This allows us to make an experimentally verifiable prediction: the average lifetimes of atomic particles and atomic nuclei must be different in different parts of the universe. Experimental evidence has been reported in this matter [25].

This proposed preon model based on the helicon is not complete since the composition of each subatomic particle is not indicated, nor is the calculation of its masses or its modes of decay. Our main objective was to provide a framework based on new principles and a radical reinterpretation of the facts. We leave for other researchers the job of proposing a complete preon theory based on this framework, highlighting three preon models (Bilson-Thompson, Yershov and Lucas) that we believe are close enough to achieve this target and that can serve as inspiration for others.

Submitted on September 21, 2018

References

1. Consa O. Helical solenoid model of the electron. *Progress in Physics*, 2018. v. 14(2), 80–89.
2. Feynman R. The Feynman Lectures on Physics. 1964 volume I; lecture 1, “Atoms in Motion"; section 1–2, “Matter is made of atoms"; p. 1–2. *If, in some cataclysm, all of scientific knowledge were to be destroyed, and only one sentence passed on to the next generations of creatures, what statement would contain the most information in the fewest words? I believe it is the atomic hypothesis.*
3. Kalman C.S. Why quarks cannot be fundamental particles. *Nuclear Physics B: Proceedings Supplements*, 2005, v. 142, 235–237.
4. Barut A.O. Unification based on electromagnetism. A simple composite model of particles. *Annalen der Physik*, 1986, v. 498(1–2), 83–92.
5. Pati J.C. Magnetism as the origin of preon binding. *Physics Letters B*, 1981 ,v. 98(1-2), 40–44.
6. Schaeffer B. Electromagnetic theory of the nuclear interaction. *World Journal of Nuclear Science and Technology*, 2016, v. 6, 199–205
7. Cook N.D., Dallacasa V. Models of the Atomic Nucleus. 2nd Edition, Springer, Berlin, 2010.
8. Cook N.D., Dallacasa V. LENR and nuclear structure theory. *J. Condensed Matter Nucl. Sci.*, 2014, v,i̇3, 68–79.
9. Kaliambos, L.A. Nuclear structure is governed by the fundamental laws of electromagnetism. *Indian Journal of Theoretical Physics*, 2003, v. 51(1), 1–37.
10. Kanarev M., Models of the atomic nuclei. *Journal of Theoretics*, 2002, v. 4, 1–7.
11. Pati J.C., Salam A. Lepton number as the fourth “color". *Physical Review D*, 1974, v. 10, 275–289.
12. Terazawa H. Unified model of the Nambu-Jona-Lasinio type for all elementary particles. *Physical Review D*, 1977, v. 15(2), 480–487.
13. Harari H. A schematic model of quarks and leptons. *Physics Letters B*, 1979, v. 86(1), 83–86.
14. Fritzsch H., Mandelbaum G. Weak interactions as manifestations of the substructure of leptons and quarks. *Physics Letters B*, 1981, v. 102(5), 319–322.
15. Dehmelt H.G. Experiments with an Isolated Subatomic Particle at Rest. *Nobel Lecture*, 1989.
16. Dugne J.J. Higgs pain? Take a preon! arXiv: hep-ph/9709227.
17. D’Souza I.A.; Kalman C.S. Preons: Models of Leptons, Quarks and Gauge Bosons as Composite Objects. *World Scientific*, 1992.
18. Bilson-Thompson S. A topological model of composite preons. arXiv: hep-ph/0503213.
19. Yershov V.N. Fermions as topological objects. *Progress in Physics*, 2006. v. 2 (4), 19–26.
20. Lucas C.W. A Classical theory of elementary particles. Part 2. Intertwining charge-fibers. *The Journal of Common Sense Science*, 2005, v. 8(2), 1–7.
21. Rañada A. Topological electromagnetism. *J. Phys A: Math. Gen.*, 1992 vol. 25, 1621–1641.
22. Schuster A. Potential matter. A holiday dream. *Nature*, 1898, v. 58, 367.
23. Dirac P.A.M. A Theory of electrons and protons. *Proc. R. Soc. Lond. A*, 1930, v. 126, 360–365.
24. Oppenheimer J.R. On the theory of electrons and protons. *Physical Review*, 1930, v. 35, 562–563.
25. Jenkins J.H. Evidence for correlations between nuclear decay rates and Earth-Sun distance, arXiv:0808.3283.

On the Acceleration of Free Fall inside Polyhedral Structures

Hartmut Müller, Renata Angeli, Roberta Baccara, Flavia Contenti, Rose Line Hofmann, Simona Muratori, Giuliana Papa, Francesca Santoni, Alessandro Turiano, Simona Turiano, Claudio Venegoni, Leili Khosravi

E-mail: hm@interscalar.com

In this paper we develop a fractal model of matter as stable eigenstates in chain systems of harmonic quantum oscillators and derive a fractal scalar field that should affect any type of physical interaction, regardless of its complexity. Based on this assumption, we discuss series of experiments on the timing of free falling solid particles inside polyhedral structures whose boundaries coincide with equipotential surfaces of the field.

Introduction

An essential aspect of scientific research is the distinction between empirical facts and theoretical models. This is not only about honesty and ethics in science, but a crucial condition of its evolution. The scientist should always be aware of this.

The nature and origin of gravitation is a key topic in modern physics. Gravitation manifests itself as universal force of attraction. It decreases with increasing distance, but it is thought as having unlimited range. Unlike electrical or magnetic forces, gravitation is considered as to be not shieldable.

The term 'gravitational shielding' is usually imagined as effect of reducing the weight of an object located in a constant gravitational field, neither changing the mass of the object nor its location in that field. Gravitational shielding is considered to be a violation of the equivalence principle and therefore inconsistent with both Newtonian theory and general relativity.

Nevertheless, some experimental evidence [1] indicates that such effect might exist under quite exotic conditions in which a superconductor is subjected to peak currents in excess of 10^4 A, surface potentials of 10^6 V, magnetic fields up to 1 T, and temperature down to 40 K.

In the context of classical physics, mass is considered as source of gravitation described by the Newtonian 'law of universal gravitation' as an instantaneous force acting through empty space. A fundamentally different understanding of gravitation arises from Einstein's general theory of relativity. In this case, gravity acts through a hypothetical 'curvature of space-time', while any kind of energy can cause it.

Gravitation is treated as dominant force at macroscopic scales that forms the shape and trajectory (orbit) of astronomical bodies including stars and galaxies. Advanced models were developed [2–4] in the last century which explain essential features of the formation of the solar system. Though, if numerous bodies are gravitationally bound to one another, classic models predict long-term highly unstable states that contradict with the astrophysical reality in the solar system.

Furthermore, many metric characteristics of the solar system are not predicted in standard models. A remarkably large number of coincidences are considered to be accidental and are not even topics of theoretical research. Until today none of the standard models of gravitation could explain why the solar system has established Jupiter's orbital period at 11.86 years and not 10.27 or 14.69 years; why the Sun and the Moon, the gas giant Jupiter and the planetoid Ceres, but also Earth and Mars have similar rotation periods; why Venus and Uranus, as well as Mars and Mercury have similar surface gravity accelerations; why several exoplanets in the Trappist 1 system have the same orbital periods as the moons of Jupiter, Saturn and Uranus etc. etc.

The standard theory of gravitation experiences also exceptional difficulties to explain the dynamics in star systems. The orbital velocities of stars should decrease in an inverse square root relationship with the distance from the Galactic Center, similar to the orbital velocities of planets in the solar system. But this is not observed. Outside of the central galactic bulge the orbital velocities are nearly constant.

Already in 1933, Fritz Zwicky [5] discovered that the fast movement of the galaxies in the Coma Cluster cannot be explained by the gravity effect of the visible galaxies only and hypothesized the existence of unseen mass that he called 'dark matter'. In 1957, Henk van de Hulst and then in 1959, Louise Volders demonstrated that the galaxies M31 and M33 do not spin as expected in accordance with Kepler's laws.

According to the hypothesis of mass as source of gravity, this deviation might be explained by the existence of a substantial amount of matter flooding the galaxy that is not emitting light and interacts barely with ordinary matter and therefore it is not observed. To explain the dynamics in galaxies and clusters, standard theories of gravitation need a lot of dark matter - 85% of the matter in the universe. Even particle physics has no idea what dark matter could be.

Nevertheless, it is still believed that gravitation of mass determines the orbits of planets and moons, planetoids and asteroids, comets and artificial satellites, and in the cosmos, the formation of stars and galaxies and their evolution. It is also thought that it is the mass of the Earth that causes all bodies to fall 'down'.

The universality of free fall means that the gravity acceleration of a test body at a given location does not depend on its mass, form, physical state or chemical composition. This

discovery, made four centuries ago by Galilei, is confirmed by modern empirical research with an accuracy of $10^{-11} - 10^{-12}$. A century ago Einstein supposed that gravity is indistinguishable from, and in fact the same thing as, acceleration. Indeed, Earth's surface gravity acceleration can be derived from the orbital elements of any satellite, also from Moon's orbit:

$$g = \frac{\mu}{r^2} = \frac{\mu}{(6372000\ \mathrm{m})^2} = 9.82\ \mathrm{m/s^2}$$

$$\mu = 4\pi\frac{R^3}{T^2} = 3.9860044 \cdot 10^{14}\ \mathrm{m^3/s^2}$$

where R is the semi-major axis of Moon's orbit, T is the orbital period of the Moon and r is the average radius of the Earth. No data about the mass or chemical composition of the Earth or the Moon is needed.

The 3^{rd} law of Johannes Kepler describes the ratio R^3/T^2 as constant for a given orbital system. Kepler's discovery is confirmed by high accuracy radar and laser ranging of the movement of artificial satellites.

Actually, Kepler's 3^{rd} law is of geometric origin and can be derived from Gauss's flux theorem in 3D-space within basic scale considerations. It applies to all conservative fields which decrease with the square of the distance and does not require the presence of mass.

It is important to underline that the orbital elements R and T are measured, but $\mu = GM$ is a theoretical presumption that provides mass as a source of gravity and the universality of the coefficient G, the 'gravitational constant'.

One of the basic principles of scientific research is the falsifiability of a theory. Occam's Razor that expresses the preference for simplicity in the scientific method is mainly based on the falsifiability criterion: simpler theories are more testable.

Obviously, any theory that postulates gravitation of mass as dominant forming factor of the solar system and the galaxy is not falsifiable, because there is no independent method to measure the mass of a celestial body. Actually, no mass of any celestial body is measured, but only calculated based on the theoretical presumption $\mu = GM$, and G is estimated in laboratory scale only.

This does not mean that those theories are compellingly wrong, but it should not surprise anyone if the assumption G = constant leads to problems in describing processes that differ by 40 orders of magnitude.

The big G is known only to three decimals, because gravity appears too weak on the scale of laboratory-sized masses for to be measurable with higher precision. As mentioned Quinn and Speake [6], the discrepant results may demonstrate that we do not understand the metrology of measuring weak forces or they may signify some new physics.

In the case of mass as source of gravity, in accordance with Newton's shell theorem, a solid body with a spherically symmetric mass distribution should attract particles outside it as if its total mass were concentrated at its center. In contrast, the attraction exerted on a particle should decrease as the particle goes deeper into the body and it should become zero at the body's center.

The Preliminary Reference Earth Model [7] affirms the decrease of the gravity acceleration with the depth. However, this hypothesis is still under discussion. In 1981, Stacey, Tuck, Holding, Maher and Morris [8, 9] reported anomalous measures (larger values than expected) of the gravity acceleration in deep mines and boreholes. In [10] Frank Stacey writes: "Modern geophysical measurements indicate a 1% difference between values at 10 cm and 1 km (depth). If confirmed, this observation will open up a new range of physics".

Anomalies have been discovered also under conditions of microgravity – in drop towers, abroad the NASA Space Shuttle and the ISS. Whenever an object is in free fall the condition of microgravity comes about. Microgravity significantly alters many processes – the behavior of liquids [11], plasma and granular materials [12, 13] as well, and there is no complete explanation for all the discovered phenomena yet.

Studies [14] of plant growth under different gravity conditions show that elongation growth is stimulated under microgravity conditions. Elongation growth is suppressed with increasing gravitational acceleration and varies in proportion to the logarithm of the magnitude of gravitational acceleration in the range from microgravity to hypergravity.

Already in 2010, Erik Verlinde [15] proposed an alternative explanation of gravitation as an entropic force caused by changes in the information associated with the positions of material bodies. An entropic force is thought as an effective macroscopic force that originates in a system with many degrees of freedom by the statistical tendency to increase its entropy. The term 'entropic force' was introduced by Bechinger and Grünberg [16] when they did demonstrate that in systems of particles of different sizes, entropy differences can cause forces of attraction between the largest particles. However, entropic models of gravitation [17] are still in development and under discussion [18].

It is remarkable that similar dynamics of plant growth observed in laboratory [19] and field experiments [20] are also known as the 'pyramid effect': Inside pyramidal constructions made of various materials, germination and elongation growth of plants are accelerated.

The diversity of sizes and materials (glass, plastic, wood, stone, metal) applied in the pyramidal constructions makes difficult to define the cause of the observed growth stimulation. At the same time, even this diversity supports the suspicion that the 'pyramid effect' could be caused by reduction of gravitation – as it is the most universal physical interaction.

To verify this hypothesis, we have designed an experimental setup that models the free fall of solid particles inside containers of various sizes, shapes and materials. The experimental design is based on global scaling [21] and considers Kosyrev's [22] temporal studies.

Methods

In [23] we have introduced a fractal model of matter as stable eigenstates in chain systems of harmonic quantum oscillators and could show the evidence of this model for all known hadrons, mesons, leptons and bosons as well. On this background, atoms and molecules emerge as eigenstates of stability in fractal chain systems of harmonically oscillating protons and electrons. Andreas Ries [24] demonstrated that this model allows for the prediction of the most abundant isotope of a given chemical element.

In [25] we have shown that the set of stable eigenstates in chain systems of harmonic quantum oscillators is fractal and can be described by finite continued fractions:

$$\mathcal{F}_{jk} = \ln(\omega_{jk}/\omega_{00}) = [n_{j0}; n_{j1}, n_{j2}, \ldots, n_{jk}]$$

where ω_{jk} is the set of angular eigenfrequencies and ω_{00} is the fundamental frequency of the set. The denominators are integer: $n_{j0}, n_{j1}, n_{j2}, \ldots, n_{jk} \in \mathrm{Z}$, the cardinality $j \in \mathrm{N}$ of the set and the number $k \in \mathrm{N}$ of layers are finite. In the canonical form, all numerators equal 1.

Any finite continued fraction represents a rational number [26]. Therefore, the ratios ω_{jk}/ω_{00} of eigenfrequencies are always irrational, because for rational exponents the natural exponential function is transcendental [27].

This circumstance provides for lasting stability of those eigenstates of a chain system of harmonic oscillators because it prevents resonance interaction [28, 29] between the elements of the system. In [30, 31] we have applied our model as criterion of stability in engineering.

The distribution density of stable eigenstates reaches local maxima near reciprocal integers $\pm 1/2, \pm 1/3, \pm 1/4, \ldots$ that are the subattractor points in the fractal set $\mathcal{F}_{jk}$ of natural logarithms (fig. 1). Integer logarithms $0, \pm 1, \pm 2, \ldots$ represent the most stable eigenstates (main attractors).

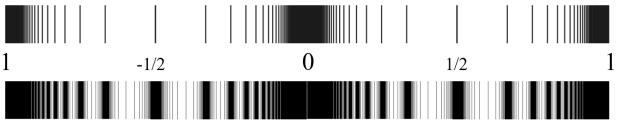

Fig. 1: The distribution of stable eigenvalues of $\mathcal{F}_{jk}$ for $k = 1$ (above) and for $k = 2$ (below) in the range $-1 \leqslant \mathcal{F}_{jk} \leqslant 1$.

In the case of harmonic quantum oscillators, the continued fractions $\mathcal{F}_{jk}$ define not only fractal sets of natural angular frequencies ω_{jk}, angular accelerations $a_{jk} = c \cdot \omega_{jk}$, oscillation periods $\tau_{jk} = 1/\omega_{jk}$ and wavelengths $\lambda_{jk} = c/\omega_{jk}$ of the chain system, but also fractal sets of energies $\mathrm{E}_{jk} = \hbar \cdot \omega_{jk}$ and masses $\mathrm{m}_{jk} = \mathrm{E}_{jk}/c^2$ which correspond with the eigenstates of the system. For this reason, we call the continued fraction $\mathcal{F}_{jk}$ the 'Fundamental Fractal' of stable eigenstates in chain systems of harmonic quantum oscillators.

The spatio-temporal projection of the Fundamental Fractal $\mathcal{F}_{jk}$ of stable eigenstates is a fractal scalar field of transcendental attractors, the Fundamental Field.

The connection between the spatial and temporal projections of the Fundamental Fractal is given by the speed of light $c = 299792458$ m/s. The constancy of c makes both projections isomorphic, so that there is no arithmetic or geometric difference. Only the units of measurement are different.

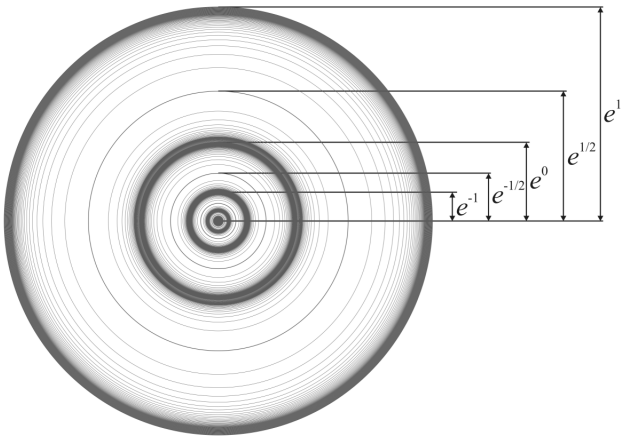

Fig. 2: The equipotential surfaces of the Fundamental Field in the linear 2D-projection for $k = 1$.

Figure 2 shows the linear 2D-projection $\exp(\mathcal{F}_{jk})$ of the first layer of the Fundamental Field for $\mathcal{F}_{j1} = n_{j0} + 1/n_{j1}$ in the interval $-1 < \mathcal{F}_{j1} < 1$. Figure 1 shows the same interval in the logarithmic representation.

At each layer k, the potential energy of the Fundamental Field is constant, therefore the layers are equipotential surfaces. The potential difference defines a gradient, a vector directed to the center of the field that causes a central force of attraction. However, the gradient exposes the logarithmically hyperbolic fractal metric of the Fundamental Field.

The Fundamental Field does not propagate, it is omnipresent. As spatio-temporal projection of the Fundamental Fractal, it is an inherent feature of the number continuum and it causes the fractality of the model space-time.

In physics, only field distortions (waves or currents), not the fields themselves have propagation speeds. In astronomic calculations, gravitation is traditionally considered as being instantaneous. First Laplace [32] demonstrated that gravitation as field does not propagate with the speed of light c. Modern estimations [33] confirm a lower limit of $2 \cdot 10^{10}\, c$.

The Fundamental Field is of pure mathematical origin, and there is no particular physical mechanism required as field source. It is all about numbers as ratios of physical quantities which inhibit destabilizing resonance. In this way, the Fundamental Field concerns all repetitive processes which share at least one characteristic — the frequency.

Therefore, we assume the universality and unity of the Fundamental Field. It might signify that everything in the universe is part of one giant oscillating chain system. This hypothesis we have called 'global scaling' and it is the basis of interscalar cosmology [34].

In fact, scale relations in particle physics [23, 35, 36] and nuclear physics [24, 37, 38], astrophysics [39, 40] and biophysics [41,42] follow always the same Fundamental Fractal calibrated on the proton and electron, without any additional or particular settings. The proton-to-electron mass ratio itself is caused by the Fundamental Fractal [34].

Planetary and lunar orbits [43] correspond with equipotential surfaces of the Fundamental Field, as well as the metric characteristics of stratification layers in planetary atmospheres [44] and lithospheres [21]. Surface gravity accelerations [45] of the planets in the solar system correspond with attractors of stability in chain systems of oscillating protons and electrons. From this point of view, the metric characteristics of stable structures origin always from the same Fundamental Fractal and different only in scale. Because of its numerical origin, we assume that the Fundamental Field affects any type of physical interaction, regardless of its complexity.

Based on this assumption, we have designed an experimental setup that models the free fall of solid particles inside a container whose boundaries coincide with equipotential surfaces of the Fundamental Field $\exp(\mathcal{F}_{jk})$. The experimental setup consists of a vacuum hourglass (sand clock) and a closed container. The duration of the hourglass was measured inside and outside the container in alternating sequence.

Three different in size, material and duration (40 s, 8 min, 60 min) hourglasses and 18 different in shape (cubic, tetrahedral, octahedral), size (0.3 – 0.6 m diameter) and material (carton, acrylic glass, metal) containers were used.

Based on relevant studies [46], we conducted mechanical tests of the utilized hourglasses and could make sure that inclination below 5 degrees, rotation below 5 Hz and microvibration (vertical and horizontal) below 10 Hz do not increase the average fluctuation level (0.2 %) of the duration of the hourglasses.

The accuracy of the vertical was controlled by two orthogonal spirit levels. The complete setup was placed in an electromagnetic shielding chamber. During the measurement, the hourglass had direct contact to an aluminum plate for conduction of eventual electrostatic charge.

The environment control included electromagnetic fields in the frequency range of 1 Hz to 5 GHz, air temperature, pressure and humidity, micro-seismic activity. The experiments were conducted in different places, but always far from the city electrification net.

Results

In general, the measured deviations of the hourglass durations inside containers of different material, shape and size in comparison with the durations outside them did not exceed the average fluctuation level of the duration of the used hourglass. However, a stable significant deviation in the hourglass duration was measured with the 8-minute vacuum hourglass inside a closed truncated octahedron (fig. 3) made of 1/16 aluminum sheet. The 'sand' of this hourglass consists of glass beads of ca. 50 μm diameter.

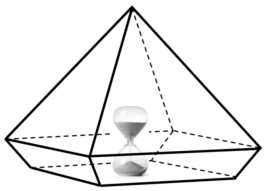

Fig. 3: The duration of the 8-minute hourglass was measured inside and outside the truncated octahedron in alternating sequence.

The truncated octahedron one can imagine as a square pyramid plus an inversed square frustum (fig. 3). The length of the edges of the pyramid coincides with the radius of the main equipotential surface $\mathcal{F}(35)$ of proton stability:

$$\mathcal{F}(35) = \lambda_{\text{proton}} \cdot \exp(35) = 33 \text{ cm}$$

Considering the height $r = 33 \text{ cm} \cdot \sqrt{2}/2 = 23$ cm of the pyramid, the orifice of the hourglass was placed in a distance from the vertices of the pyramid that equals to the radius of the main equipotential surface $\mathcal{F}(27)$ of electron stability:

$$\mathcal{F}(27) = \lambda_{\text{electron}} \cdot \exp(27) = 21 \text{ cm}$$

The height 7.5 cm of the frustum coincides with the radius of the main equipotential surface $\mathcal{F}(26)$ of electron stability:

$$\mathcal{F}(26) = \lambda_{\text{electron}} \cdot \exp(26) = 7.5 \text{ cm}$$

Furthermore, at 6 minutes after start, the continuing process of free fall passes the main temporal attractor $\mathcal{F}(54)$ of electron stability:

$$\mathcal{F}(54) = \tau_{\text{electron}} \cdot \exp(54) = 6 \text{ min}$$

The Compton angular wavelength of the electron is $\lambda_{\text{electron}} = 3.86159\dot{1}0^{-13}$ m, of the proton $\lambda_{\text{proton}} = 2,10308\dot{1}0^{-16}$ m, and the angular oscillation period of the electron is $\tau_{\text{electron}} = \lambda_{\text{electron}}/c = 1.28808\dot{1}0^{-21}$ s [47].

Probably, all these coincidences together caused an accumulated effect of damping the acceleration of free fall. Furthermore, we suppose that potential differences between equipotential surfaces of the Fundamental Field can change the entropy of the involved processes.

In series of crystallization experiments, we observed that inside the same truncated octahedron, sodium chloride crystals grow in salt solutions with concentrations far below the saturated concentration and develop octahedral shapes like diamonds instead of cubic.

The most widely accepted law that predicts the flowrate of mono-sized grains through an orifice and its dependence on different parameters was proposed by Beverloo, Leniger and van de Velde [48, 49]. They have shown that under otherwise

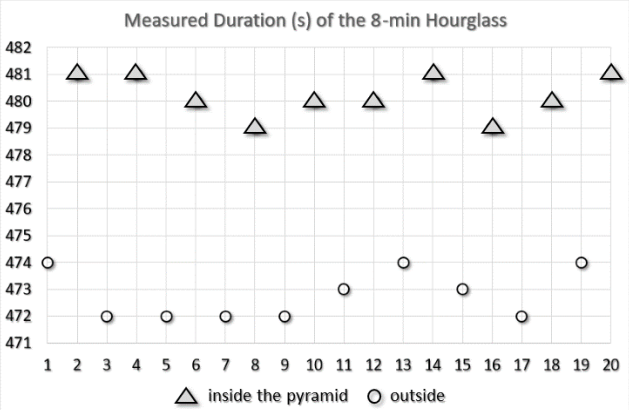

Fig. 4: Time series of the alternating measurements of the hourglass duration (s) inside the truncated octahedron (pyramid) and outside.

constant conditions k, the mass flowrate W is proportional to the square root of the gravity acceleration g:

$$W = k\sqrt{g}$$

This equation coincides with Torricelli's law for the speed of fluid flowing out of an orifice and allows for estimation of the equivalent gravity reduction Δg that corresponds to the ratio of the measured durations inside and outside the octahedron:

$$\Delta g = g\left(\frac{t_{\text{outside}}}{t_{\text{inside}}}\right)^2 - g$$

Table 1 contains representative samples of the durations measured inside and outside the truncated octahedron and the calculated corresponding equivalent gravity reduction in units of g. Fig. 1 shows time series of the alternating measurements.

series	out, s	inside, s	inside/out-1, %	Δg
1	474	481	1.48	-0.283
2	472	481	1.91	-0.364
3	472	480	1.69	-0.324
4	472	479	1.48	-0.285
5	472	480	1.69	-0.324
6	473	480	1.48	-0.284
7	474	481	1.48	-0.283
8	473	479	1.27	-0.244
9	472	480	1.69	-0.324
10	474	481	1.48	-0.283
average	473 ± 1	480 ± 1	1.57	-0.300

Table 1: The measured duration (s) of the 8-minute hourglass inside the truncated octahedron and outside, the relative deviation and the equivalent gravity reduction in units of g.

Over all series of the total 255 hours of measurements, the fluctuation level of the hourglass durations inside and outside the truncated octahedron did not exceed 0.2 %. The relative difference of the durations inside and outside the octahedron did not fall below 1.2%. The average relative difference was 1.67% that corresponds to an equivalent gravity reduction of -0.324 g inside the octahedron. Outside the octahedron, this amount of gravity reduction would correspond to an altitude of 100 km over sea level.

Only inside the described truncated octahedral container we observed a stable significant deviation in the duration of the hourglass, regardless of the location and time. In containers of different shape and size, even made of the same 1/16 aluminum sheet, the measured deviations did not exceed the average fluctuation level of the hourglass duration.

Currently we have no explanation for the extraordinariness of the octahedral (pyramidal) shape. However, in Finslerian multi-dimensional time models, the pseudo-Euclidean light cone becomes a light pyramid [50].

Conclusion

We are aware that our experiments cannot claim to be conclusive. However, they could point out that gravity is not just about the amount of the involved masses and energies. It may well be that 'subtle' factors like the spatial configuration of the system and its scale have higher influence than expected.

Acknowledgements

The authors are grateful to the Community of Living Ethics for permanent support on all stages of the study.

Submitted on September 20, 2018

References

1. Podkletnov E., Modanese G. Impulse Gravity Generator Based on Charged $YBa_2Cu_3O_{7-y}$ Superconductor with Composite Crystal Structure. arXiv:physics/0108005v2 [physics.gen-ph], (2001).
2. Williams I.O., Cremin A.W. A survey of theories relating to the origin of the solar system. *Qtly. Rev. RAS*, 1968, v. 9, 40–62.
3. Van Flandern T. Our Original Solar System – a 21st Century Perspective. *MetaRes. Bull.*, 2008, v. 17, 2–26.
4. Woolfson M.M. Planet formation and the evolution of the Solar System. arXiv:1709.07294, (2017).
5. Zwicky F. On the Masses of Nebulae and of Clusters of Nebulae. *The Astrophysical Journal*, 1937, v. 86, 217.
6. Quinn T., Speake C. The Newtonian constant of gravitation – a constant too difficult to measure? An introduction. *Phil. Trans. Royal Society A*, 2014, v. 372, 20140253.
7. Dziewonski A.M., Anderson D.L. Preliminary reference Earth model. *Physics of the Earth and Planetary Interiors*, 1981, v. 25, 297–356.
8. Stacey F.D. et al. Constraint on the planetary scale value of the Newtonian gravitational constant from the gravity profile within a mine. *Phys. Rev. D*, 1981, v. 23, 1683.
9. Holding S.C., Stacey F.D., Tuck G.J. Gravity in mines. An investigation of Newton's law. *Phys. Rev. D*, 1986, v. 33, 3487.
10. Stacey F.D. Gravity. *Science Progress*, 1984, v. 69, no. 273, 1–17.
11. Kundan A. et al. Condensation on Highly Superheated Surfaces: Unstable Thin Films in a Wickless Heat Pipe. *Phys. Rev. Lett.*, 2017, v. 118, 094501.
12. Alshibli Kh. et al. Strain Localization in Sand: Plane Strain versus Triaxial Compression. *Journal of Geotechnical and Geoenvironmental Engineering*, 2003, v. 129, no. 6.

13. Alshibli Kh. Behavior of granular materials in microgravity environment: implication for future exploration missions. *Infrastruct. Solut.*, 2017, v. 2, 22.
14. Hoson T. Plant Growth and Morphogenesis under Different Gravity Conditions: Relevance to Plant Life in Space. *Life*, 2014, v. 4, 205–216.
15. Verlinde E. On the Origin of Gravity and the Laws of Newton. arXiv:1001.0785v1 [hep-th], (2010).
16. Bechinger C., Grünberg H., Leiderer P. Entropische Kräfte. *Physikalische Blätter*, 1999, v. 55, no. 12.
17. Nicolini P. Entropic force, noncommutative gravity and ungravity. arXiv:1005.2996v3 [gr-qc], (2010).
18. Kobakhidze A. Gravity is not an entropic force. arXiv:1009.5414v2 [hep-th], (2010).
19. Motloch L.N. Effects of Pre-Sowing Incubation within a Pyramid on Germination and Seedling Growth of Phaseolus Vulgaris L. // Master of Science Thesis, Tarleton State University, (2017).
20. Skliarov A. Biological Experiments in the Egyptian Pyramids. LAH, www.lah.ru, (2009).
21. Müller H. Quantum Gravity Aspects of Global Scaling and the Seismic Profile of the Earth. *Progress in Physics*, 2018, v. 14, 41–45.
22. Kosyrev N.A. Astronomical observations through the physical properties of time. // Kosyrev N. A. Selected Works. Leningrad, 363–383, (1991).
23. Müller H. Fractal Scaling Models of Natural Oscillations in Chain Systems and the Mass Distribution of Particles. *Progress in Physics*, 2010, v. 6, no. 3, 61–66.
24. Ries A. Qualitative Prediction of Isotope Abundances with the Bipolar Model of Oscillations in a Chain System. *Progress in Physics*, 2015, v. 11, 183–186.
25. Müller H. Scale-Invariant Models of Natural Oscillations in Chain Systems and their Cosmological Significance. *Progress in Physics*, 2017, vol. 13, 187–197.
26. Khintchine A.Ya. Continued fractions. University of Chicago Press, Chicago, (1964).
27. Hilbert D. Über die Transcendenz der Zahlen e und π. *Mathematische Annalen*, 1983, v. 43, 216–219.
28. Dombrowski K. Rational Numbers Distribution and Resonance. *Progress in Physics*, 2005, v. 1, no. 1, 65–67.
29. Panchelyuga V.A., Panchelyuga M. S. Resonance and Fractals on the Real Numbers Set. *Progress in Physics*, 2012, v. 8, no. 4, 48–53.
30. Müller H. The general theory of stability and objective evolutionary trends of technology. Applications of developmental and construction laws of technology in CAD. Volgograd, VPI, (1987).
31. Müller H. Superstability as a developmental law of technology. Technology laws and their Applications. Volgograd-Sofia, (1989).
32. Laplace P. Mechanique Celeste. pp. 642–645, (1825).
33. Van Flandern T. The Speed of Gravity — What the Experiments Say. *Physics Letters A*, 1998, v. 250, 1–11.
34. Müller H. Global Scaling. The Fundamentals of Interscalar Cosmology. *New Heritage Publishers*, Brooklyn, New York, USA, (2018).
35. Müller H. Emergence of Particle Masses in Fractal Scaling Models of Matter. *Progress in Physics*, 2012, v. 8, no. 4, 44–47.
36. Ries A. A Bipolar Model of Oscillations in a Chain System for Elementary Particle Masses. *Progress in Physics*, 2012, v. 8, no. 4, 20–28.
37. Ries A., Fook M. Fractal Structure of Nature's Preferred Masses: Application of the Model of Oscillations in a Chain System. *Progress in Physics*, 2010, v. 6, no. 4, 82–89.
38. Ries A. The Radial Electron Density in the Hydrogen Atom and the Model of Oscillations in a Chain System. *Progress in Physics*, 2012, v. 8, no. 3, 29–34.
39. Müller H. Fractal scaling models of natural oscillations in chain systems and the mass distribution of the celestial bodies in the Solar System. *Progress in Physics*, 2010, v. 6, no. 4, 44–47.
40. Müller H. Global Scaling as Heuristic Model for Search of Additional Planets in the Solar System. *Progress in Physics*, 2017, v. 13, 204–206.
41. Müller H. Chain Systems of Harmonic Quantum Oscillators as a Fractal Model of Matter and Global Scaling in Biophysics. *Progress in Physics*, 2017, v. 13, 231–233.
42. Müller H. Astrobiological Aspects of Global Scaling. *Progress in Physics*, 2018, v. 14, 3–6.
43. Müller H. Global Scaling of Planetary Systems. *Progress in Physics*, 2018, v. 14, 99–105.
44. Müller H. Global Scaling of Planetary Atmospheres. *Progress in Physics*, 2018, v. 14, 66–70.
45. Müller H. Gravity as Attractor Effect of Stability Nodes in Chain Systems of Harmonic Quantum Oscillators. *Progress in Physics*, 2018, v. 14, 19–23.
46. Staude J. Untersuchung granularer Materie am Beispiel des Laufzeitverhaltes einer Sanduhr unter Einwirkung äußerer Kräfte. Bachelor Thesis Physics, Freie Universität Berlin, (2013).
47. Olive K.A. et al. (Particle Data Group), Physical Constants. *Chin. Phys. C*, 2016, v. 38, 090001.
48. Beverloo W.A., Leniger H.A., van de Velde J. The flow of granular solids through orifices. *Chem. Eng. Sci.*, 1961, v. 15, 260–269.
49. Mankoc C. et al. The flow rate of granular materials through an orifice. arXiv:0707.4550v1 [cond-mat.soft], (2007).
50. Pavlov D.G. Chronometry of the Three-Dimensional Time. // Space-Time Structure. Algebra and Geometry. Russian Hypercomplex Society, Moscow, (2007).

Janus Cosmological Model and the Fluctuations of the CMB

Jean-Pierre Petit
E-mail: jp.petit@mailaps.org

It is shown than, in the framework of the Janus Cosmological Model the gravitational instability which occurs in the negative sector makes an imprint in the positive one, which corresponds to the CMB inhomogeneities. So that their characteristic wavelength gives the ratio of the space scale factors of the two sectors, which differ from two orders of magnitude. Subsequently the speed of light in the negative sector is ten times highers than ours. So that, given to distant points, if the travel between them is managed along the negative geodesics paths, the corresponding travel time is reduced by a factor one thousand.

1 Introduction

A cosmological model must take account of the observations. From this point of view a recent paper [1] showed that the the Janus Cosmological Model (JCM) fits many.

- JCM explains the absence of observation of the so called primeval antimatter, opposite to the mainstream ΛCDM model.
- JCM describes precisely the nature of the invisible components of the universe, opposite to the mainstream ΛCDM model.
- JCM predicts that the antimatter produced in laboratory will react as the matter with respect to the gravitational field of the Earth (it will fall).
- Because positive and negative matter are repelling each other, the negative matter in the solar system is almost zero. So, JCM fits the classical relativistic observation, as presented in former papers [2, 3].
- JCM suggests a clear schema for VLS formation [4] when the mainstream model ΛCDM seems to struggle to give one.
- JCM explains the observed strange effect due to the Great Repeller [5]. The measured escape velocities of galaxies are due to the presence of an invisible repellent cluster made of negative mass, located in the centre of the big void. The mainstream model supporters suggest that such a repellent effect could be due to some kind of a hole in the dark matter field of the universe (positive masses). But, if the gravitational instability leads to the setting up of massive clusters, it does not provide ant scheme for such void formations. So that the mainstream model ΛCDM does not provide any explanation of the observation.
- JCM explains the confinement of galaxies and their flat rotation curves [1, 6]. Mysterious dark matter is no longer required, while the mainstream model ΛCDM does.
- After JCM the intensity of the observed gravitational lensing effect is mainly due to the negative matter that surrounds galaxies and clusters of galaxies. Mysterious dark matter is no longer required, while the mainstream model ΛCDM does.
- JCM suggests an explanation of the low magnitude of very young galaxies: this would be due to the negative lensing weakening, when their light are crossing the negative mass clusters located at the center of the big voids.
- JCM explains the spiral structure of galaxies, due to dynamical friction with the surrounding mass [1, 6]. The model ΛCDM don't give any model explaining the spiral structure.
- JCM explains the acceleration of the universe [1]. The so-called dark energy is the one associated to the negative mass content through $E = \rho c^2$, with $\rho < 0$.
- JCM explains the homogeneity of the primeval universe [2, 16].

JCM is definitively not a simple or pure product of mathematical physics. But it represents a deep paradigmatic change, on geometrical grounds. In the Einstein's model the universe is considered as a manifold, whose geometry corresponds to a single metric field , solution of a single field equation, without cosmological constant:

$$R_{\mu\nu} - \frac{1}{2} R\, g_{\mu\nu} = \chi T_{\mu\nu} \,. \tag{1}$$

Such model automatically generates the unmanageable runaway effect [7, 8], just because, if imbedded in a given gravitation field (the term $T_{\mu\nu}$), positive and negative masses react the same way (a single metric solution $g_{\mu\nu}$). If we give up such restrictive and non-logical hypothesis it means that, imbedded in a given gravitation field the geodesics of the two species derive from two metrics fields $g^{(+)}_{\mu\nu}$ and $g^{(-)}_{\mu\nu}$, solutions of two coupled field equations, as derived from Lagrangian method [9, 10].

$$\begin{aligned} R^{(+)}_{\mu\nu} - \frac{1}{2} R^{(+)}\, g^{(+)}_{\mu\nu} &= +\chi \left(T^{(+)}_{\mu\nu} + \sqrt{\frac{g^{(-)}}{g^{(+)}}}\, T^{(-)}_{\mu\nu} \right), \\ R^{(-)}_{\mu\nu} - \frac{1}{2} R^{(-)}\, g^{(-)}_{\mu\nu} &= -\chi \left(T^{(-)}_{\mu\nu} + \sqrt{\frac{g^{(+)}}{g^{(-)}}}\, T^{(+)}_{\mu\nu} \right). \end{aligned} \tag{2}$$

The physical meaning of the presence of the two square roots in the second members is the energy conservation requirement. We have a single manifold M_4, with two tensor fields $T^{(+)}_{\mu\nu}$ and $T^{(-)}_{\mu\nu}$, which refer to positive and negative mass contents. In some regions $T^{(+)}_{\mu\nu}$ dominates, in other $T^{(-)}_{\mu\nu}$ dominate. In others the two are zero. In any case we find everywhere two families of geodesics, as derived from the metric $g^{(+)}_{\mu\nu}$ and $g^{(-)}_{\mu\nu}$. The first refers to the paths of positive mass particles, and positive energy photons (null positive geodesics). The second refers to the paths of negative mass particles, and negative energy photons (null negative geodesics).

On pure geometric grounds the negative mass objects are invisible to us, because they emit negative energy photons that positive mass devices cannot capture. And vice versa. The positive and negative masses interact only trough (anti) gravitation.

The classical Newton's law comes from the Einstein's equation (1) through Newtonian approximation (small curvature, velocities small with respect to the speed of light, quasi Lorentzian metric).

Similarly from the system (2) we get [3, 11] the following Newtonian, and antinewtonian interaction laws:

- Positive masses do attract together, through Newton' law;
- Negative masses do attract together, through Newton's law;
- Opposed masses do repel each other, through anti Newton's law.

This interaction scheme fits the action-reaction principle.

The nature of the invisible components of the universe are determined from dynamic group theory [6, 12]. They are a copy of the ordinary antiparticles, with negative energy. This schema fits initial Sakharov's idea [13–15].

As evoked in [17], JCM may produce an original scheme for galaxies' formation. The structures of the positive and negative sectors are fairly different. After discoupling, with $\rho^- \gg \rho^+$, spheroidal globular clusters form first, the matter being confined in the remnant place, getting an alveolar structure. The compression of positive matter along flat structure is optimum for radiative cooling and Jeans' instability triggering, giving galaxies, stars and heavy atoms. At the contrary the negative mass antimatter is confined in spheroidal objects, that can be compared to huge proto-stars that will never ignite because their cooling time is longer that the age of the universe. As a consequence no galaxies, no stars, no heavy atomes and planets can form. Life is absent from such negative world.

2 A short remark about another model with negative mass

The model of L. Blanchet and G. Chardin is based on the Einstein's equation, so that the runaway effect belongs to it, which does not worry the authors.

Their scheme suggests, without theoretical grounds, that the primeval antimatter could have a negative mass.

From the Einstein's equation the interaction laws between positive and negative masses is the following (which contains the runaway effect):

- Positive masses mutually attract through the Newton's law;
- Negative masses mutually repel through "anti-Newton's law";
- Positive masses are repelled by negative masses;
- Negative masses are attracted by positive masses;

which contradicts the action-reaction principle. Howevever L.Blanchet and G.Chardin think that, thanks to such interaction scheme the primeval (negative mass) antimatter could have survived somewhere.

About cosmological evolution the authors opt for the Dirac-Milne model [17], which corresponds to a constant null gravitational field, with a constantly global zero mass. Then the expansion is linear in time, which contradicts the recent observation of the acceleration of the expansion.

JCM shows that there are two forms of antimatter. The positive mass, we can call it "Dirac antimatter" (C-symmetrical of our matter) reacts as the ordinary matter, if imbedded in a gravitational field This is the antimatter we produce in laboratory, so that we predict that the antimatter weighted if the alpha experiment will fall down.

The negative mass antimatter corresponds to the primeval antimatter and is located between galaxies. We may call it "Feynmann antimatter" (PT-symmetrical from our ordinary matter).

3 How to determine the parameters in the negative sector

According to the "variable constants" evolution schema [2, 16] the two sectors correspond to two different sets of so-called constants, time plus scale parameters:

$$\begin{aligned} &\left\{ c^{(+)};\ G^{(+)};\ h^{(+)};\ e^{(+)};\ m^{(+)};\ \mu_0^{(+)};\ a^{(+)};\ t^{(+)} \right\},\\ &\left\{ c^{(-)};\ G^{(-)};\ h^{(-)};\ e^{(-)};\ m^{(-)};\ \mu_0^{(-)};\ a^{(-)};\ t^{(-)} \right\}. \end{aligned} \tag{3}$$

Where are space and time factors. In both sectors the so-called constants and space and time factors experience "joint gauge variations" which keep the equations of physics invariant. It means that if one chooses one of the eight parameters the other seven can be expressed using that one. For example:

$$\begin{aligned} &c^{(+)} \propto \frac{1}{\sqrt{a^{(+)}}}\,, \quad G^{(+)} \propto \frac{1}{a^{(+)}}\,, \quad h^{(+)} \propto (a^{(+)})^{3/2}\,,\\ &e^{(+)} \propto \sqrt{a^{(+)}}\,, \quad m^{(+)} \propto a^{(+)}\,, \quad t^{(+)} \propto (a^{(+)})^{3/2}\,;\\ &c^{(-)} \propto \frac{1}{\sqrt{a^{(-)}}}\,, \quad G^{(-)} \propto \frac{1}{a^{(-)}}\,, \quad h^{(-)} \propto (a^{(-)})^{3/2}\,,\\ &e^{(-)} \propto \sqrt{a^{(-)}}\ ;\ \ m^{(-)} \propto a^{(-)}\,, \quad t^{(-)} \propto (a^{(-)})^{3/2}\,. \end{aligned} \tag{4}$$

What is the ontological justification of such process? It makes no necessary to invoke inflation to justify the observed homogeneity of the primeval universe. In effect, the cosmological horizon becomes an integral [2, 16]:

$$horizon^{(+)} = \int c^{(+)}\, dt^{(+)} \propto a^{(+)}. \tag{5}$$

Same thing in the "negative sector".

A question arises immediately: when does this generalized gauge process era ends? This will be examined in a next paper.

Have a look on the Jeans' lengths $L_J^{(+)}$ and $L_J^{(-)}$ and times Jeans $t_J^{(+)}$ and $t_J^{(-)}$. In this gauge process all the velocities, including thermal velocities, vary like the speed of light of their corresponding sector:

$$\langle V^{(+)} \rangle \propto c^{(+)}\,, \qquad \langle V^{(-)} \rangle \propto c^{(-)} \tag{6}$$

so that

$$\begin{aligned} L_J^{(+)}\,, &\simeq a^{(+)}\,, \qquad & t_J^{(+)} &\simeq t^{(+)}\,, \\ L_J^{(-)}\,, &\simeq a^{(-)} \qquad & t_J^{(-)} &\simeq t^{(-)}\,. \end{aligned} \tag{7}$$

The fluctuations, due to gravitational instability are not observable in a given sector, by observers who live in.

Anyway, in a fully ionized plasma the strong link to the radiation backgrounds prevents clustering of matter in both sectors. What about the "gas of photons"?

4 Photons react to gravitational field

This gives the gravitational lensing effect. On another hand the photons contribute to the curvature. If the inertial mass of the photon is zero, we can introduce an individual equivalent gravitational mass of the photon:

$$\begin{aligned} m_\varphi^{(+)} &= \frac{h^{(+)}\, v^{(+)}}{c^{(+)2}} \propto a^{(+)} \propto m^{(+)}\,, \\ m_\varphi^{(-)} &= \frac{h^{(-)}\, v^{(-)}}{c^{(-)2}} \propto a^{(-)} \propto m^{(-)}\,. \end{aligned} \tag{8}$$

We may consider than the gravitational instability occurs in the "gaz of photons" but the corresponding Jeans' length becomes:

$$\begin{aligned} L_J^{(+)} &= \frac{c^{(+)}}{\sqrt{4\,\pi\, G^{(+)}\, \rho^{(+)}}} \simeq a^{(+)}\,, \\ L_J^{(-)} &= \frac{c^{(-)}}{\sqrt{4\,\pi\, G^{(-)}\, \rho^{(-)}}} \simeq a^{(-)}\,, \end{aligned} \tag{9}$$

again, such fluctuations in one sector cannot be observed by an observer that belongs to, because it extends beyond the corresponding cosmological horizon. But, from a conceptual point of view, this links to the idea of so-called "multivers". Beyond our cosmological universe we may consider that other "universes" extend, with different sets of physical constants and scale factors. But, as such they should obey the same equations, their histories would not be different from ours, giving, in the corresponding positive sectors, atoms, stars, galaxies, planets and life.

We get an infinite set of coupled (positive/negative mass) portions of the universe.

If the gravitational instability cannot occur in our sector of the universe, before decoupling, we have the imprint of such primeval instability, which occurs in the negative sector. We think that this produces the light inhomogeneities in the CMB.

The basic fluctuation extent is two order of magnitude smaller than the whole angular extent. It gives directly the order of magnitude of the ratio of the space scale factoirs. In the negative sector the fluctuations have a characteristic wavelength, so that the measure of the imprints in our sector gives the order of magnitude according to:

$$\frac{a^{(-)}}{a^{(+)}} \approx \frac{1}{100}\,. \tag{10}$$

As a conclusion, if we consider two points A and B of the manifold, we have two different lengths, which differ from the same ratio.

5 Link to the interstellar travel problem

During the gauge process era the two sectors experience evolution of their constants according to:

$$a^{(+)}\, c^{(+)2} = a^{(')}\, c^{(')2} = constant. \tag{11}$$

Combining with (10) we get:

$$\frac{c^{(-)}}{c^{(+)}} \approx 10. \tag{12}$$

According to the Einstein's model (1), interstellar travels at sub-relativistic velocity implies durations fairly incompatible with human lifetime. But if some distant civilizations could invert the mass of a vehicle (plus passengers) and travel along geodesics of the negative sector at $V^{(-)} < c^{(-)}$ the gain in time travel would correspond to three order of magnitude. So that a travel to, or from the nearest systems could be possible.

6 Conclusion

We review the many observational confirmations of the Janus Cosmological Model. We deal with the origin of the fluctuations in the CMB. Based on our primeval gauge process era, which explains the homogeneity of the primeval universe, without need to the inflation schema, we look at the gravitational instability during that era and show that the corresponding Jeans's length follows the extension of the cosmological horizon in both sectors. We notice that, even if we

cannot make observation beyond the horizon, other portions of the universe could be ruled by different sets of so-called constants and scale factors. This links to the idea of "Multiverse". But, according to ou scheme such sets should derive from the same set of equations, so that the physical, an biological evolution in such sectors should give the same patter (atoms, stars, planets, life).

We point out that such primeval gravitational instability, occurring in the negative sector, make an imprint in ours, and that corresponds to the observed fluctuations in the CMB.

Then it gives the measure of the ration of the two scale factors $\frac{a^{(+)}}{a^{(-)}} \approx 100$.

According to our gauge process scheme it corresponds to $\frac{c^{(-)}}{c^{(+)}} \approx 10$.

As a conclusion it shortens the travel time, for sub-relativist journeys, by a factor 1000, which makes the impossibility of travels to nearest stars questionable, if mass inversion technique would be someday possible.

Submitted on September 26, 2018

References

1. D'Agostini G. and Petit J.P. Constraints on Janus Cosmological Model from recent observations of supernovae type Ia. *Astrophysics and Space Science*, 2018.
2. Petit J.P. Twin universe cosmology. *Astrophysics and Space Science*, 1995, v.222, 273.
3. Petit J.P. and D'Agostini G. Negative mass hypothesis and the nature of dark energy. *Astrophysics And Space Science*, 2014, v.353, issue 2.
4. De Lapparent V., Geller M.H. and Huchara J.P. A slice of the Universe. *Astrophysical Journal*, 1986, v. 102, L1–L2.
5. Hoffman Y., Pomarede D., Tully R.B. and Courtois H.M. The Dipole Repeller. *Nature Astronomy*, 2017, 0036.
6. Petit J.P., Midy P. and Landsheat F. Twin matter against dark matter. International meeting on astrophysics and Cosmology "Where is the matter"?, Marseille, June 2001, 25–29.
7. Bondi H. Negative mass in General Relativity. *Review of Modern Physics*, 1957, v. 29, no. 3.
8. Bonnor W.B. Negative mass in General Relativity. *General relativity and Gravitation*, 1989, v. 21, no. 11, 1143–1157.
9. Hossenfelder S. Antigravitation. *Physics Letters B*, 2006, v. 636, 119–125.
10. Hossenfelder S. A bimetric theory with exchange symmetry. *Physical Review D*, 2008, v. 78, 044015.
11. Petit J.P. and D'Agostini G. Cosmological model with interaction positive and negative masses and two different speeds of light, in agreement with the observed acceleration of the universe. *Modern Physics Letters A*, 2014, v. 29, no. 34.
12. Souriau J.-M. Structure des Systèmes Dynamiques. Dunod, Paris, 1970. (English translation: Souriau J.-M. Structure of Dynamical Systems. Birkhäuser, Boston, 1997).
13. Sakharov A.D. *ZhETF Pis'ma*, 1967, v. 5, 32; *JETP Lett.*, 1967, v. 5, 24.
14. Sakharov A.D. *ZhETF*, 1979, v. 76, 1172; *ZhETF*, 1979, v. 49, 594).
15. Sakharov A.D. (1980). Cosmological model of the Universe with a time vector inversion. *ZhETF*, 1980, v. 52, 349–351; *ZhETF*, 1980, v. 79, 689–693.
16. Petit J.P. Cosmological model with variable velocity of light. *Modern Phys. Letters A*, 1988, v. 3, 1988, 1527.
17. Petit J.P. The missing mass problem. *Il Nuovo Cimento*, 1994, v. 109, 697–710.
18. Benoit-Levy A. and Chardin G. Introducing the Dirac-Milne universe. arXiv:1110.3954v2 (astro-ph).

On the Supersymmetry Realization of Involving β^+-Orthopositronium. Phenomenology

Boris M. Levin

N. N. Semenov Inst. Chem. Phys. Russian Acad. of Sci., Moscow (1964–1987),
The creative cooperation with B. P. Konstantinov Leningrad Inst. Nucl. Phys. Russian Acad. of Sci., Gatchina (1984–1987),
A. F. Ioffe Phys. Tech. Inst. Russian Acad. of Sci., St. Petersburg (2005–2007)
E-mail: bormikhlev@yandex.ru

The absence of a Coulomb barrier in the interaction of the Vacuum-Like State of Matter with normal matter is the basis of the phenomenology of the Project of the New (Additional) $G\hbar/ck$-Physics "Outside" the Light Cone.

"*Of course, the most intriguing question is whether NEC-violation fields exist in Nature. Needless to say, no such fields have been discovered. The situation is not entirely hopeless, however: we may learn at some point in future that Universe went through the bounce or Genesis epoch, and that will be an indication that NEC-violation indeed took place in the past*" [1].

Closely adjoins this problem the phenomenology of the extension of the Standard Model/SM (as the possibility of two-valued/± vacuum states), the formulation of which is stimulated by observations (1956/USA, 1965/USA, 1967/Russia, 1975/USA, 1975/England, 1975/Canada, 1987/Russia, 1982–1990/USA, 2003/USA) anomalies of annihilation of β^+-decay positrons (β^+-orthopositronium) in the system

$$^{22}\mathrm{Na}\,(3^+) \xrightarrow{e^+_\beta+\nu} {}^{22*}\mathrm{Ne}\,(2^+) \xrightarrow{\gamma_n\simeq 1.274\ \mathrm{MeV}} {}^{22}\mathrm{Ne}\,(0^+) - \text{gaseous neon (8.86\% } {}^{22}\mathrm{Ne}).$$

The necessary definiteness in the construction of the model to explain the anomalies in neon is the result of our critical experiment [2] (the hypothesis about paradoxical realization of the Mossbauer effect/EM): at the indicated "*resonance conditions*" there is doubling 1.85 ± 0.1 of the contribution of the orthopositronium component $\boldsymbol{I}_2$ of the lifetime spectra of the β^+-positrons e^+_β at decrease in the fraction of the isotope ^{22}Ne in the natural isotope composition — from 8.86% to 4.91% — in the sample for comparison. From the SM position, the possible change in $\boldsymbol{I}_2$ is vanishingly small: $10^{-7} - 10^{-6}$.

Self consistent phenomenology in the proposed model is formulated with reference to the results and conclusions of a number of creative searches for theorists (1962–2012) — by including in the final state of the β^+-decay of nuclei ^{22}Na, ^{64}Cu, ^{68}Ga and the like ($\Delta J^\pi = 1^\pi$) of the bounded 4-volume of space-time "outside" the Light Cone, instead of counterproductive phenomenology "*tachyon*, as a particle" [3].

Otherwise, it is impossible to explain the "isotope anomaly".

It is necessary to return to this fact ignored by the scientific community: among the known and presumed vacuum effects — from the Lamb shift of atomic levels and Casimir effect to the birth of the universe "in the Laboratory" [1, 4] — there is no discussion of a paradoxical realization of EM in the "resonance conditions".

The effect can be represented as the result of a *Topological Quantum Transition/TQT* of a bounded 4-volume of space-time in the final state of β^+-decay into a two-valued/± *Vacuum-Like State of Matter/VSM*$^{\text{"}+''}$ "*Through the Looking Glass*"/*TLG*$^{\text{"}-''}$ — *Long-Range Atom/LRA* with a *LRA Core*. In phenomenology, this is a kind of realization of a string (the Hamiltonian chain), at the nodes of which there are quasiparticles of all the ingredients of stable matter – quasiprotons ($\bar{p}$), quasielectron ($\bar{e}$), quasineutrino ($\bar{\nu}$) [2, 3].

According to the SM, negative masses are not physically realized, since otherwise such physical states would be unstable with respect to the catastrophic generation of an unlimited number "particle-antiparticle" pairs (disintegration of the vacuum). The prohibition of such "pathological states" underlies the Weak Energy Condition/WEC (NEC) of the General Relativity.

The model proposed in [3] of the LRA of the two-valued/± Planck mass

$$\pm M_{\mathrm{Pl}} = \pm\sqrt{\frac{(\pm\hbar)\cdot(\pm c)}{G}}\,, \quad G > 0,$$

with the total number of cells/nodes

$$\pm N^{(3)} = \frac{\pm M_{\mathrm{Pl}}}{\pm m_{\bar{p}} \pm m_{\bar{e}} \pm m_{\bar{\nu}}} \simeq 1.3\cdot 10^{19}$$

and a LRA Core [5]

$$\pm n \simeq 5.3\cdot 10^4,$$

in the final state of the β^+-decay type $\Delta J^\pi = 1^\pi$ stops the disintegration of the vacuum and substantiated the EM in "resonance conditions".

The main thing is that presented model is based on the assumption of a fundamental difference between the QED-orthopositronium formed in the substance as result of the production of the $e^+ - e^-$ pair from the β^+-orthopositronium/β^+-o-Ps, since it is possible to justify [3] that in the process of

formation and lifetime β^+-o-Ps in the substance a supersymmetry is realized [6]. The process is limited by the lifetime of β^+-o-Ps, which, being formed "inside" the Light Cone — oscillates due to single-quantum (virtual) annihilation.

So β^+-o-Ps objectively formalized the status of the physical observer.

In this case, the causality principle (global) is realized as a local causality principle due to the presence of β^+-o-Ps.

Because of the fundamental difference in the radii of interactions — infinite radius for electromagnetic and gravitational interactions and submicroscopic radii of "nuclear" interactions (weak ones, $r_w \sim 10^{-16}$ cm and $r_{str} \sim 10^{-13}$ cm) — there is no Coulomb barrier at interaction the LRA Core with ordinary substance.

In the gravitational field of the ground laboratory, the two-valued/± components of the LRA Core ($\text{VSM}^{\text{“}+''}/\text{TLG}^{\text{“}-''}$) diverge vertically by a distance h_G in the vertical during the lifetime of β^+-o-Ps ($\tau_{\text{o–Ps}} \leqslant 1.42 \cdot 10^{-7}$ s)

$$h_G = 2 \cdot \frac{g\,\tau^2_{\text{o–Ps}}}{2} \leqslant 10^{-11}\ \text{cm}.$$

Since $h_G \gg r_w$ and r_{str}, in the final start of the β^+-decay of ^{22}Na, ^{64}Cu, ^{68}Ga nuclei (TQT in the presence of β^+-o-Ps) at the nodes of the LRA Core, the quasiprotons of the $\text{VSM}^{\text{“}+''}$ ($\bar{p}$) are released (decompensation of the baryon charge) but the electric charges of the quasiprotons and the charges of the quasi-electrons of the $\text{VSM}^{\text{“}+''}$ ($\bar{p}^+$, $\bar{e}^-$) are compensated by the $\text{TLG}^{\text{“}-''}$ ($\bar{p}^-$, $\bar{e}^+$).

This means that there is no Coulomb barrier in the interaction of the LRA Core with the nuclei of the substance atoms. As a result, a Rigid Body/RB is formed (^{22}Ne) in the system

$$^{22}\text{Na}\,(3^+) \longrightarrow {}^{22*}\text{Ne}\,(2^+) \longrightarrow {}^{22}\text{Ne}\,(0^+) - \text{gaseous neon (8.86\% } {}^{22}\text{Ne).}$$

by way exchange interaction of the quasiprotons of the ^{22}Na nuclei from gas with the quasiprotons of the LRA Core at nodes ($\bar{n}$) during the lifetime of the β^+-o-Ps ($\tau_{\beta^+-o-Ps} \leqslant 1.42 \cdot 10^{-7}$)-collectivization of the γ_n-quantum ("resonance conditions" — the Mössbauer effect)

$$^{*22}\text{Ne}\,(2^+) \xrightarrow{\gamma_n \simeq 1.274\ \text{MeV}} {}^{22}\text{Ne}\,(0^+).$$

It is interesting that the ratio of the macroscopic dimensions of the LRA to the size of the LRA Core on the order of magnitude is equal to this ratio for atoms of the ordinary substance

$$\sqrt[3]{\frac{N^{(3)}}{\bar{n}}} \simeq \frac{r_H}{r_p} \simeq 10^5,$$

where r_H and r_p, respectively, are the radii of the hydrogen atom and the proton.

Conceptually, the stated phenomenology seems to have for a long time been foreseen:

"*A week energy conditions is not satisfied for the 'C-field' proposed by Hoyle and Narlikar* ⟨[7]⟩*, which is also a scalar field* $m = 0$*; only this time the energy-momentum tensor has the opposite sign and, consequently, the energy density is negative. In view of this, simultaneous production of quanta of fields with positive energy and C-field with negative energy is possible. This process take place in a stationary universe proposed by Hoyle and Narlikar, in which, as the particles increase, a new substance is continuously created as a result of the general expansion of the universe, so that a constant average density is maintained. However, such a process causes difficulties in terms of quantum mechanics. Even if the cross section of such process is very small, the presence of an infinite phase volume for quanta of positive and negative energy would lead to the production of an infinite number of pairs in a finite region of space-time*" [8].

With the adoption of the considered model, the process of real one-quantum annihilation of the β^+-o-Ps is

$$\beta^+\text{–o–Ps/p-Ps}' \longrightarrow \gamma\, U^{\pm}(\gamma^{\circ}/2\gamma'),$$

where γ° is a notoph [9], p-Ps′ is a parapositronium in the TLG, γ' is a photon/notoph in TLG and β^+-decay of nuclei of the type $\Delta J^{\pi} = 1^{\pi}$ with "resonance conditions" (EM) in the final state of the TQT [2, 3]

$$^{22}\text{Na}\,(3^+) \xrightarrow{e^+_{\beta} + \nu + U^{\pm}} {}^{22*}\text{Ne}\,(2^+) \xrightarrow{\gamma_n \simeq 1.274\ \text{MeV}} {}^{22}\text{Ne}\,(0^+) - \text{gaseous neon (8.86\% } {}^{22}\text{Ne).}$$

At the same due to the interaction of the neon atoms from the gas (90.88% ^{20}Ne, 0.26% ^{21}Ne) with the lattice nodes of the LRA Core, a quasi-nucleus [^{22}Ne–$\bar{p}$] ⇔ ^{22}Na is formed, since the nuclear-mass defect ^{23}Na (−9.5296) is maximal in comparison with ^{22}Na (−5.1840) and ^{21}Na (−2.1858).

The model realizes the thought first expressed in the report of M. Faraday to the Royal Society "*On the possible connection of gravity to electricity*" (November 28, 1850) — "*A long and unchanging conviction that all the forces of Nature are in mutual communication, having a common or rather, representing different manifestations of the single basic force…*" — the connection of physical interactions, including strong and weak (electroweak) interaction [10], open in the twentieth century.

Submitted on September 27, 2018

References

1. Rubakov V.A. The Null Energy Condition and its violation. arXiv: 1401.4024v2 [hep-th]; *Phys. Usp.*, 2014, v. 57(2), 128.
2. Levin B.M., Kochenda L.M., Markov A.A., Shantarovich V.P. Time spectra of annihilation of positrons (^{22}Na) in gaseous neon of various isotopic compositions. *Sov. J. Nucl. Phys.*, 1987, v. 45(6), 1119.
3. Levin B.M. Atom of Long-Range Action Instead of Counter-Productive Tachyon Phenomenology. Decisive Experiment of the New (Additional) Phenomenology Outside of the Light Cone. *Progress in Physics*, 2017, v.13(1), 11; Levin B.M. Half-Century History of the Project of New (Additional) Physics. *Progress in Physics*, 2017, v. 13(1), 18.

4. Rubakov V.A. Consistent NEC-violation: towards creating a universe in the laboratory. arXiv:1305.2614v2 [hep-th]; *Phys. Rev. D*, 2013, v. 88, 044015.
5. Levin B.M. On the kinematics of one-photon annihilation of orthopositronium. *Phys. Atom. Nucl.*, 1995, v. 58(2), 332.
6. Di Vecchia P., and Schuchhardt V. $N = 1$ and $N = 2$ supersymmetric positronium. *Phys. Lett. B*, 1985, v. 155(5/6), 427.
7. Hoyle F., Narlikar J.V. C-field as direct field of particles. *Proc. Roy. Soc. A*, 1964, v. 282, issue 1382, 178.
8. Hawking S.W., Ellis J.F.R. Large-Scale Structure of Space-Time. Camb. Univ. Press, 1973.
9. Ogievetsky V.I. and Polubarinov I.V. The notoph and its possible interactions. *Sov. J. Nucl. Phys.*, 1967, v. 4(1), 156.
10. Kotov B.A., Levin B.M., Sokolov V.I. Orthopositronium: "On the possible relation of gravity to electricity". Preprint No. 1784, A. F. Ioffe Physical Technical Institute Russian Academy of Sciences, Saint-Petersburg, 2005; arXiv: quant-ph/0604171.

On the Nature and Values of the Gravitational and Cosmological Constants

Anatoly V. Belyakov
E-mail: belyakov.lih@gmail.com

Stable particles of the Universe — protons and electrons — are in constant motion (there is a background component of their velocity), which is the source of the vacuum energy, explains the non-Newtonian vacuum potential and the curvature of space and determines the values of the gravitational and cosmological constants. This follows from the balance of interactions between a free electron and a proton, provided that there are no electrical forces and external influences.

1 Introduction

The origin and nature of the gravitational constant γ and, in particular, the cosmological constant Λ, introduced by Einstein into the equations of the general theory of relativity, are still the subject of discussion [1–3]. The cosmological constant determines the non-Newtonian gravitational forces and characterizes the curvature of empty space, as if additional mass or energy was introduced into it, and has a dimension of m^{-2}.

One of the points of view is that the vacuum itself is material, and the space containing it rotates. That is, for the Universe being in the stationary state, it is necessary that the inertial forces field generated by rotation compensate for the vacuum gravitational attraction [3]. However, the question arises, is it really necessary to endow vacuum with a mass and space with rotation to maintain such a balance?

Indeed, there is a geometrodynamic concept (J. Wheeler et al. [4, 5]), in which, in fact, the materiality of space itself is postulated, and in this space the initial one-dimensional spatial elements can be organized into the three-dimensional objects that one can observe. Then the original primary elements, if they are real entities, not mathematical abstractions, should in its physical incarnation be vortex structures being based on the phase boundary (surface).

So, according to Wheeler, charged microparticles are singular points on the three-dimensional surface of our world, connected by a "wormhole", i.e. a vortex tube or a power current line (of the input-output kind) located in an additional dimension. As a result, a *closed* contour is formed which a physical vacuum or some medium circulates along. Wheeler's idea, even in a simple mechanistic interpretation, allows to use macroanalogies successfully for objects of any matter organization levels: see [6, 7] etc. In particular, in determining the speed of light, it was sufficient to apply Wheeler's scheme for a single closed proton-electron contour [8].

2 The gravitational constant in geometrodynamics

Let us consider, as in the case of determining of the light speed, a single spatial-material cell, where there is a balance of forces acting between a proton and an electron. Assume that in this case the particles are in a free state, not bound to an atom, and there are no electrical forces and external influences. That is, it is assumed that a hydrogen atom is formed only when the particles approach the distance of the Bohr radius, and as for the atom larger size (the excited state), it arises only when the atom receives additional energy.

Indeed, if the contour *is not closed*, then the "photon exchange" does not occur, and there are no electric forces between the proton and the electron, and the electron can not "rotate" around the proton if the distance between them exceeds the Bohr radius. Then, in the state of equilibrium particles must move rectilinearly, changing only their mutual position. The particles themselves, according to Wheeler, if the contour is open, can be considered as single-pole vortex formations. They interact with each other through gravity and also retain the magnetic interactions between their vortex tubes (force lines) extending into "extra" dimension. These forces between the particles must be compensated by the inertial quasi-centrifugal forces, determined in the case of rectilinear motion of particles with respect to the instantaneous radius equal to the distance between the particles.

We recall that in [6, 7] the formula for electric and magnetic forces are written in the "Coulombless" form, where the charge is replaced by the electron ultimate momentum. It is assumed that the unit element of such a tube is an element having the size of the classical electron radius r_e and its mass m_e. In this case, the electric and magnetic constants have the form:

$$\varepsilon_0 = \frac{m_e}{r_e} = 3.23 \times 10^{-16}\ \mathrm{kg/m}, \tag{1}$$

$$\mu_0 = \frac{1}{\varepsilon_0 c^2} = 0.0344\ \mathrm{N}^{-1}, \tag{2}$$

where m_e, r_e, c are the electron mass, the electron radius, and the light speed. The balance between magnetic, inertial and gravitational forces has the form:

$$z_{e_1} z_{e_2} \mu_0^{-1} \frac{l}{2\pi r} \left(\frac{r_e}{c \times [\mathrm{sec}]} \right)^2 + z_{g_1} z_{g_2} \mu_0^{-1} \frac{\varepsilon_0 \gamma / c^2}{r^2} = z_g \mu_0^{-1} \frac{(v_0/c)^2}{r}, \tag{3}$$

where l, r, v_0, z_e, z_g are the relative length of the vortex tube in units of r_e, the relative distance between the particles in

units of r_e, the relative to each other velocity of the particles, the relative charge and mass in electron charges and masses. Making transformations and neglecting the electron mass, we represent (3) in the form:

$$r\,\frac{l}{m_p}\,\frac{r_e^2}{2\pi\times[\mathrm{sec}^2]}-rv_0^2=\varepsilon_0\gamma\,, \tag{4}$$

where m_p is the relative proton mass in units of m_e. Thus, an equation has been obtained having the velocity squares dimension, and these terms of the equation are proportional to the energies of the corresponding interactions.

As for the vortex tube length, then $a < l < m_p$ (a is the fine structure inverse constant), since the electron spin ($ar_em_ec/2$) means the presence of either a "hidden" mass or a linear parameter in its structure which is increased not less than 137 times with respect to the electron standard parameters, even if the spin speed of rotation is equal to the light speed. On the other hand, l can not exceed of the proton vortex tube length (with correction for the projection angle) [7].

To maintain the equilibrium state, the velocity v_0 must be constant for any distance between particles, including for limiting cases. Neglecting the gravitational component at $r\to\infty$ and $l = m_p$, we obtain from (4):

$$v_0=\frac{r_e}{(2\pi)^{1/2}\times[\mathrm{sec}]}=1.12\times10^{-15}\ \mathrm{m/sec}. \tag{5}$$

Neglecting the magnetic component, when the distance between the particles is equal to the Bohr radius R_B, i.e. for $r = a^2$, we obtain:

$$v_0=\frac{(\varepsilon_0\gamma)^{1/2}}{a}=1.07\times10^{-15}\ \mathrm{m/sec}, \tag{6}$$

which actually coincides with the previous value. It can be reasonably assumed that this velocity is constant throughout the entire range of distances between particles — from the Bohr radius size to infinity — and it is a fundamental value, so that one can derive a formula for the gravitational constant. Bearing in mind (4) and (5), we obtain:

$$\gamma=r\left(1-\frac{l}{m_p}\right)\frac{v_0^2}{\varepsilon_0}\,. \tag{7}$$

At the Bohr radius distance, substituting $r = a^2$, $l = 137$ and the v_0 value, we find $\gamma = 6.79\times10^{-11}\ \mathrm{m^3kg^{-1}sec^{-2}}$, which is close to the actual value. Since $\gamma = const$, an increase in the distance between particles must be accompanied by in the vortex tubes length increase (the "hidden" mass) up to the value m_p.

We note that homogeneous particles behave otherwise. From the balance of interactions it follows that the free electrons must come together, and the free protons, on the contrary, move away from each other, starting from some distance between them. This difference, perhaps, contributes to the separation of particles in outer space.

The correct value of the gravitational constant for a single proton-electron unit cell has been obtained, and its value does not change when passing to cosmological scales. This gives grounds to believe that this scheme can be extended to the Universe level as a whole.

3 The cosmological constant

The equation (4) can be interpreted in the sense that the gravitational energy proportional to $\varepsilon_0\gamma$ is, as it were, a background or additional constant that ensures the equilibrium state of an elementary space-material cell regardless of its size, and the motion of free particles with velocity v_0 is something similar to cosmic "Brownian motion". Within the framework of this model, it is this motion of free particles that, when passing to cosmological scales, creates its own vacuum potential (which is perceived by an external observer as a manifestation of non-Newtonian forces) and determines the cosmological constant magnitude.

The inverse quantity Λ^{-1} can be regarded as the surface area on which the inertial forces, arising during rotation of the Universe as a whole with a background velocity v_0 over some radius L, act.

These forces counteract gravitational forces. In this case, the magnetic forces can be neglected, since in space macrobodies are in general electrically neutral. For the Universe being in equilibrium state, taking into account only the forces associated with masses, bearing in mind (4), one can write down the balance of pressures produced by these forces:

$$\frac{M\varepsilon_0\gamma}{L^3}=\frac{Mrv_0^2}{L\,\Lambda^{-1}}\,, \tag{8}$$

where M is an arbitrary mass, L is a linear parameter (radius).

The balance does not depend on the mass of the Universe, but depends on its parameter L. Both the shape of the Universe and the position of its center are undefined, and any of its points can be taken as the center of rotation, so its volume can be taken equal to L^3, and the radius of rotation is equal to the parameter L. In [9] the basic parameter of the Universe L_v is uniquely defined as the length of a vacuum structural unit (vortex tube):

$$L_v=\frac{R_c^2}{R_B}\,, \tag{9}$$

where R_c is a mean geometric, the linear parameter obtained from the balance of electric and magnetic forces and equal to $(2\pi)^{1/2}c\times[\mathrm{sec}] = 7.51\times10^8$ m. The parameter L_v is the *greatest* length to which the *lowest* peripheral speed v_0 corresponds.

The formal increase in the kinetic energy component in formula (8) a multiple of r, while maintaining the balance of pressures, requires that in this case there should be $L = L_v r^{-1/2}$, so the parameter r in (8) is reduced. As a result,

referring to (5), (9) and revealing R_c and R_B, (8) we obtain:

$$\Lambda = \frac{\varepsilon_0 \gamma}{(L_v\, v_0)^2} = \frac{1}{2\pi}\left(\frac{a}{c}\right)^4 \varepsilon_0 \gamma \times [\sec^{-2}] = \\ = 1.49 \times 10^{-52}\ \mathrm{m}^{-2}, \quad (10)$$

and such a value must correspond to the equilibrium state of the Universe. At present, based on the assumed age of the Universe, the value of Λ is estimated at 10^{-52} m^{-2} [10].

Perhaps there are regions of space filled with free elementary particles that are not bound to atoms (voids). Then it is necessary to consider the sum of set of unit elementary cells, taking into account the magnetic forces, and then the sum in brackets in an analogous formula is close to one:

$$\Lambda = \left(\frac{l}{m_p} + \frac{\varepsilon_0 \gamma}{r v_0^2}\right)\frac{1}{L^2} \approx L^{-2}. \quad (11)$$

In this case, there is a trivial uncertain result, depending only on the region size $\Lambda^{-1/2}$.

As for the hypothetical form of the Universe, the ratio $L_v/\Lambda^{-1/2} = 130.6$ is a very characteristic value close to a. Let us assume that the properties of vorticity and helicity are inherent in the structure of the Universe as a whole, as well as of its constituent units. Then the size $\Lambda^{-1/2} = 8.2 \times 10^{25}$ m can be associated with the diameter of its vortex tube, and the size $L_v = 1.06 \times 10^{28}$ m with the size of a spiral turn, the number of turns is indeterminate and they are directed along the time axis to infinity. Note that this size has the same order of magnitude as the ultimate radius of the event horizon (0.59×10^{28} m), calculated by di Bartini [11]. Some hints on the unusual form of the Universe are found in [12], where cosmological effects are given, which the authors explain by the shape of the Universe resembling a horn or a saddle.

4 Conclusions

The stable particles of matter — protons and electrons are in continuous motion (the background component of its velocity). This follows from the balance of magnetic, gravitational and inertial interactions under the condition that there are no electrical forces and external influences. At cosmological scales, the field of inertial forces generated by their motion compensates for the gravitational attraction of the Universe matter as a whole. It is this balance applied to a unit cell containing a proton and an electron that determines the gravitational constant value, and, as applied to the Universe as a whole, determines the cosmological constant value. From the observer's point of view, Λ-field manifests itself as a result of the action of non-Newtonian gravitational forces, and therefore there is no need to involve dark energy and dark matter to substantiate this field.

Submitted on September 18, 2018

References

1. Weinberg C. S. The cosmological constant problem. *Reviews of Modern Physics*, 1989, v.61, 1–23.
2. Carroll S.M. The Cosmological Constant. *The Living Reviews in Relativity*, 2001, v.4, 1–56.
3. Yermolenko Yu. The cosmological constant problem. http://cdn.scipeople.ru/materials/55751/The_cosmological_constant_problem.pdf
4. Dewitt B.S. Quantum gravity. *Scientific American*, December 1983, v.249, 112–129.
5. Berera A., Buniy R.V., Kephart T.W., Päs H., and Rosa J.G. Knotty inflation and the dimensionality of spacetime. arXiv: 1508.01458.
6. Belyakov A.V. Charge of the electron, and the constants of radiation according to J.A.Wheeler's geometrodynamic model. *Progress in Physics*, 2010, v.6, issue 4, 90–94.
7. Belyakov A.V. Macro-analogies and gravitation in the micro-world: further elaboration ofWheeler's model of geometrodynamics. *Progress in Physics*, 2012, v.8, issue 2, 47–57.
8. Belyakov A.V. On the Speed of Light and the Continuity of Physical Vacuum. *Progress in Physics*, 2018, v. 14, issue 4, 211–212.
9. Belyakov A.V. On the independent determination of the ultimate density of physical vacuum. *Progress in Physics*, 2011, v. 7, issue 2, 27–29.
10. Borissova L., Rabounski D. Fields, Vacuum and the Mirror Universe. Swedish Physical Archive, Stockholm, 2009, Ch. 5, §5.4.
11. Oros di Bartini R. Relations Between Physical Constants. *Progress in Physics*, 2005, v.1, issue 3, 34–40 (English translation from the 1966 original manuscript).
12. Aurich R., Lustig S., Steiner F., and Then H. Hyperbolic Universes with a Horned Topology and the CMB Anisotropy. arXiv: astro-ph/0403597.

Progress in Physics is an American scientific journal on advanced studies in physics, registered with the Library of Congress (DC, USA): ISSN 1555-5534 (print version) and ISSN 1555-5615 (online version). The journal is peer reviewed and listed in the abstracting and indexing coverage of: Mathematical Reviews of the AMS (USA), DOAJ of Lund University (Sweden), Scientific Commons of the University of St.Gallen (Switzerland), Open-J-Gate (India), Referential Journal of VINITI (Russia), etc. Progress in Physics is an open-access journal published and distributed in accordance with the Budapest Open Initiative: this means that the electronic copies of both full-size version of the journal and the individual papers published therein will always be accessed for reading, download, and copying for any user free of charge. The journal is issued quarterly (four volumes per year).

Electronic version of this journal: http://www.ptep-online.com

Postal address:
Department of Mathematics and Science, University of New Mexico,
705 Gurley Avenue, Gallup, NM 87301, USA